# N-terminal Regulatory Domains of Phosphodiesterases 1, 4, 5 and 10 examined with an Adenylyl Cyclase as a Reporter

**Dissertation**

der Mathematisch-Naturwissenschaftlichen Fakultät

der Eberhard Karls Universität Tübingen

zur Erlangung des Grades eines

Doktors der Naturwissenschaften

(Dr. rer. nat.)

vorgelegt von

**Ana Banjac**

Tübingen

2011

Tag der mündlichen Qualifikation: 10. 3. 2011

| | |
|---|---|
| Dekan: | Prof. Dr. Wolfgang Rosenstiel |
| 1. Berichterstatter: | Prof. Dr. Joachim E. Schultz |
| 2. Berichterstatter: | Prof. Dr. Peter Ruth |

# Acknowledgement

The experimental part of this thesis work was done within the period from November 2005 to July 2010 under the supervision of Prof. Dr. J. E. Schultz at the Pharmaceutical Institute of Tübingen University.

I would like to thank Prof. Dr. J. E. Schultz for his support and encouragement as well as for the beneficial scientific discussions. His kind support and guidance have been of great value in this study.

I am grateful to Prof. Dr. Peter Ruth for taking part in the evaluation of my thesis.

I would like to show my gratitude to Prof. Dr. Klaus Hantke and Priv. Doz. Dr. Martina Düfer for participation in the thesis examination.

Prof. Dr. Frank Böckler and Markus Zimmermann, I want to thank you for your valuable suggestions.

I appreciate the help of Ursula Kurz and Anita Schultz for cloning and training me on handling different methods. Special thanks to Karina Hofbauer, Sandra Bruder and Iman Mansi for the interest they showed at the beginning of my work in the lab. I would also like to thank Jürgen Linder for his detailed and constructive comments.

And not to forget my lab colleagues Laura García Mondéjar, Kajal Kanchan, Karin Winkler and Janani Natarajan for creating a nice working atmosphere and very interesting discussions.

My special thanks to my family for their patience and support during these five years. Without their encouragement and understanding it would have been impossible for me to finish this work.

# Content

Content ..... I
Abbreviations ..... III
1 Introduction ..... 1
1.1 Signal transduction ..... 1
1.1.1 Cyclic nucleotides as second messengers ..... 2
1.2 Phosphodiesterases ..... 2
1.2.1 Catalytic Domain Structures ..... 2
1.2.2 Regulatory Domain Structures ..... 3
1.3 Small molecule binding domains (SMBD) - GAF domains ..... 5
1.4 PDE families ..... 7
1.4.1 PDE1 ..... 7
1.4.2 PDE2 ..... 7
1.4.3 PDE4 ..... 8
1.4.4 PDE5 ..... 9
1.4.5 PDE10 ..... 10
1.4.6 PDEs in cNMP signaling compartments ..... 10
1.5 Class III Adenylyl cyclases ..... 10
1.6 Aim of work ..... 11
2 Materials and equipments ..... 13
2.1 Chemicals and materials ..... 13
2.2 Equipments ..... 14
2.3 Buffers and Solution ..... 14
2.3.1 Buffers and solutions for molecular biology ..... 15
2.3.2 Buffers and solutions for protein chemistry ..... 15
2.4 Oligonucleotides ..... 22
2.4.1 Cloning primers ..... 22
2.4.2 Sequencing primers ..... 26
2.5 Plasmids ..... 27
2.6 Bacterial strains ..... 28
3 Methods ..... 29
3.1 Molecular biology methods ..... 29
3.2 Protein chemistry ..... 35
3.2.1 Protein expression in *E.coli* ..... 35
3.2.2 Cell harvesting and lysis ..... 36
3.2.3 Protein purification ..... 36
3.2.4 SDS-PAGE gel electrophoresis and Western blotting ..... 37
3.3 Densitometry of the SDS-PAGE gels or Western blots ..... 38
3.4 Chromatography methods ..... 38
3.5 Adenylyl cyclase assay ..... 39
3.6 Crystallization ..... 40
3.7 Cloning ..... 40
3.7.1 Starting clones ..... 41
3.7.2 PDE5-CyaB1 AC Chimeras ..... 43
3.7.3 PDE10, PDE5 linker-CyaB1 AC chimeras ..... 45
3.7.4 PDE1-CyaB1 AC chimeras ..... 49
3.7.5 PDE4-CyaB1 AC chimeras ..... 50
3.7.6 Crystal constructs ..... 57

# Content


4 Results ..... 59
4.1 hPDE5 N-terminus in tandem GAF signaling ..... 59
4.1.1 Expression and characterization of shortened PDE5-CyaB1 AC chimeras ..... 59
4.2 Insertion of NAAIRS between hPDE5 GAF-B and CyaB1 AC ..... 63
4.2.1 Expression and characterization of PDE5 NAAIRS-CyaB1 AC ..... 63
4.3 hPDE10 and hPDE5 α-helical linker in tandem GAF signaling ..... 66
4.3.1 Expression and characterization of PDE10, PDE5 (G311-S346)-CyaB1 AC chimeras (No.1-16) ..... 67
4.3.2 Expression and characterization of chimeras No.17 and 18 ..... 75
4.3.3 Expression and characterization of chimeras No.19-21 ..... 78
4.3.4 Expression and characterization of chimeras No.22 and 23 ..... 81
4.4 Tandem CaM-binding domains in signaling: hPDE1-CyaB1 AC chimeras ..... 85
4.4.1 Expression and characterization of PDE1A3- and PDE1B1-CyaB1 AC chimeras ..... 86
4.5 Tandem UCR domains in signaling: hPDE4-CyaB1 AC chimeras ..... 91
4.5.1 Expression and characterization of hPDE4D3-CyaB1 AC chimeras ..... 92
4.5.2 Expression and characterization of hPDE4A4-CyaB1 AC chimeras ..... 95
4.5.3 Expression and characterization of hPDE4B1-CyaB1 AC chimeras ..... 100
5 Discussion ..... 103
5.1 Role of hPDE5 N-terminus in tandem GAF signaling ..... 104
5.2 Role of the linker between GAF-A and B in hPDE5 and 10 ..... 105
5.3 Tandem CaM-binding domains from hPDE1 in regulation of CyaB1 AC activity 107
5.4 Tandem UCR domains from hPDE4 in regulation of CyaB1 AC activity ..... 108
5.4.1 hPDE4D3 tandem UCR domains in regulation of CyaB1 AC activity ..... 109
5.4.2 hPDE4A4 tandem UCR domains in regulation of CyaB1 AC activity ..... 109
5.4.3 hPDE4B1 tandem UCR domains in regulation of CyaB1 AC activity ..... 110
5.5 Crystallization of hPDE5 GAF domains ..... 111
5.6 Possible pharmacological meaning of PDEs N-tandem domains ..... 112
5.7 Open questions and outlook ..... 113
6 Summary ..... 116
Appendix ..... 117

# Abbreviations

| | |
|---|---|
| AA/Bis | Acrylamide / bisacrylamide (37.5:1) |
| Ab | Antibody |
| AC | Adenylyl cyclase |
| aa | Amino acid |
| bp | Base pair |
| CaM | $Ca^{2+}$-calmodulin |
| CyaB1/CyaB2 | Adenylyl cyclase from *Anabaena sp.* |
| cpm | Counts per minute |
| EtBr | Ethidium bromide |
| GC | Guanylyl cyclase |
| IDA | Iminodiacetic acid |
| IMAC | Immobilized metal affinity chromatography |
| IPTG | Isopropyl thiogalactoside |
| IBMX | 3 –isobutyl–1– methylxanthin, non-selective PDE activator |
| *Kappa* | Kappa polymerase |
| LB-medium | Luria-Bertani culture medium |
| MCS | Multiple cloning site |
| NTA | Nitrilotriacetic acid |
| OD | Optical density |
| ORF | Open reading frame |
| PDE(s) | Phosphodiesterase(s) |
| PEG | Polyethylene glycol |
| *Pfu*-polymerase | DNA polymerase from *Pyrococcus furiosus* |
| *Phusion*-polymerase | DNA polymerase, *Pyrococcus*-like enzyme |
| PKA | cAMP dependent protein kinase |
| PKB | Protein kinase B |
| PKC | Protein kinase C |
| PKG | cGMP dependent protein kinase |
| PVDF | Polyvinylidendifluorid |
| RT | Room temperature |

| | |
|---|---|
| SMBDs | Small molecules binding domain |
| TAE | Tris-acetate-EDTA buffer |
| *Taq*-polymerase | DNA polymerase from *Thermus aquaticus* |
| TE | Tris-EDTA buffer |
| TEV | Tobacco etch virus |
| TBS | Tris buffered saline |
| TM | Transmembrane domain(s) |
| UCR | Upstream conserved region |
| WT | Wild type |
| X-Gal | 5-bromo-4-chloro-3-indolyl-β-D-galactopyranoside |

# 1 Introduction

Several mammalian PDEs and cyanobacterial ACs share a similar domain organization, an N-terminal tandem GAF domain (GAF-A and GAF-B) linked to a C-terminal catalytic domain. These N-terminal tandem GAF domains (acronym originates from proteins in which these domains were initially identified: c***G***MP binding PDEs, ***A***denylyl cyclases, and ***F***hlA transcription factor) have sequence and structural similarities in spite of three billion years of evolution distancing mammals and cyanobacteria [1-6].

In 2002, T. Kanacher successfully replaced the N-terminal tandem GAF domain of the AC from cyanobacterium *Anabaena cylindrica* (CyaB1 AC) with the rat PDE2 tandem GAF domain [7]. CyaB1 AC holoenzyme is activated by cAMP binding to GAF-B and the mammalian PDE2 by cGMP binding to GAF-B [8, 9]. By this exchange CyaB1 AC was converted into a cGMP regulated chimera. To biochemically characterise the PDE2 tandem GAF, such a chimera was useful as its substrate and allosteric activator were not identical.

CyaB1 AC in our laboratory has been used extensively for investigations of mammalian PDE2, PDE5, PDE10 and PDE11 tandem GAF domains. Results demonstrated that tandem GAF domains from mammalian PDEs and CyaB1 AC share common mechanisms for regulation [10-13]. Since all PDEs share a similar basic domain structure, the question was whether there exists a general mechanism of PDE regulation?

To answer this question, I prepared chimeras of the N-terminal regulatory domains from PDE1, PDE4, PDE5 and PDE10 and the catalytic domain from CyaB1 AC, to study the regulatory domains with the respect to ligand specificity, the role of phosphorylation and the role of defined protein regions in regulation.

## 1.1 Signal transduction

All cells respond to different environmental demands. Extracellular stimuli are detected, amplified and integrated in signal–transduction cascades. The results are responses such as changes in gene expression (DNA transcription and translation), changes in enzyme activity or ion-channel conductivity [14].

Ligands such as hormones, neurotransmitters, odorants and chemicals form complexes with membrane receptor proteins, change their conformation and affect second messenger concentrations. This can result in altered gene expression or further signal amplification which finally (de)activates ion channels or enzymes. Common second messengers are cAMP and cGMP, $Ca^{2+}$, inositol tris phosphate (IP3) and diacyl glycerol (DAG).

Multiple signaling pathways are involved in cross-talk and integrate a variety of signals in fine tuning cell activity.

### 1.1.1 Cyclic nucleotides as second messengers

The discovery of cAMP in liver homogenates by Sutherland and Rall was the beginning of the second messenger-story [15-17]. The levels of cAMP (cGMP) in cells and the duration of the signal are determined by AC and GC, respectively, which catalyse their synthesis and by PDEs which hydrolyse them into 5`-nucleotide monophosphates [18-21].

## 1.2 Phosphodiesterases

PDE activity was observed immediately after the cAMP discovery [15]. PDEs are metal hydrolases which participate in regulation of cAMP and cGMP. PDEs are subdivided into three distinct classes (I, II and III) according to differences in their primary structures. All known mammalian PDEs are class I as are PDEs from *Dictyostelium discoideum, Drosophila melanogaster, Caenorhabditis elegans* and *Saccharomyces cerevisiae.* Class I PDEs selectively hydrolyses the 3` phosphate bond of cAMP or cGMP. Class II PDEs from yeast, *Dictyostelium discoideum* and *Vibrio fischeri* also hydrolyses the phosphodiester bond, but do not show the same substrate selectivity. PDEs from prokaryotes are class III [20, 22, 23].

21 genes encode 11 PDE families (PDE1-11), which differ in their amino acid sequence, substrate specificities, kinetic properties, modes of regulation, inhibitor sensitivities, intracellular localization, cellular expression and tissue distribution. Every gene has several different isoforms because of alternative transcriptional start sites, secondary modifications and alternative splicing of mRNA. Current estimates are for more than 100 mRNA, most of which can be translated into various PDEs [22-24]. The question is what is the physiological role of these multiple isoforms?

It has been established that PDEs are multi-domain proteins which share a conserved domain organisation consisting of a C-terminal catalytic domain of about 270 aa and an N-terminal domain containing structural elements which regulate PDE activity.

### 1.2.1 Catalytic Domain Structures

The overall structures of catalytic domains are very similar among all PDE families although the sequence identity of catalytic domains is only approximately 25% (within each family 75%) [23-25]. According to their substrate specificity, PDEs can be divided into three groups:

1) cAMP - specific (PDE4, 7 and 8)

2) cGMP - specific (PDE5, 6 and 9)

3) PDEs with dual specificity (PDE1, 2, 3, 10 and 11).

Substrate selectivity is likely to be determined by a "glutamine switch" in the catalytic domain [26-29]. PDEs that hydrolyse both cAMP and cGMP have an invariant glutamine which is free to rotate; in PDEs which are cAMP selective this glutamine is fixed by neighbouring residues into a favoured position for cAMP binding; in PDEs which prefer cGMP, the glutamine is fixed into another, cGMP favoured position. This invariant glutamine probably stabilises purine ring binding in the binding pocket.

### 1.2.2 Regulatory Domain Structures

Despite structural and functional diversity, there is a remarkable homology in the overall domain organization of PDEs (Fig 1.1). The N-terminal regulatory domains contribute to modulation of cNMP levels.

Different PDE families have different N-terminal domains [23, 24]: PDE2, 5, 6, 10 and 11 contain tandem GAF domains; PDE1 has a tandem $Ca^{+2}$-calmodulin (CaM)-binding domain; at the N-terminus of PDE4 is a tandem of upstream conserved regions (UCR1/2); PDE3 is activated by phosphorylation at the N-terminus; PDE7 has not been studied much; PDE8 contains two regulatory regions of unknown function, a REC domain (homologous to the receiver domains of bacterial two-component signaling systems) and a PAS domain (*Drosophila* **P**eriod clock protein, **a**ryl hydrocarbon receptor nuclear translocator, *Drosophila* **s**ingle-minded protein); PDE9 is the most recently discovered PDE, apparently without any N-terminal regulatory sequences found in other PDEs.

Currently, several structures of PDE regulatory domains have been solved: the parallel dimer structure of mouse PDE2 tandem GAF domain with cGMP bound, near full-length hPDE2 (aa 215-900), GAF-B domain of hPDE10A with cAMP bound and NMR solution structure of PDE5 GAF-A domain with cGMP bound [30-33].

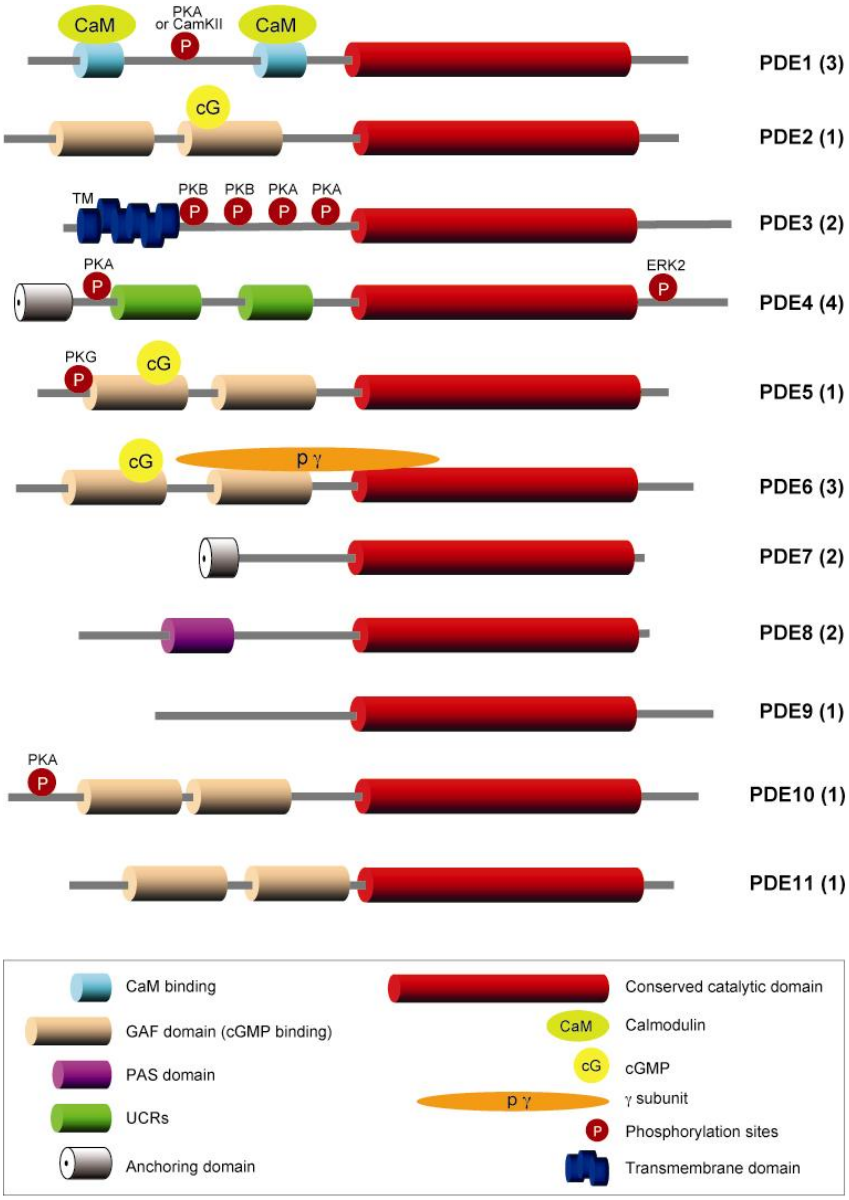


Conti M, Beavo J. 2007.
Annu. Rev. Biochem. 76:481–511

Fig. 1.1: Domain organization of the eleven PDE families from [23]
The number of genes encoding different members of the families is in brackets; CaMKII: calmodulin regulated kinase II, ERK2: extracellular signal-regulated kinase 2, Pγ: PDE6 γ-subunit, PKA: protein kinase A, PKB: protein kinase B, TM: transmembrane domains, UCR: upstream conserved region;

Since several PDEs have a conserved domain organization, there might be similarities in regulatory mechanisms.

## 1.3 Small molecule binding domains (SMBD) - GAF domains

The ability of sensing small molecules is of great importance for every life form in regulation of different cellular processes. 21 different SMBD were described according to sequence analysis and protein structure comparisons of thousands of proteins from bacteria, Archaea and eukaryotes [34] .

Usually SMBDs consist of approximately 100 aa. They bind ligands and transmit their effects to a catalytic domain through allosteric regulation. Some prominent SMBDs are PAS (**P**er-**A**rnt-**S**im), GAF (c**G**MP phosphodiesterase, **A**denylate cyclase, **F**hlA transcription factor), HAMP (**H**istidine kinase, **A**denylate cyclase, **M**ethyl-accepting chemotaxis protein and **P**hosphatase), STAS (**S**ulfate **t**ransporter, **A**nti-**s**igma factor-binding domain) and DSBH (**D**ouble-**s**tranded **ß**-helix **d**omain).

GAF domains were identified in 1997 by Aravind and Ponting [35]. More than 7400 proteins contain GAF domains from Archaea to mammals [36]. For most of them the function is yet to be understood. Evidences of ligand binding are confirmed for a very few GAF domains [7, 10, 37-40]. Proteins with GAF domains mostly participate in cell signal transduction processes and transcription regulation and are especially prominent among bacteria.

GAF domains are usually ~200 aa long and exist as stand alone proteins or more often as multi-domain proteins with usually a single or a tandem GAF. Tandem GAF domains are present at the N-terminal ends of five mammalian PDE, PDE2, 5, 6, 10, and 11 (Fig. 1.2). In these GAF tandems, one GAF binds cyclic nucleotide and the other has a structural role [11, 12]. Removing one GAF from a tandem abolishes signaling and regulation. PDE2 is activated by cGMP binding to GAF-B, PDE5 and 11 by cGMP to GAF-A, PDE10 by binding of cAMP to GAF-B and PDE6 GAF-A binds cGMP, which activates the enzyme by removal of the inhibitory γ subunit [10, 37, 38, 41, 42].

The crystal structure of the tandem GAF domain from PDE2 shows a parallel dimer with cGMP bound to GAF-B domains and GAF-A domains involved in dimerization [8, 30]. Both domains are separated by a long α-helical linker which is also used for dimerization contacts (Fig. 1.3 - A).

More recently, the crystal structure of PDE10 GAF-B with bound cAMP, the NMR structure of PDE5 GAF-A with bound cGMP, and, most recently a near full length PDE2 without ligand demonstrated similar overall structures of all GAF domains: a six-stranded antiparallel β-sheet is sandwiched between 2-4 α-helices involved in the dimerization interface on one side and a mixture of short α-helices and loops on the other side [31-33]. Surprisingly, CyaB1 and CyaB2 ACs from *Anabaena* contain tandem GAF domains which are closely related to

mammalian GAF tandems. Their N-terminal tandem GAF domain is linked to the C-terminal output domain via a PAS-domain of unknown function (Fig. 1.2). The crystal structure of the tandem GAF domain from CyaB2 AC has been solved [43], showing the antiparallel homodimer, in which cAMP was bound in both GAF-A and GAF-B domains. As in PDE2, the length conserved α-helical linker connects two GAF domains and it is involved in dimerization (Fig. 1.3 – B).

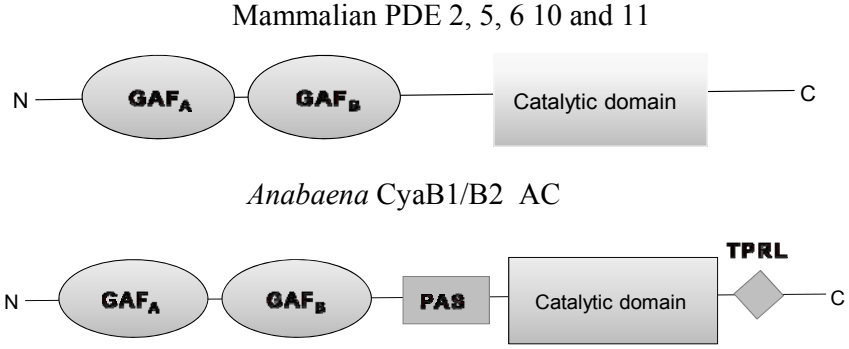


Fig. 1.2: Domain organization of PDE with a tandem GAF domain and *Anabaena sp.* AC (modified from [30])
PAS: **P**er-**A**rnt-**S**im, TPRL: **T**etratrico **p**eptide **r**epeat-**l**ike-domain;

Despite the enormous evolutionary distance, tandem GAF domains from mammalian PDE2 (later from PDE5, PDE10 and PDE11) can substitute that in CyaB1 and regulate cyclase activity [7], suggesting highly conserved mechanisms of activation established early in evolution.

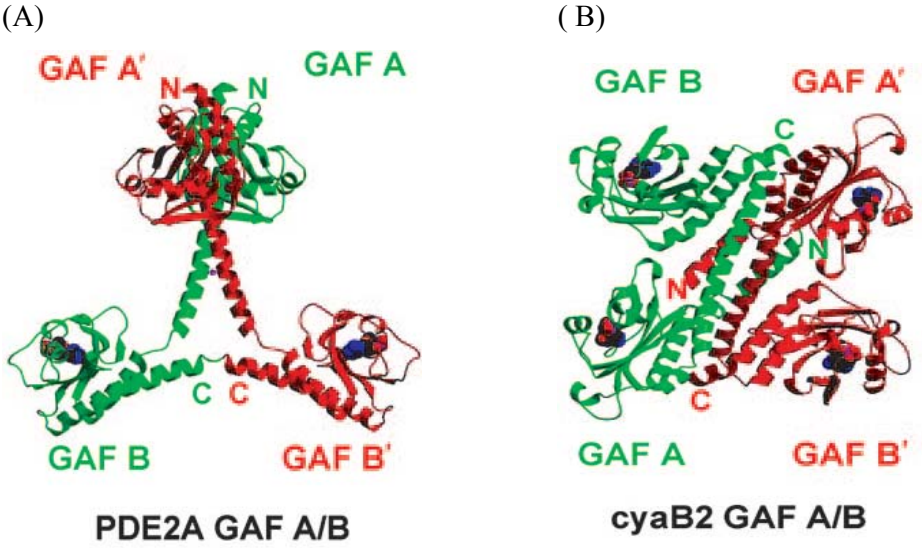


Fig. 1.3: Crystal structures of GAF-domains from mouse PDE2A and CyaB2 fom *Anabaena sp.*
Ribbon structure views: (A) PDE2A GAF A/B parallel dimer structure [30] and (B) CyaB2 GAF A/B antiparallel dimer structure [43];

## 1.4 PDE families

### 1.4.1 PDE1

PDE1 family is calcium-calmodulin (CaM) activated and one of the first identified [44]. There are several PDE1 isoforms encoded from three PDE1 genes: PDE1A, B and C, expressed in various cell types and tissues. They all have a similar domain organization: an N-terminal tandem CaM-binding domains with short autoinhibitiory sequences between them and a C-terminal catalytic domain [45-49]. The catalytic domains are highly conserved and have dual specificity for cAMP and cGMP. PDE1As and PDE1Bs are more specific for cGMP hydrolysis, while PDE1Cs hydrolyse both cAMP and cGMP equally well. PDE1s are dimers and each monomer binds one molecule of CaM which activates the catalytic domain, probably by relieving an inhibition [50, 51].

As a consequence of unique N-terminals in different isoforms, PDE1s have different affinities to CaM even within the isoforms of the same gene family: e.g. PDE1A1 has a 10-fold higher affinity for CaM than PDE1A2. Phosphorylation of PDE1As by PKA and of PDE1Bs by CaMKII at specific N-terminal sites decreases CaM affinity. The activity of PDE1Cs is likely inhibited by PKA phosphorylation [51].

Due to unique N-terminal sequences, different isoforms have distinct functional properties and localization [24, 47, 50-52].

Currently, there is no specific cell-permeable inhibitor for the PDE1 family which makes the investigation of this family difficult.

### 1.4.2 PDE2

PDE2 hydrolyses both cAMP and cGMP with high Vmax and low Km values. It is allosterically stimulated by cGMP binding to GAF-B. cGMP binds to GAF-B with high affinity and selectivity [8, 30, 38].

Recently, the crystal structure of a near full-length enzyme has been solved (aa 215-900) [33]. It demonstrated a dimer in which each monomer has a parallel, extended, linear organization containing tandem regulatory domains GAF-A and GAF-B and the catalytic domain connected by linker α-helices (Fig. 1.4). Two linker helices between GAF-A and GAF-B domains are roughly parallel with a lot of hydrophobic contacts along the entire length. Linkers between GAF-B and the catalytic domain cross over, so that the catalytic domain of one molecule is directly below the GAF-B domain of the other molecule of the dimer.

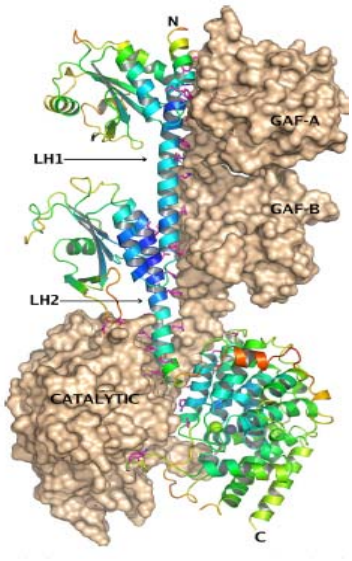


Fig. 1.4: Crystal structure of PDE2A (aa 215-900), from [33]
The surface/ribbon presentation of asymmetric unit which contains two molecules A and B. The three domains are labelled in the figure as well as the linker helices LH1 and LH2 that connect them;

Three isoforms of PDE2 are described, soluble PDE2A1 and membrane associated PDE2A2/3. PDE2s mediate the negative cross-talk between cAMP and cGMP pathways in adrenal medulla, brain, platelets, heart and macrophages. In adrenal gland they are highly expressed and regulate aldosteron secretion: atrial natriuretic peptide (ANP) released from the cardiac tissue during high blood pressure activates GC and increases the cGMP level. This cGMP activates PDE2 and decreases the levels of cAMP inhibiting aldosterone secretion which in turn leads to reduction in blood pressure and volume [53].

A few selective PDE2 inhibitors facilitate investigation of PDE2 functions in different tissues under physiological and pathophysiological conditions especially in sepsis, localised inflammatory responses and for memory improving.

### 1.4.3 PDE4

PDE4 is the best studied family of PDEs, rolipram inhibited and cAMP specific. Four genes A, B, C and D encode more than 20 different variants by means of alternative splicing with almost identical kinetic characteristics [54, 55]. C-terminal catalytic domains in PDE4s exhibit 75% sequence identity. Isoforms have unique N-terminal regions which regulate catalytic activity and direct the proteins to specific cellular regions by binding to different targets or into the membrane. In each family there are so called long and short isoforms with differences at their N-termini. Long isoforms have two UCR domains, UCR1 and UCR2, short isoforms have a single UCR and supershort ones only a truncated UCR domain. UCR1 and UCR2 are conserved in PDE4s, but lack homology among themselves [29].

At the beginning of UCR1 in all long isoforms, a conserved RRESF motif is localized; the phosphorylation of Ser in this motif activates the catalytic domain 60-250% [56, 57]. An additional role of Ser phosphorylation is to alter binding of PDE4 to various scaffold proteins. There is one more phosphorylation site at the C-terminal for ERK I which is involved in a feedback mechanism in long PDE4 isoforms [58].

UCR1 and UCR2 are independent domains which interact with each other through electrostatic interaction and with the catalytic domain, probably via UCR2, holding the enzyme in the "off" position [59]. As cAMP levels in the cell increase, PKA phosphorylates the serine in the RRESF motif (S54 in PDE4D3) and disrupts the interaction. This UCR1-UCR2 interplay probably removes the autoinhibitory effect of UCR2 on the catalytic site and increases the affinity for $Mg^{2+}$ in the catalytic center [56, 57, 59].

Dimerization of long isoforms is an additional function of UCR1 and 2 domains [60, 61]. All short isoforms are monomers and that explains differences in the regulatory properties between long and short PDE4s.

Long PDE4s are activated by phosphatidic acid via UCR1 [62, 63]. Probably the negative charge input in this region (like the PKA phosphorylation) is important for enzyme activation.

The PDE4 family is very well studied due to several available selective inhibitors and via knockout mice. PDE4s are drug targets [29, 64-68]. A potent PDE4 inhibitor - rolipram is a smooth muscle relaxant, antidepressant and anti-inflammatory agent, but with strong emetic side effects (probably through PDE4D3 inhibition in the CNS). A new generation PDE4 inhibitor, rofumilast [69, 70] with less side effects was approved in July 2010 for treatment of chronical obstructive pulmonary disease (COPD). PDE4 inhibitors are good anti-inflammatory agents by suppressing the release of inflammatory mediators and immune cell infiltration. There are preclinical evidences that PDE4 inhibitors may have a role in the treatment of schizophrenia, depression, Alzheimer`s disease and some neurodegenerative conditions. Variations in PDE4D gene were found to confer increased risk of ischemic stroke and osteoporosis [24, 71].

### 1.4.4 PDE5

PDE5s are cGMP specific and cGMP binding PDEs [4, 72, 73]. They are allosterically activated by cGMP binding to a high affinity binding site in GAF-A, which stimulates catalytic activity up to ten fold by increasing substrate affinity and promoting PKG phosphorylation at the Ser-102 (numbering in hPDE5) [37, 74, 75]. Phosphorylation of serine further increases the affinities for cGMP at both sites, allosteric and catalytic. This feedback

could be the mechanism for a prolonged activation of PDE5. However, Ser-102 phosphorylation also directly stimulates the PDE5 catalytic site independent of cGMP binding to the allosteric site [76].

PDE5 is responsible for cGMP hydrolysis in many tissues: vascular smooth muscle, pancreas, kidney, Purkinje neurons, lung, heart and platelets. PDE5 inhibitors sildenafil, vardenafil and tadalafil are highly selective inhibitors used in the treatment of the erectile dysfunction (ED), [77-81] and pulmonary hypertension [82]. PDE5 inhibitors are regulators of vascular smooth muscle.

### 1.4.5 PDE10

PDE10s have dual substrate specificity for cAMP and cGMP [83-85]. One gene, PDE10A encodes six isoforms with differences at their N- and C-termini. PDE10A1 and 2 are the major human isoforms [86]. Crystal structures of the catalytic domain and recently of GAF-B domain with bound cAMP are available [31]. This is the only PDE which is allosterically activated by cAMP via GAF-B [10]. The highest levels of PDE10s are in the brain, testis, thyroid, pituitary gland and heart [83, 84, 87-89].

### 1.4.6 PDEs in cNMP signaling compartments

The new concept in understanding of cNMP signaling is that cNMPs cannot diffuse freely in the cell. In this hypothesis PDEs have an important role and together with protein kinases (or other effector proteins) establish microdomains of discrete subcellular compartments.

This hypothesis originated from work on cardiac myocytes but since then has been extended to other cell types and confirmed by fluorescence-resonance-energy-transfer (FRET) used to visualize spatial and temporal gradients of cAMP [29, 66-68].

cAMP is localized in pools below the plasmamembrane near the site of synthesis and at sufficient concentrations for PKA activation. PDEs are anchored to specific scaffold proteins and spatially restrict these cAMP pools.

## 1.5 Class III Adenylyl cyclases

Adenylyl cyclases catalyze the synthesis of cAMP from ATP. Based on the sequence similarities, they are grouped into six classes (I-VI).

Class III AC is wide spread, present in eukaryotes as well as in prokaryotes, and studied well [1, 2, 90, 91]. It is further subdivided into four classes IIIa-IIId [90]. The catalytic domain of these ACs is often linked to different protein domains with regulatory properties: PAS, GAF,

BLUNT, histidine kinase receiver and some cation channels. In mammals, AC III is a pseudoheterodimer with a single catalytic pocket, and in prokaryotes and lower eukaryotes, AC III proteins homodimerize with two catalytic pockets.

Cyanobacteria are a group of prokaryotes known as blue-green algae. The cyanobacterium *Anabaena sp. PCC 7120* has six genes which encode different AC isoenzymes [1, 7, 90] As already mentioned tandem GAF domains from CyaB1 and CyaB2 are closely related to tandem GAF domains from mammalian PDEs. CyaB1 AC is a homodimer in which cAMP binding to GAF-B activates the catalytic domain and increases the cAMP production [7]. That is an autoactivating feed-forward mechanism.

## 1.6 Aim of work

According to previous results from our laboratory the catalytic domain of CyaB1 AC can be regulated by the tandem GAF domains of mammalian PDEs. In this way CyaB1 AC served as a reporter for tandem GAF domains from hPDE2, 5, 10 and 11 [7, 9-13].

Chimeras of different human PDE`s N-terminal domains and CyaB1 AC were prepared and employed as a tool to study the role of these domains in regulation.

This work started with investigations of the role of the N-terminus which precedes the PDE5 GAF-A. According to S. Bruder, a step-wise removal of the N-terminus up to Ser-102 (phosphorylation site) did not affect basal activity and cGMP affinity. Removal of 102 and more aa increased basal activity and caused kind of a disengagement of the GAF domains and AC, since cGMP could not activate the reporter any more [11]. The questions I tried to answer were:

- How does the regulation of the catalytic domain change when 89, 91 and 95 aa are removed from the N-terminus?
- Are PDE5-CyaB1 AC chimeras optimally linked, since in all constructs we made, the end of PDE5 GAF-B domain was Glu-513? The linker between PDEs and AC is a short α-helix.

Work was continued with attempts to crystallize PDE5 tandem GAF domain.

Further experimental work is divided into two parts.

First, different mutations were made in the α-helical linker between GAF domains in PDE5 and PDE10. The work from K. Hofbauer suggested specific domain interactions within tandem GAF domains which are not visible in crystal structures, since swapping the linkers between PDE5 and PDE10 GAF tandem domains abrogated regulation [12]. It seems that this

linker is directly involved in specific interactions. The questions I tried to answer in this part were following:

- What is the role of the α-helical linker between GAF-A and GAF-B in PDE5 and 10 in transmitting the signal from the N-terminus to the catalytic domain?
- Which aa are responsible for the loss of regulation in PDE10-CyaB1 AC containing a PDE5 linker?

Second, the role of N-terminal tandem domains from PDE1s and long PDE4s in CyaB1 AC regulation was examined. Different isoforms were used: PDE1A3 and B1 and of PDE4D3, A4 and B1. I tried to answer the questions:

- Can tandem N-terminal regulatory domains from PDE1A3 and B1 and from PDE4A4, B1 and D3 functionally couple with the catalytic domain of CyaB1 AC?
- Long PDE4s are activated by PKA phosphorylation of serine at the beginning of UCR1. Does phosphomimetic mutation of the respective Ser to Asp in chimeras have the same effect?
- Can phosphatidic acid activate PDE4D3-CyaB1 AC chimeras?
- What is the role of the N-terminus ahead of UCR1 in PDE4D3?

At the end, the additional question can be formulated:

- Is there a similar mechanism for the regulation of all PDEs despite differences in the primary structure, since they have the same overall structural arrangement?

# 2 Materials and equipments

Only those suppliers are listed whose products were very important for the replication of the experiments described herein.

## 2.1 Chemicals and materials

**AGS, Heidelberg:** Restriction Endonucleases with their 10×reaction buffer

**Amersham Biosciences, Freiburg** (2,8-$^{3}$H)-cAMP (ammonium salt), *ECL Plus Western Blotting Detection System, Hyperfilm ECL*, Formamide, *Thermosequenase Primer Cycle Sequencing Kit*

**Applied Biosystems, California, USA:** *BigDye Terminator Cycle Sequencing Kit Version 3.1* with *HiDi*

**BIO-RAD, München:** *BIO-RAD Protein Assay-reagent*, *Profinity$^{TM}$ IMAC Ni-Charged Resin*

**Dianova, Hamburg:** Secondary goat-anti-mouse IgG horseradish peroxidase conjugated antibodies

**Finnzymes, Espoo (Finnland):** *Phusion High-Fidelity* PCR kit with *Phusion* DNA Polymerase and 5×HF/GC buffer

**Fluka BioChemika, Buchs (Switzerland):** Glucose, PEG 1000, SDS

**Hampton Research, Aliso Viejo (USA):** *Crystal Screen, Crystal Screen 2, Crystal Screen Lite*, VDX 24-well crystallization plates, siliconized cover slides, reagent kits for protein crystallization screening, PEG 400, PEG 3350, PEG 8000

**Hartmann Analytik, Braunschweig:** ($\alpha$-$^{32}$P)-ATP

**Invitrogen, Karlsruhe**: *pRSET-A*-expression vector, *DH5α* cells

**Macherey-Nagel, Düren:** *Nucleotrap*-Kit, *PCR clean-up Gel extraction*, *Porablot PDVF*-blotting membrane (2µm pore size)

**Millipore, Molsheim (France):** Concentrators *Amicon Ultra-15 (Ultracel-5k)* and *ULTRAFREE-0.5*

**New England Biolabs (NEB), Frankfurt/Main:** BSA 100×(10 mg/ml) for molecular biology, Restriction Endonucleases with 10×reaction buffers, *T4*-Polynucleotide Kinase and 10×kinase buffer

**Novagen R&D systems, Wiesbaden:** *pET16b*-expression vector, *PETDuet-1*-expression vector, *E. coli BL-21(DE3)-[pREP4]* cells, *E.coli BL21 Rosetta (pLysS)* cells

**Pall Life Sciences, Ann Arbour (USA):** *NANOSEP 10k OMEGA* centrifugal devices

**PEQLAB Biotechnologie, Erlangen:** peq Gold-Agarose, peq Gold Protein-Marker, dNTP`s, *KAPAHiFi* ™ Proofreading DNA Polymerase

**Promega, Madison (USA):** *Wizard Plus Minipreps* and *Wizard Plus SV Minipreps, Pfu*-DNA-Polymerase with 10×reaction buffer, *T4*-DNA-Ligase

**Qiagene, Hilden:** $Ni^{2+}$*-NTA Agarose*, *pQE30*, *pQE60* and *pQE80*- expression vectors, *pREP4*, mouse monoclonal *RGS-His*$_4$ antibody, *Tetra-His* antibody, *Taq*-DNA-polymerase with 10×reaction buffer

**Roche Diagnostics, Mannheim:** Alkaline phosphatase, λ-DNA, Restriction Endonucleases with 10×buffers, Klenow-Polymerase, *Rapid DNA Ligation Kit*, ATP, dNTP`s, *Complete EDTA-free* protease inhibitor tablets, Proteins for chromatography (aldolase, katalase, albumin, Cyt c, chymotrypsinogen, ferritin)

**Roth, Karlsruhe:** Brilliant Blue R250 and G250, Ampicillin, Kanamycin, Chloramphenicol, Agarose *Rotigarose*

**Sartorius, Göttingen:** Cellulose-Nitrate-Filter (0.2 µm and 0.45 µm), concentrators *Vivaspin 2* (10.000 MWCO PES)

**Serva, Heidelberg:** Coomassie-Brilliant Blue G250, *VISKING dialysis tubing 8/32* (∅6 mm) and *27/32* (∅21 mm), Polyethylenglycol

**Stratagene, Heidelberg:** *pBluescript II SK (-)* cloning vector, *E.coli XL1 Blue*-cells

**Süd-Laborbedraf GmbH, Gauting:** *Hi Yield* Gel/PCR DNA Fragments Extraction Kit

**Vivascience, Hannover:** Vivaspin 500 µl and 2 ml (for protein concentration)

## 2.2 Equipments

**Amersham Pharmacia, Freiburg:** *ÄKTA* FPLC with fraction collector *frac-950*, Gel filtration column *Supradex 200 10/30*, *Liquid Scintillation Counter Rockbeta 1209* (LKB Wallac)

**Applied Biosystems, California, USA:** Capillary electrophorese *System ABI 3130×1*

**BIO-RAD München:** Blotting apparatus *Trans-Blot SD Semi-dry Transfer Cell*

**GE Healthcare, München:** *HiLoad 16/60 Superdex 200 prep grade*

## 2.3 Buffers and Solution

For all buffers and solutions MilliQ water was used. pH values were adjusted at RT, unless indicated otherwise.

### 2.3.1 Buffers and solutions for molecular biology

All solutions and buffers for molecular biology methods were sterile-filtered or autoclaved.

***Solutions for DNA***

*TAE-buffer*
40 mM Tris/Acetate pH 8.0
1 mM EDTA

*TE buffer*
10 mM Tris/HCl pH 7.5
1 mM EDTA

*10xKlenow buffer*
200 mM Tris/HCl pH 7.9
60 mM $MgCl_2$
10 mM Dithiothreitol

*10xTBE buffer (LI-COR)*
1.34 mM Tris
440 mM Boric acid
25 mM EDTA

*4xLoading sample buffer (BX)*
0.5% Bromophenol blue
0.5% Xylencyanol
5% Glycerol
1× TAE

*dNTP's*
20 mM of each dNTP

*10xdephosphorylation buffer*
500 mM Tris/HCl pH 8.5
1 mM EDTA

*10xCM buffer*
100 mM $CaCl_2$
400 mM $MgCl_2$

***Solutions for blue/white selection***

*IPTG*
1 M IPTG in $H_2O$

*X-GAL*
20 mg/ml in Dimethylformamide

***Solutions for bacterial culture media***

*LB-agar plates*
35 g/L LB Agar (powder)

*LB-Medium*
20 g/L LB Broth (powder)

*LB-Medium for permanent cultures*
20 g/l LB Broth (powder)
28.7% Glycerol (w/w)

### 2.3.2 Buffers and solutions for protein chemistry

***SDS-PAGE gel electrophoresis***

*Resolving gel buffer*
1.5 M Tris/HCl pH 8.8
0.4% SDS

*Stacking gel buffer*
500 mM Tris/HCl pH 6.8
0.4% SDS

*10xelectrophoresis buffer*
25 mM Tris
192 mM Glycin
0.1% SDS

*Coomassie staining solution*
0.1% Brilliant Blue R250
40% Methanol
1% Acetic acid

*4xsample buffer*
130 mM Tris/HCl pH 6.8
10% SDS
20% Glycerol
0.06% Bromophenol blue
10% β-Mercaptoethanol

*Destaining solution*
10% Acetic acid
30% Ethanol

***Western Blot***

*TBS buffer (Tris Buffer Saline)*
20 mM Tris/Cl pH 7.6
140 mM NaCl

*Ponceau S staining solution*
0.1% (w/v) Ponceau S
5% Acetic acid

*TBS-T*
0.1 % Tween 20 in TBS buffer

*M-TBS-T*
5% Milk powder in TBS-T Buffer

*Towbin- Blot buffer*
25 mM Tris/HCl
192 mM Glycin
20 % Methanol

*Primary antibody*
RGS-$His_4$-antibody
0.04-0.2 µg/ml in M-TBS-T

Tetra-His antibodies
0.1 µg/ml in M-TBS-T

Secondary antibody
Goat anti-mouse antibody (polyclonal) conjugated with horseradish peroxidise diluted 1:5000 in M-TBS-T

***Cell harvesting, cell lysis and protein purification***

pH-values were adjusted at 4°C (pH of imidazole was 8.5). For protein purifications the following buffers were used (optimal conditions are listed):

*Pellet wash buffer*
50 mM Tris/HCl pH 8.5
1 mM EDTA

*Cell lysis buffer*
50 mM Tris/HCl pH 8.5
20 % Glycerol
50 mM NaCl
±7.5-40 mM Imidazole
*Complete-EDTA-free-protease-inhibitor* from Roche (1 tablet/50 ml)
(optional 10 mM Thioglycerol/2-Mercaptoethanol)

*Elution buffer*
50 mM Tris/HCl pH 8.5
20% Glycerol
10/50 mM NaCl (optional)
300 mM Imidazole
2 mM $MgCl_2$

*Dialysis buffer (for protein storage at -20°C)*
50 mM Tris/HCl pH 8.5
10 mM NaCl
2 mM $MgCl_2$
10%/35% Glycerol (10% for fractionation of PDE4A4-CyaB1)

*Dialysis buffer (after hydrophobic interaction chromatography)*
100 mM Tris/HCl pH 7.5
10 mM NaCl
2 mM $MgCl_2$

*Shortened PDE5 A89-/N91-/G95-CyaB1 AC*
(pH of all buffers is 8.5)

*Equilibration mixture for $Ni^{2+}$-NTA agarose*
250 mM NaCl
5 mM $MgCl_2$
15 mM Imidazole

*Wash buffer A*
50 mM Tris/HCl pH 8.5
400 mM NaCl
2 mM $MgCl_2$
20% Glycerol
5 mM Imidazole

*Wash buffer B*
Wash buffer A + 15 mM Imidazole

*Wash buffer C*
Wash buffer A + 25 mM Imidazole + 10 mM NaCl

*PDE5 L136-A517 (cryst.)*
(pH of buffers 8 or 8.5)

*Equilibration mixture for $Ni^{2+}$-NTA/ $Ni^{2+}$-IDA agarose I*
250 mM NaCl
5 mM $MgCl_2$
(±15 mM Imidazole pH 8/8.5)

*Equilibration mixture for $Ni^{2+}$-NTA/ $Ni^{2+}$-IDA agarose II*
Cell lysis buffer
(±10/15/30 mM Imidazole pH 8/8.5)

Different concentrations of imidazole (5-75 mM) and NaCl (400 mM/10 mM) have been used in wash buffers.

*Wash buffer A/B*
50 mM Tris/HCl pH 8/8.5
400 mM NaCl
2 mM $MgCl_2$
20% Glycerol
5-75 mM Imidazole

*Wash buffer C*
Wash buffer A + 25-75 mM Imidazole + 10 mM NaCl

*PDE5 NAAIRS-CyaB1 AC*
(pH of all buffers is 8.5)

*Equilibration mixture for $Ni^{2+}$-IDA*
0.75 ml Cell lysis buffer (+ 7.5 mM Imidazole)

*Wash buffer A*
50 mM Tris/HCl pH 8.5
400 mM NaCl
2 mM $MgCl_2$
20% Glycerol
35 mM Imidazole

*Wash buffer B*
Wash buffer A + 70 mM Imidazole

*Wash buffer C*
Wash buffer A + 70 mM Imidazole + 10mM NaCl

*PDE10- (constructs No.1-22)* and WT PDE10-CyaB1 AC*
(pH of all buffers is 8.5)

*Equilibration mixture for $Ni^{2+}$-IDA agarose*
400 mM NaCl
5 mM $MgCl_2$
25 mM Imidazole

*Wash buffer A*
50 mM Tris/HCl pH 8.5
400 mM NaCl
2 mM $MgCl_2$
20% Glycerol
35 mM Imidazole

*Wash buffer B*
Wash buffer A + 55 mM Imidazole

*Wash buffer C*
Wash buffer A + 75 mM Imidazole + 10 mM NaCl

*- The list of constructs is in Appendix (p.117)

*PDE5- (No.23) and WT PDE5-CyaB1 AC*
(pH of all buffers is 8.5)

*Equilibration mixture for $Ni^{2+}$-NTA (No.23)*
250 mM NaCl
5 mM $MgCl_2$
15 mM Imidazole

*Equilibration mixture for $Ni^{2+}$-IDA (WT PDE5)*
Cell lysis buffer (7.5 mM Imidazole)
400 mM NaCl

*Wash buffer A*
50 mM Tris/HCl pH 8.5
400 mM NaCl
2 mM $MgCl_2$
20% Glycerol
7.5 mM Imidazole

*Wash buffer B*
Wash buffer A + 15 mM Imidazole

*Wash buffer C*
Wash buffer A + 25 mM Imidazole + 10 mM NaCl

*PDE1A3- (A, B and C) and PDE1B1-CyaB1 AC (D, E and F)*
(pH of all buffers is 8.5)

*Equilibration mixture for $Ni^{2+}$-IDA agarose (for A, B, C)*
400 mM NaCl
5 mM $MgCl_2$

*Wash buffer A*
Cell lysis buffer

*Wash buffer B*
Cell lysis buffer + 20 mM Imidazole

*Equilibration mixture for $Ni^{2+}$-IDA agarose (for D, E, F)*
400 mM NaCl
5 mM $MgCl_2$
15 mM Imidazole

*Wash buffer C*
50 mM Tris/HCl pH 8.5
400 mM NaCl
2 mM $MgCl_2$
20% Glycerol
10 mM Thioglycerol
20 mM Imidazole

*Wash buffer D*
Wash buffer C + 20 mM Imidazole + 50 mM NaCl

*PDE4D3-CyaB1 AC (I-IV)*
(pH of all buffers is 8.5)

*Equilibration mixture for $Ni^{2+}$-NTA agarose*
400 mM NaCl
5 mM $MgCl_2$
40 mM Imidazole

*Wash buffer A*
50 mM Tris/HCl pH 8.5
400 mM NaCl
2 mM $MgCl_2$
20% Glycerol
60 mM Imidazole

*Wash buffer B*
Wash buffer A + 60 mM Imidazole + 10 mM NaCl

*PDE4A4- (V and VI) and PDE4B1-CyaB1 AC (VII and VIII)*
(pH of all buffers is 8.5)

*Equilibration mixture for $Ni^{2+}$-IDA*
400 mM NaCl
5 mM $MgCl_2$
40 mM Imidazole (without imidazole for VII and VIII)

*Wash buffer A (V and VI)*
50 mM Tris/HCl pH 8.5
400 mM NaCl
2 mM $MgCl_2$
20% Glycerol
60 mM Imidazole

*Wash buffer B*
Wash buffer A + 60 mM Imidazole + 10 mM NaCl

*Wash buffer C (VII and VIII)*
Cell lysis buffer

*Wash buffer D*
Cell lysis buffer + 20 mM Imidazole

***Adenylyl cyclase assay***

*2×AC-Cocktail*
43.5% Glycerol
100 mM Tris/HCl pH 7.5
1 mg/ml BSA
20 mM $MgCl_2$

*ATP Stock Solution*
5 mM pH 7.5 (adjusted with Tris)

*cAMP or cGMP Stock solution*
40 mM pH 7.5 (adjusted with Tris)

*10×ATP-substrat solution*
750 µM ATP pH 7.5
Inkl.16-30 kBq ($\alpha$-$^{32}$P)-ATP

*$^{3}$H-cAMP internal standard*
20 mM cAMP
10-20 kBq/ml (2,8-$^{3}$H-cAMP)

*AC Stop buffer*
3 mM cAMP/Tris pH 7.5
3 mM ATP
1.5 % SDS
pH adjusted to 7.5 with Tris

***Buffers for chromatography***

In all buffers MilliQ water was used; all buffers were filtrated (0.2 µm).

*Buffers for hydrophobic interaction chromatography*

*Equilibration buffer*
0.05 M Tris/HCl pH 7.5
1 mM 2-Mercaptoethanol
0.1 mM $CaCl_2$

*Wash buffer*
0.05 M Tris/HCl pH 7.5
1 mM 2-Mercaptoethanol
0.1 mM $CaCl_2$
0.5 M NaCl

*Elution buffer*
0.05 M Tris/HCl pH 7.5
1 mM 2-Mercaptoethanol
2 mM EGTA

*Buffers for anion exchange chromatography*

*Buffer A - equilibration buffer (start buffer)*
50 mM Tris/HCl pH 7.5
10% Glycerol
2 mM $MgCl_2$

*Buffer B*
Buffer A+ 1M NaCl

*Buffer for gel filtration chromatography*

*Buffer A*
100 mM Tris/HCl pH 7.5
150 mM NaCl

***Crystallization***

10% Glycerol
Tris/HCl pH 7.5 10 mM
1 mM $MgCl_2$
90% Thioglycerol

## 2.4 Oligonucleotides

### 2.4.1 Cloning primers

Restriction sites are in small letters, mutations in bold, inserted bases underlined; All numberings are according to bp position in holoenzymes (Tables 2.1)
s-sense primer, as-antisense primer;

***Cloning primers for PDE5 A89-/N91-/G95-CyaB1 AC chimeras***

| Name | Position in template (bp) | Sequence (5`-3`) | Description |
|---|---|---|---|
| P5A89BglIIs | 264-285 (PDE5) | AAA aga tct GCA GAT AAC AGT GTC CCT GGA | Bgl II |
| P5N91BglIIs | 271-291 (PDE5) | AAA aga tct AAC AGT GTC CCT GGA ACA CCA | Bgl II |
| P5G95BglIIs | 283-304 (PDE5) | AAA aga tct GGA ACA CCA ACC AGG AAA ATC | Bgl II |
| P5XbaIas | 1020-1037 (PDE5) | AAA tct aga GAT TGT TGT TCT TCA AAA | Xba I (from S.Bruder) |

***Cloning primers for PDE5 NAAIRS-CyaB1 AC chimera***

| Name | Position in template (bp) | Sequence (5`-3`) | Description |
|---|---|---|---|
| P5NAAIRSs (II) | 1162-1180 (PDE5) | GTG GAG AAT GCT GCT ATA CGA TCG AAA CAA TAT CAA AAA GAC | Inserted NAAIRS aa |
| P5NAAIRSas | 1525-1540 (PDE5) | CGA TCG TAT AGC AGC ATT CTC CAC TGC TTC ATA | Inserted NAAIRS aa |
| P5BglIIs | 1-18 (PDE5) | AAA aga tct ATG GAG CGG GCC GGC CCC | Bgl II |
| ACEnd SmaIas | 2613-2632 (CyaB1 AC) | TTT ccc ggg CTG CAG GAA TTC ACT | Sma I |

***Cloning primers for PDE10-CyaB1 AC chimeras (constructs No.1-22)***

For all PDE10-CyaB1 AC constructs with linker mutations, fusion PCR was performed with BamHI G73 PDE10 (s) and PDE11 Mfe (as) as end primers.

| **Name** | **Position in template (bp)** | **Sequence (5`-3`)** | **Description/ introduced mutations/inserted aa** |
|---|---|---|---|
| BamHI G73 PDE10 | 180-198 (PDE10) | AAA gga tcc GGA GTT GTA TAT GAA CTA | BamHI (from K. Hofbauer) |
| MfeI PDE11as | 1339-1363 (CyaB1) | TTT caa ttg GTA CAA TTT CCC AAA | MfeI (from M. Gross-Langenhoff) |
| PDE5/10 1as | 646-675 (PDE10) | CAC CTG ATG TAT TGC **AAT ACC** AGC CCA GGC | GI |
| PDE5/10 2s | 646-675 (PDE10) | GCC TGG GCT **GGT ATT GTT CTT** CAT CAG GTG | GIVL |
| PDE5/10 3as | 660-693 (PDE10) | AAG GCC TCT GCA TAC CTG **AGC ATT** ATG AAG AAC | NA |
| PDE5/10 4s | 660-693 (PDE10) | GTT CTT CAT **AAT GCT** CAG **CTC TAT** AGA GGC CTT | NALY |
| PDE5/10 5as | 675-705 (PDE10) | TGT CTG TTT GGC AAG **AGT CTC** ATA GAG CTG | ET |
| PDE5/10 6s | 675-705 (PDE10) | CAG CTC TAT **GAG ACT TCA CTG** AAA CAG ACA | ETSL |
| PDE5/10 7as | 687-717 (PDE10) | GTC ATT CAA TTC TGT **CTC CAG** CAG TGA ATG | LE |
| PDE5/10 8s | 687-717 (PDE10) | ACT TCA CTG **CTG GAG AAC AAG** TTG AAT GAC | LENK |
| PDE5/10 9as | 699-729 (PDE10) | GTC GAG TAG GAA GTC ATT **TCT** CTT GTT CTC | R |
| PDE5/10 10s | 699-729 | GAG AAC AAG **AGA** AAT **CAG GTG** CTA CTC GAC | RQV |
| PDE5/10 11as | 720-750 (PDE10) | ATC AAA ATA TGT TTT **AGC AAG** GTC GAG TAG | LA |
| PDE5/10 12s | 720-750 (PDE10) | CTA CTC GAC **CTT GCT AGT TTA** TAT TTT GAT | LASL |
| PDE5/10 13as | 731-762 (PDE10) | TGC AAC TAT GTT ATC AAA **AAT TAA** ACT AGC | I |
| PDE5/10 14s | 731-762 (PDE10) | GCT AGT TTA **ATT** TTT **GAA GAA** ATA GTT GCA | IEE |
| PDE5/10 15as | 744-771 (PDE10) | AGA ATC TAT TGC **TTG TTG** TTC TTC AAA | QQ |
| PDE5/10 16s | 744-771 (PDE10) | TTT GAA GAA **CAA CAA TCT** ATA GAT TCT | QQS |
| PDE10LYs | 669-696 (PDE10) | CAG GTG CAG **CTC TAT** AGA GGC CTT GCC | LY |
| PDE10LYas | 669-696 (PDE10) | GGC AAG GCC TCT **ATA GAG** CTG CAC CTG | LY |
| PDE10Ls | 669-696 (PDE10) | CAG GTG CAG **CTC** TGC AGA | L |

| | | | |
|---|---|---|---|
| | | GGC CTT GCC | |
| PDE10Las | 669-696 (PDE10) | GGC AAG GCC TCT GCA **GAG** CTG CAC CTG | L |
| PDE10Ys | 669-696 (PDE10) | CAG GTG CAG GTA **TAT** AGA GGC CTT GCC | Y |
| PDE10Yas | 669-696 (PDE10) | GGC AAG GCC TCT **ATA** TAC CTG CAC CTG | Y |
| inPDE10s | 747-771 (PDE10) | gct cag ctc tat gag act tca ctg ctg gag aac aag aga aat cag gtg ctg ctt gac ctt gct agt tta att ttt GAT AAC ATA GTT GCA ATA GAT TCT | Inserted aa from PDE5 K298-F341 |
| inPDE10as | 591-615 (PDE10) | cag cag tga agt ctc ata gag ctg agc att atg aag aac aat acc aca aaa tgc caa ata agc agc aaa gtc ctt ttc atc ttt AAG ACA GAA GGC TTC TTT GCC CCA | Inserted aa from PDE5 K298-F341 |
| No.3+Ls | 669-696 (PDE10) | AAT GCT CAG **CTC** TGC AGA GGC CTT GCC | L |
| No.3+Las | 669-696 (PDE10) | GGC AAG GCC TCT GCA **GAG** CTG AGC ATT | L |
| No.3+Ys | 669-696 (PDE10) | AAT GCT CAG GTA **TAT** AGA GGC CTT GCC | Y |
| No.3+Yas | 669-696 (PDE10) | GGC AAG GCC TCT **ATA** TAC CTG AGC ATT | Y |

***Cloning primers for PDE5, PDE10 (S218-F261)-CyaB1 AC chimera (construct No.23)***

| **Name** | **Position in template (bp)** | **Sequence (5`-3`)** | **Description** |
|---|---|---|---|
| in PDE5s | 867-891 (PDE5) | cag gtg cag gta tgc aga ggc ctt gcc aaa cag aca gaa ttg aat gac ttc cta ctc gac gta tca aaa aca tat ttt GAA GAA CAA CAA TCT CTA GAA GTA | Inserted aa from PDE10 S218-F261 |
| in PDE5as | 1023-1047 (PDE5) | ttt ggc aag gcc tct gca tac ctg cac ctg atg tat tgc tac tga agc cca ggc aag att tgc tgt tgc aac ctc ctg gtg act TTC AGT AAA TGT CCC ACC GTT TCC | Inserted aa from PDE10 S218-F261 |
| PDE5BglIIs | 1-18 (PDE5) | AAA aga tct ATG GAG CGG GCC GGC CCC | BglII (from S. Bruder) |
| MfeI PDE11as | 1339-1363 (CyaB1) | TTT caa ttg GTA CAA TTT CCC AAA | MfeI (from M. Gross-Langenhoff) |

***Cloning primers for PDE1A3- and PDE1B1-CyaB1 AC chimeras (A-F)***

| Name | Position in template (bp) | Sequence (5`-3`) | Description |
|---|---|---|---|
| PDE1A3BamHIs | 1-18 (PDE1A3) | AAA gga tcc ATG GGG TCT ATG GCC ACA | BamHI |
| PDE1A3 XhoI M178as | 513-534 (PDE1A3) | AAA ctc gag AAA CTT CAG ACT ATG CTC TCC | XhoI |
| PDE1A3 XhoI L206as | 598-619 (PDE1A3) | AAA ctc gag AGC TTC TGC AAA GGT GAT TAG | XhoI |
| PDE1A3 XhoI M234as | 682-702 (PDE1A3) | AAA ctc gag TAT GTA ATG CAC AGT TTG AGT | XhoI |
| PDE1B1BamHIs | 1-18 (PDE1B1) | AAA gga tcc ATG GAG CTG TCC CCC CGC | BamHI |
| PDE1B1 SalI T182s | 526-547 (PDE1B1) | AAA gtc gac GGT CCT CAG GGC ATG GTC ATC | SalI |
| PDE1B1 SalI A210s | 610-631 (PDE1B1) | AAA gtc gac GGC ATC CAG GAA ACT CAT CAA | SalI |
| PDE1B1 SalI F238s | 693-714 (PDE1B1) | AAA gtc gac GAA GCA ATG GAC TGT CTG GGT | SalI |

***Cloning primers for PDE4D3-CyaB1 AC chimeras (I-IV) and PDE4D3 UCR1/2 cryst.***

| Name | Position in template (bp) | Sequence (5`-3`) | Description /inserted aa |
|---|---|---|---|
| PDE4D3BglIIs | 1-21 (PDE4D3) | AAA aga tct ATG ATG CAC GTG AAT AAT TTT | BglII |
| PDE4D3XhoIas | 615-636 (PDE4D3) | AAA ctc gag AGA AGG AAT TTC CAC TTC ATG | XhoI |
| PDE4D3BamHIs | 117-138 (PDE4D3) | AAA gga tcc CTA ATT CTC CAA GCA AAT TTT | BamHI |
| PDE4D3SfuIs | 147-168 (PDE4D3) | AAA ttc gaa CAA CGA CGG GAG TCC TTC CTG | SfuI |
| PDE4D3HincIIs | 144-174 (PDE4D3) | AAA gtc aac GAC GGG AG**G AC**T TCC TGT ATC GA | HincII |
| PDE4D3SfuIS54Ds | 147-168 (PDE4D3) | AAA ttc gaa CAA CGA CGG GAG **GAC** TTC CTG TAT CGA | SfuI |
| PDE4D3NcoI(pET16b)s | -6-12 (PDE4D3-CyaB1,pQE30) | AAA acc atg GGA TCT ATG ATG CAC GTG | NcoI |
| PDE4D3BglII(pET16)as | 2040-2058 (PDE4D3-CyaB1,pQE30) | AAA aga tct CTT TGT GAA AAT TGT CCA | BglII |
| PDE4D3BglIIs cryst | 1-18 (PDE4D3) | AAA aga tct GAG AAC TTA TAC TTC CAG GGA ATG ATG CAC GTG AAT AAT | BglII Tev-rest. site ENLYFQG |
| PDE4D3HindIIIas cryst | 616-636 (PDE4D3) | AAA aag ctt AGA AGG AAT TTC CAC TTC ATG | HindIII |

***Cloning primers for PDE4A4- and PDE4B1-CyaB1 AC chimeras (V-VIII)***

| Name | Position in template (bp) | Sequence (5`-3`) | Description |
|---|---|---|---|
| PDE4A4BamHIs | 1-21 (PDE4A4) | AAA gga tcc ATG GAA CCC CCG ACC GTC CCC | BamHI |
| PDE4A4 XhoIas | 885-906 (PDE4A4) | AAA ctc gag TGA TGG GAT CTC CAC TTC ATT | XhoI |
| PDE4B1BglIIs | 1-21 (PDE4B1) | AAA aga tct ATG AAG AAA AGC AGG AGT GTG | BglII |
| PDE4B1XhoIas | 849-870 (PDE4B1) | AAA ctc gag AGA TGG GAT CTC CAC ATC ATT | XhoI |
| PDE4A4S145Ds | 421-445 (PDE4A4) | CAG CGC CGG GAG **GAC** TTC CTG TAC | S145D |
| PDE4A4S145Das | 421-445 (PDE4A4) | GTA CAG GAA **GTC** CTC CCG GCG CTG | S145D |
| PDE4B1S133Ds | 420-444 (PDE4B1) | CAG CGC AGA GAG **GAC** TTT CTC TAC | S133D |
| PDE4B1S133Das | 420-444 (PDE4B1) | GTA GAG AAA **GTC** CTC TCT GCG CTG | S133D |
| MfeI PDE 11as | 1339-1363 (CyaB1) | TTT caa ttg GTA CAA TTT CCC AAA | MfeI |

***Cloning primers for PDE5 L136-A517 (cryst.)***

| Name | Position in template (bp) | Sequence (5`-3`) | Description |
|---|---|---|---|
| hPDE5SphIs (cryst) | 406-424 (PDE5) | AA Agc atg cTA ACC CCT CCA AGG TTT | SphI |
| hPDE5BglIIas (cryst) | 1533-1553 (PDE5) | AAA aga tct GGC CAT GGC TCT CTC CAC | BglII |

Tables 2.1: Cloning primers

### 2.4.2 Sequencing primers

Primers used for sequencing with *LI-COR,* were tagged with IRD 800.
Stock concentrations of all primers were 5 µM (Tables 2.2).

| Name | Direction | $T_{annealing}$ | Sequence (5`-3`) | Position (bp) | Description |
|---|---|---|---|---|---|
| T3 | s | 56°C | aat taa ccc tca cta aag gg | 772-791 | pBSKII(-) |
| T7 | as | 56°C | taa tac gac tca cta tag gg | 626-646 | pBSKII(-) |
| U-pQE-IR | s | 54°C | gaa ttc att aaa gag gag aaa | 88-108 | pQE30 |
| R-pQE-IR | as | 54°C | cat tac tgg atc tat caa cag g | 212-233 | pQE30 |
| R-800-pET MSC-pQE30 | as | 56°C | acc cct caa gac ccg ttt aga | 5423-5443 | pET16 MCS-pQE30 |
| U-IR-800 CyaB1-PAS2 | s | 56°C | gct tgt cag atg ctg taa ttt c | 1190-1211 | CyaB1Holo |

| | | | | | |
|---|---|---|---|---|---|
| R-IR-800 CyaB1-GAF | as | 56°C | act ttt atg att agc atc acc | 1279-1299 | CyaB1Holo |
| U-IR-800 CyaB1-Cat | s | 56°C | gat gcc tta atg gtt ggt g | 1768-1786 | CyaB1Holo |
| U-IR-800 PDE5 GAF | s | 56°C | cat gat gaa ggg gac cag tgc t | 427-448 | PDE5Holo |

For capillary DNA sequencing, it is not necessary that primers are tagged.

| **Name** | **Direction** | **$T_{annealing}$** | **Sequence (5`-3`)** | **Position (bp)** | **Description** |
|---|---|---|---|---|---|
| PAS CyaB1 | s | 56°C | aaa tca gat gct gta att tct aca gat | 1195-1208 | CyaB1Holo |
| PDE10/5Kpn | s | 56°C | gat gaa ggg gac cag tgc | 430-447 | PDE5Holo (from K.Hofbauer) |
| PDE5 D488A | s | 56°C | atg **ccg** aac agt ttc tgg **agg** ctt ttg tca tc | 1460-1481 | PDE5Holo (from S. Bruder) |
| PDE5 D299A | s | 56°C | act gaa aaa gct gaa aag gac ttt gc | 886-903 | PDE5Holo (from S. Bruder) |
| Sma ACend | as | 56°C | ccc ggg ctg cag gaa ttc act | 2612-2632 | CyaB1Holo |
| CyaB1 end | s | 56°C | tca gca tta gat atg cgc caa | 2017-237 | CyaB1Holo |
| pETDuet down 1 | as | 56°C | cga tta tgc ggc cgt gtacaa | 273-294 | pETDuet |
| pETDuet up 2 | s | 56°C | ttg tac acg gcc gca taa tcg | 273-294 | pETDuet |
| PDE10 SalI | as | 56°C | gcg aat tct atg ata cat att | 1245-1266 | PDE10Holo |

Tables 2.2: Sequencing primers

## 2.5 Plasmids

pBluescript (II)SK (-), Stratagene
pQE30, pQE60, pQE70, pQE82 Qiagen
pRSET A, Invitrogen
pETDuet-1, pET16b Novagen
Descriptions are on respective homepages. Some vectors were developed further by Anita Schultz to improve cloning and expression properties. These were:

1) PET16b with MCS pQE30, cloning and expression vector (5634bp)

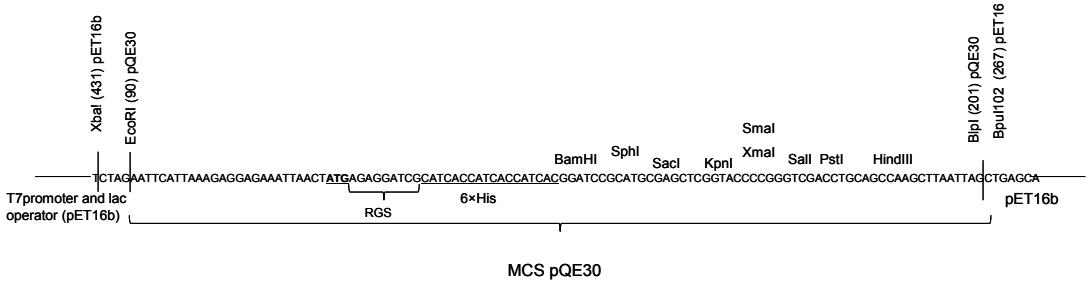


pET16b MCS-pQE30

2) PET16b with MCS pQE60, cloning and expression vector (5599bp)

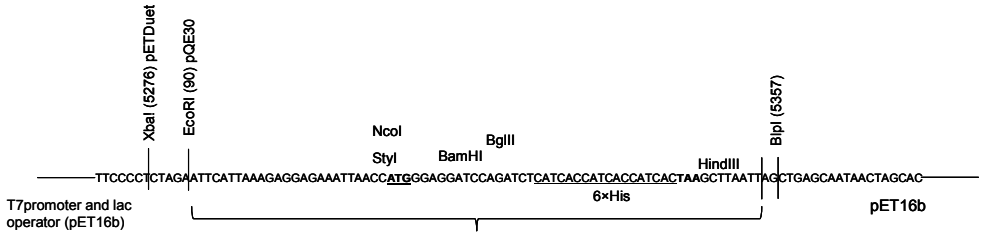


pET16b MCS-pQE60

3) PETDuet-1 with MCS pQE30, cloning and expression vector (5393bp)

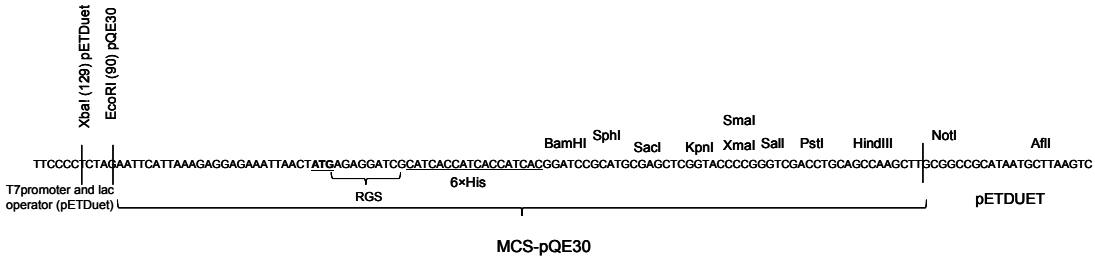


pETDuet MCS-pQE30

## 2.6 Bacterial strains

*E.coli XL1 Blue*, Stratagene
*E.coli DH5α*, Invitrogen
*E.coli BL-21 (DE3) [pREP4],* Novagen
*E.coli BL21 Rosetta (pLysS)*, Novagen
Their genotypes, antibiotic resistance and other characteristics can be found on homepages of the respective companies.

# 3 Methods

## 3.1 Molecular biology methods

***Plasmid isolation from E.coli***

LB-medium (5 ml) inoculated from a permanent cell culture or with a single clone from an agar plate was incubated with antibiotics (depending on the strain) overnight at 37°C, shaking. The cell culture was pelleted and the plasmid was purified using *Wizard Plus Minipreps DNA Purification* kits according to the manufacturer`s protocol. Plasmid-DNA was eluted with 50-100 µl water. In some cases phenol-chloroform extraction was used for further purification and than 50-70 µl TE-buffer was used for the elution. DNA was stored at 4°C or -20°C.

***Polymerase chain reaction (PCR)***

In PCR, DNA polymerase amplifies certain DNA fragment using specific primers. In this way introduction of point mutations, restriction sites as well as insertion or deletion of aa was possible.

A PCR tube contained in 50 µl:

DNA template 1-10 ng (after plasmid isolation)

0.5 µM s and as primer

0.2 mM dNTP`s

10 µl buffer 5×

1U Taq / Kappa / Phusion / 1.75U Pfu polymarase

(optional 3-5% DMSO for GC-rich sequences)

Negative controls contained water instead of template DNA. Different DNA-polymerases were used according to the manufacturer's protocol (Tables 3.1).

Temperature program for Taq and Pfu polymerase:

| *Phase* | *T(°C)* | *Time* | |
|---|---|---|---|
| *Denaturation (hold)* | 95 | 5 min | |
| *Denaturation* | 95 | 1 min | 25-30 cycles |
| *Primer annealing* | Tm | 1 min | |
| *Elongation* | 72 | 1min/1kb | |
| *Final elongation (fill up)* | 72 | 10 min | |
| *End (cooling)* | 4 | | |

Temperature program for κ polymerase:

| *Phase* | *T(°C)* | *Time* | |
|---|---|---|---|
| *Denaturation (hold)* | 95 | 2 min | |
| *Denaturation* | 98 | 20s | 25-30 cycles |
| *Primer annealing* | Tm | 15s | |
| *Elongation* | 68 | 30s/1kb | |
| *Final elongation (fill up)* | 68 | 5 min | |
| *End (cooling)* | 4 | | |

Temperature program for Phusion polymerase:

| *Phase* | *T(°C)* | *Time* | |
|---|---|---|---|
| *Denaturation (hold)* | 98 | 30s | |
| *Denaturation* | 98 | 10s | 25-30 cycles |
| *Primer annealing* | Tm | 30s | |
| *Elongation* | 72 | 30s/1kb | |
| *Final elongation (fill up)* | 72 | 5-10 min | |
| *End (cooling)* | 4 | | |

Tables 3.1: PCR-programs

The annealing temperature was calculated according to the formula:

Tm (C°) = 2·(AT) + 4·(GC)

AT and GC are the number of AT and GC pairs in the primer sequence; the lower Tm was used in cases where the annealing temperatures were different.

A temperature gradient was used for annealing of longer primers. 5 cycles were run at a 5-7°C lower temperature followed by 20-25 cycles at the calculated Tm.

Sense and antisense primers often contained unique restriction sites used later in cloning and at least 20 bp complementary to the DNA template in each direction. When a unique restriction site was not available or feasible, a fusion PCR was used for introduction of mutations.

In fusion PCR, two separate PCR reactions (PCR1 and PCR2) were carried out each with its pair of primers. The as primer of PCR1 and the s primer of PCR2 were overlapping by 20-25 bp. PCR1 and PCR2 products were purified from the gel and used as new templates for a third PCR reaction which fuses two DNA fragments into one.

Test tube for a fusion PCR contained (50 µl):

DNA template PCR1 10-30 ng

DNA template PCR2 10-30 ng

0.5 μM s and as primers

0.2 mM dNTP`s

10 μl κ buffer ($MgSO_4$ included)

κ polymerase 1U

or with 1U Pfu polymerase the same 50 μl sample as above except with 30-100 ng of PCR1 and PCR2 template DNA product.

***Agarose gel electrophoresis***

The agarose gel (0.6-2%) was placed in electrophoresis chamber in TAE buffer. DNA samples (10-20 μl) mixed with loading sample buffer were applied and run at 80-100 V, 30 min at RT. After incubation in EtBr (10 μg/100 ml) for 2 min, electrophoresis was continued for 10-20 min and DNA bands were detected. Under UV light the gel was documented. The size of the product was determined by comparison with a DNA ladder. DNA ladders used are *EcoRI/HindIII* digested λ-DNA (λ-marker) and *MspI/SspI* digested *pBluescript II (-)* (π-marker).

The concentration of agarose gel was dependent on DNA fragment size.

***Purification of DNA fragments from agarose gel***

After DNA gel electrophoresis bands were excised and purified by *NucleoTrap* or *Hi Yield* DNA purification kit according to the manufacturer's protocol. The purified DNA was eluted using 25-50 μl water and stored at 4°C (sticky ends) or -20°C (blunt ends).

***Purification, desalting and concentration of DNA***

Desalting was done with *NucleoTrap* or *Hi Yield* kits.

Phenol-chloroform extraction was advisable to prevent degradation of plasmids isolated from *E.coli BL-21 (DE3) [pREP4]* by DNAses. DNA was mixed with half its volume of phenol (saturated with Tris/HCl pH 8), vortexed for 1 min and centrifuged at 12,000×g for 1 min. Three phases formed: lower organic phase, white interphase with proteins and upper aqueous phase with DNA. The aqueous layer was transferred to a new cup and extracted with the same volume of chloroform-isoamylalcohol (24:1), vortexed and centrifuged. The chloroform layer was discarded and the aqueous phase was concentrated by ethanol precipitation. To the volume of DNA solution (measured by pipetting - $V_{DNA}$), 0.375 × $V_{DNA}$ 10 M ammonium acetate and 2.5 × $V_{DNA}$ 96% ethanol was added, mixed and incubated at RT for 30 min. DNA was pelleted at 12,000×g (30 min at 4°C). Pellets were washed once with 70% ethanol, briefly centrifuged, dried at RT and DNA was dissolved in 20-50 μl water by heating and vortexing.

*Wizard Plus SV Minipreps DNA Purification* kits contain alkaline protease which inactivates endonuclases and other proteins during cell lysis. This kit was preferred for plasmid DNA isolation from *E.coli BL-21 (DE3) [pREP4]*. This way phenol-chloroform extraction was avoided.

Water DNA solutions were often concentrated in a *SpeedVac* at 30-35°C for 10-40 min.

***Determination of DNA concentration***

DNA concentration was determined at $OD_{260}$. The content of protein impurities can be estimated from the $OD_{260/280}$ ratio (aromatic aa from protein impurities absorb light at 280 nm). For well purified DNA the $OD_{260/280}$ is around 1.8.

***Restriction digestion of DNA***

In 10 µl 200-800 ng plasmid DNA or PCR product was incubated with 1U restriction enzyme, 1.5 × enzyme volume of BSA (10 mg/ml) and the respective enzyme buffer. Incubation at 37°C (unless otherwise recommended) was for 1-2 h, or overnight. The digested fragments were separated by agarose gel electrophoresis, isolated and purified.

***Generation of blunt ends***

When necessary the ends of DNA fragment were blunted using Klenow. 500-1000 ng of DNA was incubated with 1 µl of 10×Klenow buffer, 1U of Klenow fragment and 0.5 µl BSA (10 mg/ml) in 10 µl (10 min, 37°C). 3`overhangs were removed and for adding nucleotides to the 5`ends, 1 µl of dNTP-mix (each 20 mM) was added and incubated for 30-40 min at 37°C. Klenow was inactivated by heating at 70°C for 10 min.

***Phosphorylation***

For ligation, 5`ends of DNA have to be phosphorylated. 10 µl of Klenow treated DNA or purified PCR product was incubated with 7-10U *T4 polynucleotide kinase* (PNK), T4-PNK buffer and 1.5 µl 10 mM ATP in 15 µl at 37°C for 1 h. PNK enzyme was inactivated by heating at 70°C for 10 min.

***5`-Dephosphorylation***

To avoid vector religation, 5' ends of DNA were dephosphorylated with alkaline phosphatase (AP). DNA was incubated usually in 20 µl with 1U of AP and dephosphorylation buffer at 37°C for 1 h. The compatibility of AP with all buffer systems allowed dephosphorylation directly after restriction digestion of the plasmid. The dephosphorylated fragments were separated by agarose gel electrophoresis, purified as described above and used for ligation.

***Ligation***

DNA fragments (insert and vector) were ligated using the *Rapid DNA Ligation Kit* according to the instructions of the manufacturer. 50 ng of vector was used in the reaction and the molar ratio of vector to insert was 1:1 to 1:3.

***Transformation of recombinant DNA into E.coli competent cells***

*Preparation of the competent E.coli cells*

5 ml LB-medium was inoculated with competent cells and grown overnight at 37°C. Antibiotics were added depending on the type of the strain: for *E.coli XL1 Blue* tetracycline (10 µg/ml), for *E.coli BL-21 (DE3) [pREP4]* kanamycin (50 µg/ml), for *E.coli Rosetta (pLysS)* chloramphenicol (34 µg/ml) and for *DH5α* no antibiotic was added. The preculture was transferred into 200 ml fresh LB-medium and incubated at 37°C for 2-3 h to an $OD_{600}$ 0.5-0.6 with respective antibiotics. Cells were cooled in ice for 10 min, centrifuged at 3,200×g for 10 min at 4°C. Pellets were resuspended in 50 ml 0.1 M $CaCl_2$ (sterile, 4°C), cooled in ice for 20 min and centrifuged as before. Pellets were resuspended in 10 ml 0.1 M $CaCl_2$ /20% glycerol (sterile, 4°C) and cooled in ice for 4-6 h. Cells were aliquoted (100 µl) and stored at -80°C.

1µl of empty pBSKII(-) vector (1 ng/µl) was added to an aliquot of competent cells and transformed (see *Transformation* below). 110 µl of the cell culture was spread over pre-warmed LB-agar plates (for *DH5α* and *XL1* ampicillin plates were used, for *BL-21 (DE3) [pREP4]* ampicillin/kanamycin plates and for *BL21 Rosetta* ampicillin/chloramphenicol plates) and incubated overnight at 37°C. Next morning at least 150 clones should be seen.

*Transformation*

To the DNA ligation reaction (21 µl, see *Ligation*) 10 µl×CM buffer was added and filled up with water to 100 µl. This was poured over competent cells and cooled in ice for 20-30 min. Cells were then heat-shocked at 42°C for exactly 1 min and cooled on ice for next 10-20 min. 500 µl of the LB-medium (without antibiotic) were added and cells were incubated for 1 h at 37°C (210 rpm). 100-200 µl of this mixture were spread over the pre-warmed LB agar plate(s) with antibiotic(s) depending on kind of strain. By retransformation of plasmid DNA in *E.coli* cells 1µl of DNA solution (Miniprep) was added to competent cells.

*E.coli permanent cultures*

For storage of single clones, permanent cultures were prepared. 5 ml of LB medium with antibiotics were inoculated with a single clone and incubated overnight at 37°C (210 rpm).

1.5-3 ml of the culture was centrifuged and pellets were resuspended in 1 ml of LB-medium/glycerol (all sterile), (4:1) and stored at -80°C.

***Blue-white colony screen***

After PCR the insert was ligated into *pBSKII(-)*. For discrimination of cells with recombined plasmid from the cells with religated vector, *E.coli XL1* cells were incubated 75 min at 37°C and spread over the plate with 40 µl 2 % X-gal and 40 µl 0.1 M IPTG. After overnight incubation at 37°C, clones with insert were white and those with an empty vector were blue. If the insert is absent, ß-galactosidase, expressed from *LacZ* gene cleaves X-gal yielding galactose and 5-bromo-4-chloro-3-hydroxyindole which is oxidized to 5,5`-dibromo-4,4`-dichloro-indigo an insoluble blue dye visible in blue colonies.

***DNA sequencing***

*Chain termination sequencing*

The DNA sequencing was carried out using Sanger´s dideoxy method [92]. The *Thermo Sequenase Primer Cycle Sequencing Kit* which contains each of ddNPT`s (fluorescent labelled), all four dNTP´s, *Thermo Sequenase DNA polymerase*, reaction buffer with $MgCl_2$ and *pyrophosphatase.* 2 µl from each reaction solution was mixed with 3-4 µl of the following mixture:

- purified DNA (1.5-4 µg DNA from *E.coli XL1 Blue*; 2-7 µg DNA *E.coli BL-21 (DE3) [pREP4]*)
- 1.3 µl sequencing primer (5`-IRD 800 labelled, 4 µM with T7)
- 0.7 µl DMSO (3 %)
- water ad 20 µl

Each sample was covered with a drop of *Chill-Out 14 Liquid Wax*, briefly centrifuged and run in a thermocycler according to the program in the table:

| Temperature | Time | Cycles | Phase |
|---|---|---|---|
| 95°C | 2 min | | Initial denaturation |
| 95°C<br>56°C<br>72°C | 20s<br>20s<br>30s | 20-25 | Denaturation<br>Annealing<br>Elongation |
| 4°C | | | Cooling |

Table 3.2: PCR-program for DNA sequencing

After PCR, samples were mixed with 6 µl stop buffer and 1-1.2 µl of each sample was loaded on 6 % polyacrylamide gel with 7 M Urea. Electrophoresis was with TBE buffer at 50°C, 50 W, 1500 V and 37 mA using *LI-COR*-Sequenator. The results were analysed using *BaselImagIR version 4.0* and *DNA-Star*-software.

*Capillary DNA sequencing*

Samples consisted of:

- 4 µl diluted (1:6) *BigDye Terminator Cycle Sequencing Kit Version 3.1* with ddNTP`s (labelled with fluorescent color), dNTP`s and DNA polymerase in corresponding buffer
- 1.2 µl primer (0.6 pmol/µl)
- 5µl purified DNA

Samples were centrifuged shortly and set for a PCR according to the program in the table:

| Temperature | Time | Cycles | Phase |
|---|---|---|---|
| 96°C | 1 min | | Initial denaturation |
| 96°C<br>50°C<br>60°C | 10s<br>5s<br>4 min | 25 | Denaturation<br>Annealing<br>Elongation |
| 4°C | | | Cooling |

Table 3.3: PCR-program for capillary DNA sequencing

DNA was precipitated with 40 µl isopropanol, left at RT for 10 min and centrifuged at 13,000 rpm for 30 min, isopropanol layer was discarded. The DNA was then washed with 150 µl 80% ethanol, centrifuged for 5 min, ethanol was discarded and DNA pellets were dried in a *SpeedVac* for 10 min. DNA was dissolved in *HiDi* (formamide) buffer, left at RT for 15 min, vortexed and centrifuged. Samples were automatically loaded by the capillary sequencing robot. Results were analysed using *Sequence scanner* software from the manufacturer.

## 3.2 Protein chemistry

### 3.2.1 Protein expression in *E.coli*

Proteins were expressed in *E.coli BL-21 (DE3) [pREP4]* or *Rosetta BL21 (pLysS)*. A preculture was prepared by inoculating 50-150 ml of LB-broth containing 100 µg/ml ampicillin and 50 µg/ml kanamycin for *BL-21 (DE3) [pREP4]* or 100 µg/ml ampicillin and 34 µg/ml chloramphenicol for *Rosetta BL21 (pLysS)* with a permanent culture (37$^{o}$C, 12 h, 210 rpm). Usually, protein was expressed in 400-800 ml cell culture, in cases of poor protein expression in 3.6 or 7.2 L.

5-10 ml of preculture were inoculated and grown in 200 ml LB-broth containing antibiotics as above at 30°C, 210 rpm, to an $OD_{600}$ of 0.4-0.6 (approx. after 2-6 h). The temperature was set and cells were induced with IPTG. Constructs with CyaB1 AC were induced in the presence of 10 mM $MgCl_2$. Usually at temperatures 12-20°C, expression was 12-15 h and at temperatures 20-30°C for 5-7 h. 0.1 µM-1 mM IPTG was used for induction.

An empty vector was induced under identical conditions. 2-4 h after induction, 1 ml cell culture and empty vector culture was centrifuged (13,000 rpm, 2 min), washed with 1 ml cell wash buffer and centrifuged again (13,000 rpm, 15min). Pellet were resuspended in 100 µl of cell lysis buffer, sonicated (3 times, 5 s) on ice and centrifuged for 15 min. Pellet were suspended in 50 µl water. 20 µl of the latter and 5µl of supernatant were mixed with 5 µl SDS sample buffer, heated at 95°C for 5 min and loaded on SDS-PAGE.

### 3.2.2 Cell harvesting and lysis

At an $OD_{600}$ between 1.8 and 4.0 cells were harvested - centrifuged at 4,100×g for 10 min at 4°C. Pellet from each 400 ml cell culture were resuspended in 40-50 ml cell wash buffer (on ice), transferred to 50 ml Falcon tubes and centrifuged (4,300×g, 20 min, 4°C). Supernatants were discarded and pellet were lysed or stored at -80°C.

Pellet were resuspended in 25-30 ml cell lysis buffer and broken with *French Press* at 1000 psi. Homogenate was centrifuged at 41,300×g (1 h, 4°C). Pellet were discarded. From pellet and supernatant after cell lysis probes were taken for SDS-PAGE analysis. 2-10 µg of protein were used. Probes were stored at -20°C.

### 3.2.3 Protein purification

In the $Ni^{2+}$-IDA affinity chromatography iminodiacetic acid (IDA) is the ligand coupled to *Unosphere* base matrix. Supernatant after cell lysis was incubated with 250 µl $Ni^{2+}$-IDA resin (*Profinity™ IMAC Ni-charged Resin*) for 3h on ice and gentle shaking. $Ni^{2+}$ material was usually equilibrated with low concentrations of imidazole (15 mM or 25 mM) to reduce unspecific binding and NaCl (up to 400 mM) to prevent ionic binding of *E.coli* proteins. $Ni^{2+}$ material was centrifuged at 1,100×g for 5 min at 4°C. In some cases when the yield of protein was low, supernatant was incubated with new $Ni^{2+}$-IDA for another 3h and/or overnight. 2-5 µl of this supernatant was used for SDS-PAGE analysis.

Pellet were poured into a 10 ml syringe with an attached *Wizard® Plus* mini-column and washed with different wash buffers (2-6 ml) with increasing imidazole concentrations (max. 70 mM imidazole). The protein was eluted twice with 300-600 µl elution buffer containing

300 mM imidazole. Purified protein was analysed by SDS-PAGE gel and dialysed overnight in 35% or 10% glycerol.

Some proteins were purified with $Ni^{2+}$-NTA agarose. There nitrilotriacetic acid (NTA) is coupled to *Sepharose CL-6B*. Purification procedure with $Ni^{2+}$-NTA agarose was the same as with $Ni^{2+}$-IDA. In the wash steps higher concentrations of imidazole could be used.

*Dialysis*

To remove imidazole (affects the stability of CyaB1 AC chimeras) or to change buffer after elution, protein was dialysed overnight at 4°C in 0.5-1 L dialysis buffer against 35% glycerol (10% for some proteins and crystallization). Protein was assayed immediately after dialysis or stored at -20°C in corresponding buffer.

*Protein concentration*

After dialysis, protein for crystallization was concentrated using *NANOSEP 10K OMEGA* centrifugal devices or *ULTRAFREE-0.5*-protein concentrators at 10,000-11,000 rpm (*Cool centrifuge 5402, Eppendorf*). 2-15 ml protein solution was concentrated in *Vivaspin 2*- or *Amicon Ultra-15*-concentrators at 4,200 rpm (*Megafuge 1.0 R, Heraeus*) at 4°C to the volume of 200-500 µl. Before concentrating membranes were washed with dialysis buffer (crystallization buffer).

Protein determination was according to [93] (Bradford test).

### 3.2.4 SDS-PAGE gel electrophoresis and Western blotting

SDS-PAGE was carried out according to Laemmli [94] to separate proteins according to their molecular weights. *PeqGold* was used as a protein marker (marked as M on gel photos). After electrophoresis, gel(s) were used further for Western blotting or stained with Coomassie blue for 30 min during gentle shaking, decolorized for another 30 min and washed with water until bands could be clearly detected.

For Western blotting proteins were transferred with *Semi-Dry*-electrotransfer according to Towbin onto a PVDF membrane [95]. PVDF membrane (6×8.5 cm) and six *Whatman* papers (6×9 cm) were successively soaked 10 min in methanol, 10 min in water and together with the gel for 10 min in Towbin buffer. For the electric transfer the following set-up was made on the anode plate: 3 *Whatman* papers, blot membrane, gel and again 3 *Whatman* papers. During handling with membranes, gloves and forceps were used. Excess buffer was wiped off with a tissue. The cathode plate with the lid was fixed and blotting was started (20 V, 200 mA pro gel, 3 h). After blotting, the gel was stained in Coomassie blue and decolorized to check

transfer efficiency. The membrane was stained in Ponceau S for 5 min and decolorized with water until protein bands were clear enough and protein markers were marked with pencil.

The membrane was blocked with M-TBS-T buffer for 30 min at RT or overnight at RT or 4°C during shaking. After a membrane wash (twice 2 min in TBS-T) it was incubated with primary Ab (mouse monoclonal RGS-$His_4$ Ab 1:2000 or Tetra-His Ab 1:1000, diluted in M-TBS, depending on the expression plasmid), 1 h, RT. Again, the membrane was washed in TBS-T buffer for 15 min and twice for 5 min and incubated 1h with secondary Ab (goat anti-mouse IgG-Fc horseradish peroxidase conjugated Ab 1:5000 diluted in M-TBS-T). Membrane was washed in TBS-T as above.

For detection of protein-Ab complex *ECL plus Western Blotting Detection* reagents were used according to manufacturer`s instructions. Chemiluminescent signal was detected by exposing the membrane to *hyperfilm ECL* (exposure time 3 s - 5 min) and the films were developed.

## 3.3 Densitometry of the SDS-PAGE gels or Western blots

This is the method for quantification of the protein´s SDS-PAGE or Western blots. ImageJ software calculates the area and pixel value statistics of defined selections. Intensity of the band is determined as area under peak (AUP).

*Densitometry of SDS-PAGE gels:*

The sum of AUPs of all proteins from the sample represented as a SDS-PAGE gel plot was taken as 100% (see Table 4.1). The amount of protein of interest was calculated accordingly (% of that sum - protein purity). Proteins usually had similar purities and their specific activities were compared.

*Densitometry of Western blot signals:*

When SDS-PAGE gel densitometry was impossible, Western blot signals were digitized. It is important that Western blot signals have the same background and exposure time. Signal with the strongest intensity (AUP with the highest value) was taken as 100% and the other signal(s) were calculated accordingly. Specific activities were recalculated and compared.

## 3.4 Chromatography methods

***Gel filtration chromatography***

Proteins are separated according to their size as they pass through the column. To purify PDE5 crystal construct Superose 12 was used (H/R of columns was 30/1, sample volume Vs=270 µl, flow rate 0.5 ml/min; Vtot =23.7 ml, $V_0$ =7.7 ml). Markers were: BSA, phosphorylase b, ovalbumine and aldolase (2 mg/ml).

***Anion-exchange chromatography***

For purification construct PDE4A4-CyaB1 AC, anion exchange chromatography on Mono Q columns was used (10 µm diameter spherical beads, H/R was 5/5, V=1 ml, flow rate 1 ml/min, back pressure 1.0-1.5 MPa) at 4°C.

pH of the equilibration buffer determines the charge of the protein of interest. In the experiment Tris/HCl buffer pH 7.5 was used since the pI of PDE4A4 protein is 6.2. A NaCl step gradient was used (100 mM - 1 M NaCl) and proteins were eluted at different ionic strengths.

***Hydrophobic interaction chromatography***

This was used for calmodulin purification, using Phenyl Sepharose (H/R was 10/2.5 cm, flow rate 2 mil/min, back pressure 0.3 MPa) at room temperature.

$Ca^{2+}$ was added to the protein prior to chromatography (up to 5 mM) thus that hydrophobic residues are exposed. CaM binds reversibly to the phenyl groups. Low affinity proteins are washed away with equilibration buffer. To prevent high affinity basic proteins to bind to acidic CaM absorbed on the column, buffer with high ionic strength (0.5 M NaCl) was applied (wash buffer). CaM was eluted from the column with the elution buffer containing 1 mM EGTA.

## 3.5 Adenylyl cyclase assay

The activity of adenylyl cyclase was determined according to Salomon et al. [96]. Substrate [α-$^{32}$P]-ATP was converted into [$^{32}$P]-cAMP, which was isolated using a two-column system. [2, 8-$^{3}$H]-cAMP, internal standard to monitor yield was added with the stop solution.

Every test was repeated at least twice in duplicate ($n \geq 4$).

100 µl assay sample contained:

- in 40µl: protein, test reagents, 50 µg BSA (5 µl) (mix of total amount of protein and BSA for all samples was prepared and calculated amount for one sample was pipetted on the bottom of the tube)
- 50 µl AC-cocktail
- 10 µl 750 µM [α-$^{32}$P]-ATP

Blank samples contained water instead of protein.

10 µl 750 µM [α-$^{32}$P]-ATP (16-30 kBq) was added to start the reaction. Samples were shortly vortexed and incubated at 37°C for 10 min with shaking. Final concentrations of reactants were: 22 % glycerol, 50 mM Tris/HCl pH 7.5 (unless indicated otherwise), 10 mM $MgCl_2$, 75

µM [α-$^{32}$P]-ATP and 5-200 nM protein. The reaction was stopped by addition of 150 µl stop buffer. 10 µl of 20 mM [2, 8-$^{3}$H]-cAMP (final, 2 mM, approx.150 Bq) and 750 µl water were then added. Samples were poured on *Dowex* columns (9×1 cm, glass column, with 1.3 g *Dowex-50WX4*), washed with 3 ml water and eluted with 5 ml water onto *Alox* columns (10×0.5 cm, plastic column, with 1 g active, neutral $Al_2O_3$ *90*). Radioactive cAMP was eluted with 4.5 ml 0.1 M Tris/HCl pH 7.5 in vials filled with 4 ml *Ultima Gold XR* Scintillator. They were vigorously shaken and counted in a *Liquid Scintillation Counter*.

For regeneration, columns were washed with:

- 5 ml 2 N HCl, 10 ml water and 5 ml water, for Dowex and
- 2 × 5 ml 0.1 M Tris/HCl pH 7.5, for Alox

Specific activity (A) – pmol cAMP/mg (protein)·min was calculated with the following formula:

$$A = \frac{Substrate\,(\mu M) \times 100\,\mu l}{time\,(\min)} \times \frac{1000}{protein\,(\mu g)} \times \frac{cpm\left[^{3}H\right]_{total}}{cpm\left[^{3}H\right]_{sample} - 3\%\left[^{32}P\right]_{sample}} \times \frac{cpm\left[^{32}P\right]_{sample} - cpm\left[^{32}P\right]_{blank}}{cpm\left[^{32}P\right]_{total}}$$

3 % of phosphorus counts were subtracted from tritium value for each sample because of the spillover of $^{32}$P into the tritium channel. Activities lower than double backgrounds were considered as zero activity.

## 3.6 Crystallization

Hanging drop vapour diffusion method was used for crystallization.

500 µl of different precipitants (*Wizard I* and *II* and *Crystal screen I, II* and *lite*) were placed in each of 24 well of *VDX 24-well* crystallization plates (reservoir). 1µl of it was mixed with 1 µl protein (5-15 µg/µl) on a siliconized coverslip. Usually 2 mM cGMP was added. The coverslip with the drop was greased and inverted over the reservoir, forming the hanging drop. The plates were kept at 4°C, 12°C or 18°C for 4-5 days and analysed every other day for 15 days under a polarization microscope (*Axioskop 40*).

## 3.7 Cloning

In construct`s schemes, CyaB1 AC has been omitted. Vectors are depicted by black lines. Final clones, used for expression are framed.

Sequenced clones were used for expression and as templates. Most of the constructs were transformed first in *E.coli XL1 Blue* or *DH5α*. Final clones were sequenced and transformed in *E.coli BL-21 (DE3) [pREP4]* or *E.coli BL21 Rosetta (pLysS)* for expression.
All numberings are from holoenzymes. Starting clones used as templates were from Anita Schultz, Sandra Bruder, Karina Hofbauer, Nycomed and Marco Conti.

### 3.7.1 Starting clones

WT CyaB1 AC, pQE30 (A. Schultz)
WT CyaB1 AC, pBSKII(-) (A. Schultz)
hPDE5-CyaB1 AC, pET16b MCS-pQE30 (S. Bruder)
hPDE5-CyaB1 AC, pQE30 (S. Bruder)
hPDE10-CyaB1 AC, pRSETA (K. Hofbauer)
hPDE2-CyaB1 AC, pET16b MCS-pQE30 (A. Schultz)
hPDE1A3 Holo (Nycomed)
hPDE1B1 Holo (Nycomed)
hPDE4D3 Holo, pcDNA3 (M.Conti, Stanford University)
hPDE4A4 Holo, pVL1393 ( Nycomed)
hPDE4B1 Holo, pER-Bac (Nycomed)

All constructs* were attached to the identical reporter CyaB1 AC (L386-K859), which was cloned onto 3`-terminals of PDEs via XhoI whenever possible. When this was impossible fusion PCRs were performed with a sense primer from the respective PDE and an antisense primer covering a Mfe site CyaB1 AC. This is indicated in the graphs.

*- The list of all constructs is in Appendix (p.117)

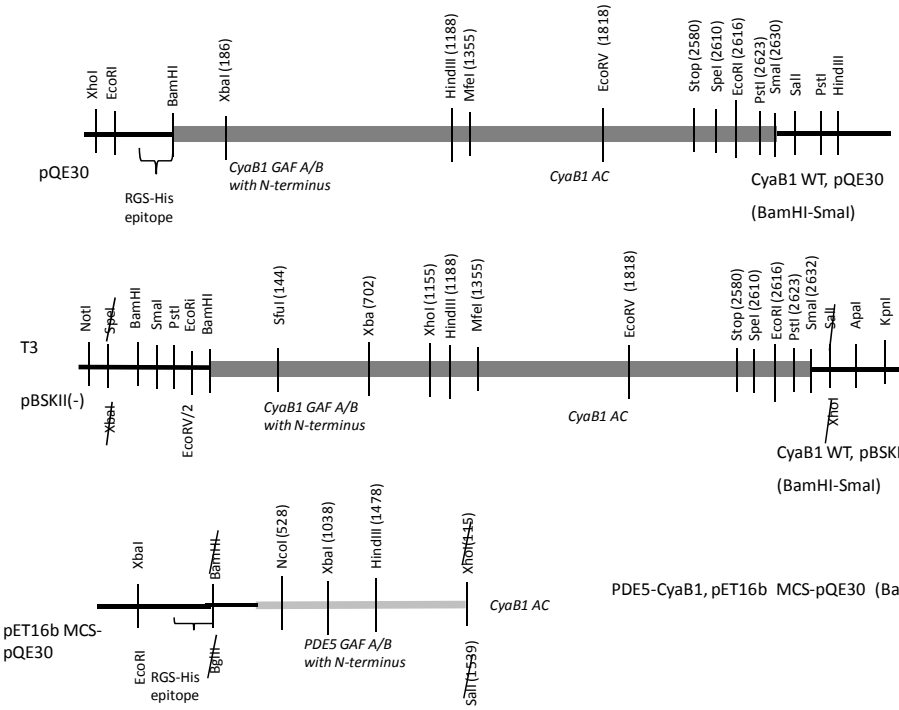
XhoI
EcoRI
BamHI
XbaI (186)
HindIII (1188)
MfeI (1355)
EcoRV (1818)
Stop (2580)
SpeI (2610)
EcoRI (2616)
PstI (2623)
SmaI (2630)
SalI
PstI
HindIII
pQE30
RGS-His epitope
CyaB1 GAF A/B with N-terminus
CyaB1 AC
CyaB1 WT, pQE30
(BamHI-SmaI)
T3
T7
pBSKII(-)
NotI
SpeI
BamHI
SmaI
PstI
EcoRi
BamHI
SfuI (144)
Xba (702)
XhoI (1155)
HindIII (1188)
MfeI (1355)
EcoRV (1818)
Stop (2580)
SpeI (2610)
EcoRI (2616)
PstI (2623)
SmaI (2632)
SalI
ApaI
KpnI
XbaI
EcoRV/2
CyaB1 GAF A/B with N-terminus
CyaB1 AC
XhoI
CyaB1 WT, pBSKII (-)
(BamHI-SmaI)
XbaI
BamHI
NcoI (528)
XbaI (1038)
HindIII (1478)
XhoI (1545)
CyaB1 AC
pET16b MCS-pQE30
EcoRI
RGS-His epitope
BglII
PDE5 GAF A/B with N-terminus
SalI (1539)
PDE5-CyaB1, pET16b MCS-pQE30 (BamHI/BglII-SacI)

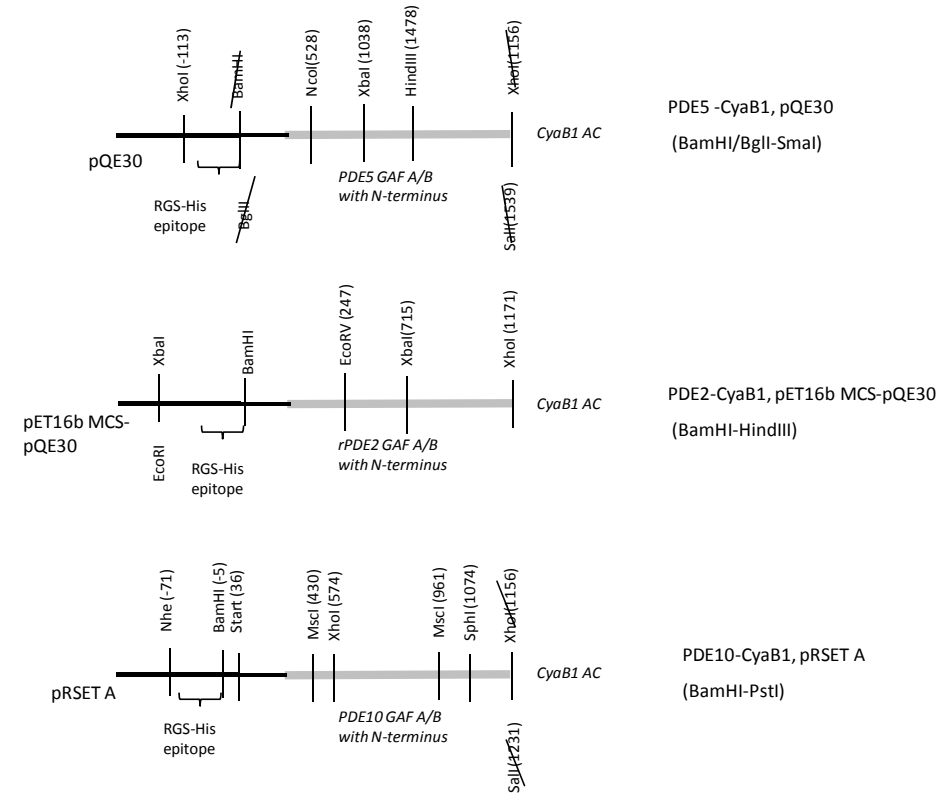
XhoI (-113)
BamHI
NcoI(528)
XbaI (1038)
HindIII (1478)
XhoI(1156)
CyaB1 AC
pQE30
RGS-His epitope
BglII
PDE5 GAF A/B with N-terminus
SalI(1539)
PDE5 -CyaB1, pQE30
(BamHI/BglII-SmaI)
XbaI
BamHI
EcoRV (247)
XbaI(715)
XhoI (1171)
CyaB1 AC
pET16b MCS-pQE30
EcoRI
RGS-His epitope
rPDE2 GAF A/B with N-terminus
PDE2-CyaB1, pET16b MCS-pQE30
(BamHI-HindIII)
Nhe (-71)
BamHI (-5)
Start (36)
MscI (430)
XhoI (574)
MscI (961)
SphI (1074)
XhoI(1156)
CyaB1 AC
pRSET A
RGS-His epitope
PDE10 GAF A/B with N-terminus
SalI(1231)
PDE10-CyaB1, pRSET A
(BamHI-PstI)

### 3.7.2 PDE5-CyaB1 AC Chimeras

#### *PDE5 A89-/N91-/G95-CyaB1 AC*

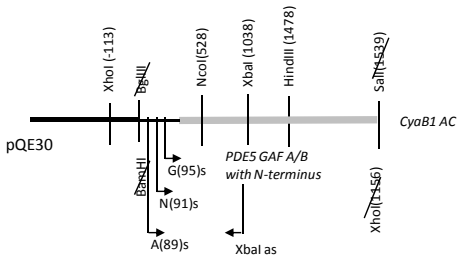


PDE5 -CyaB1, pQE30
(BamHI/BglI-SmaI), template

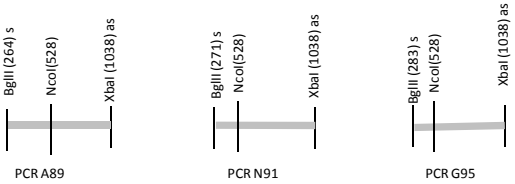


Ligation of PCR products (≈ 800bp) in EcoRV digested pBSKII(-) (≈ 2900bp), transformation in XL-1 cells, sequencing and checking the orientation.

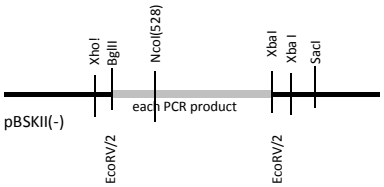


Digestion with BglII-SacI (≈850bp) and ligation in BamHI-SacI digested (≈5700), dephosphorylated pET16b MCS-pQE30 (expression vector), transformation in DH5α cells.

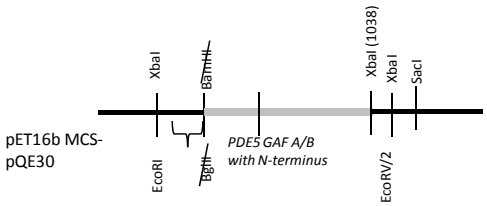


PDE5 A89-/N91-/G95- BglII-XbaI, pET16b MCS-pQE30 (BamHI/BglII-SacI)

Digestion with NcoI-SacI from PDE5 -CyaB1, pET16b MCS-pQE30 (≈2700bp) and ligation in NcoI-SacI digested, dephosphorylated PDE5 A89-/N91-/G95 -BglII-XbaI, pET16b MCS-pQE30 vector (≈ 6000bp). Transformation in E.coli BL21 cells, control digestion with NcoI-MfeI (≈1250bp), sequencing and expression .

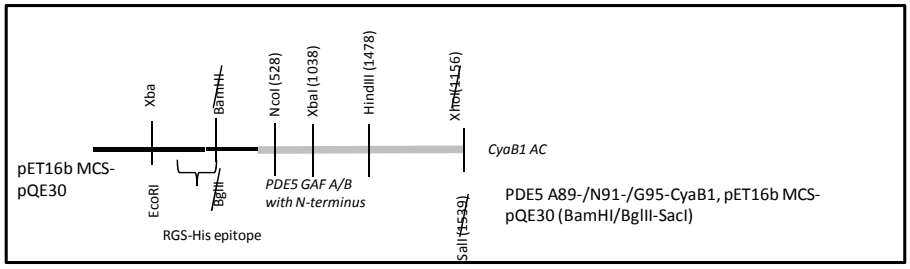


PDE5 A89-/N91-/G95-CyaB1, pET16b MCS-pQE30 (BamHI/BglII-SacI)

## *PDE5 NAAIRS-CyaB1 AC*

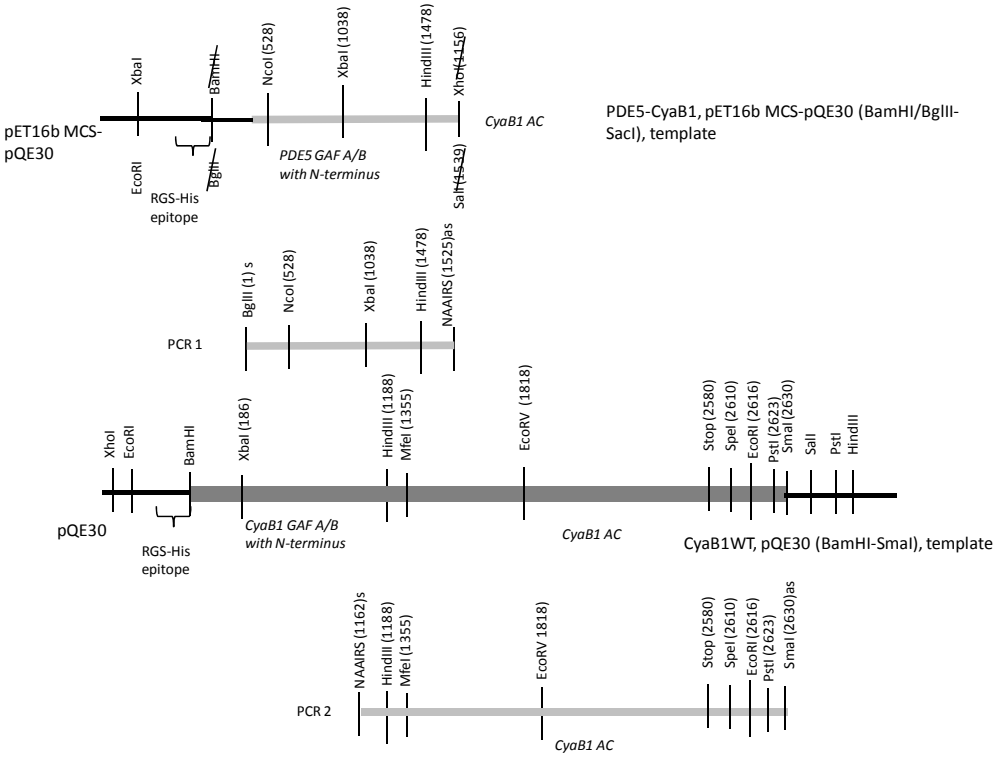


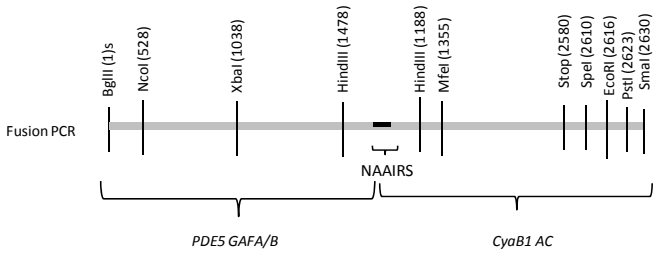


Digestion with NcoI- MfeI (≈1200bp) ligation in NcoI-MfeI digested, dephosphorylated vector PDE5-CyaB1,pET16b MCSp-QE30 (≈7000), transformation in E.coli BL21 (pREP4) cells, sequencing and expression.

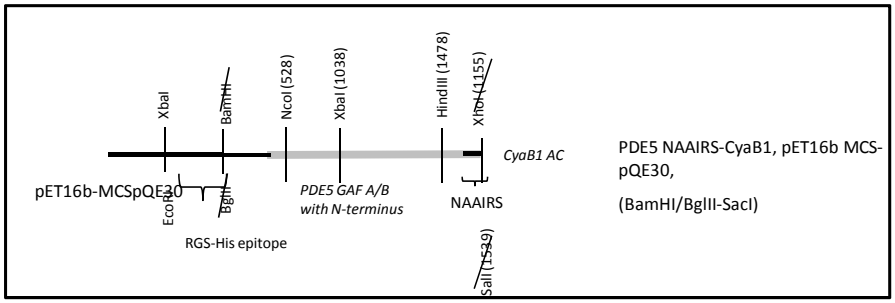

### 3.7.3 PDE10, PDE5 linker-CyaB1 AC chimeras

***PDE10 WT- and PDE10, PDE5 (G311-S346)-CyaB1 AC (No.1-15)***

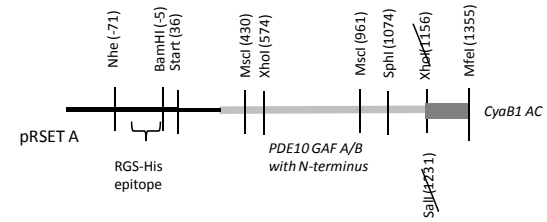


PDE10-CyaB1, pRSET A, (BamHI-PstI), template

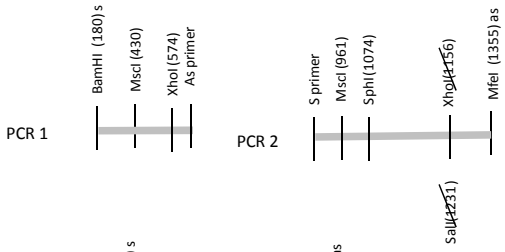


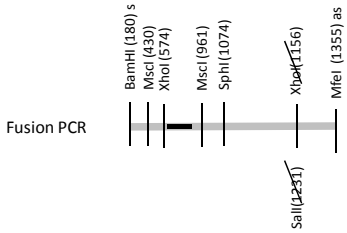


For cloning No.1 the template was PDE10-CyaB1, pRSET A and for each next construct (No.2-No.15), the template was the previous final clone in pETDuet MCS-pQE30 vector. Fusion PCR was digested with MscI-MscI (≈530bp) or XhoI-SphI (≈500bp) and ligated in MscI-MscI or XhoI-SphI digested and dephosphorylated vector WT PDE10-CyaB1, pETDuet MCS-pQE30 (≈7400bp), sequenced and expressed in E.coli B21 Rosetta (pLysS) cells. WT PDE10-CyaB1, pETDuet MCS-pQE30 was cloned between BamHI and PstI.

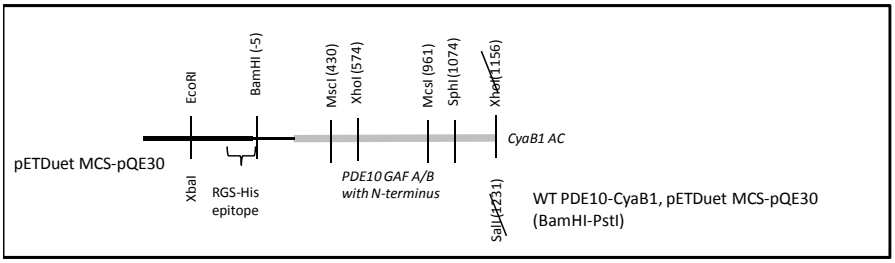


WT PDE10-CyaB1, pETDuet MCS-pQE30 (BamHI-PstI)

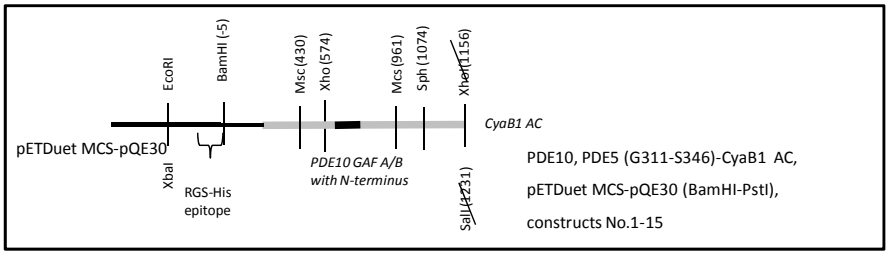


PDE10, PDE5 (G311-S346)-CyaB1 AC, pETDuet MCS-pQE30 (BamHI-PstI), constructs No.1-15

## *PDE10 V239L-/ C240Y-/ V239L, C240Y-/, No. 3 V239L- and No. 3 C240Y- CyaB1 AC (No.17-21)*

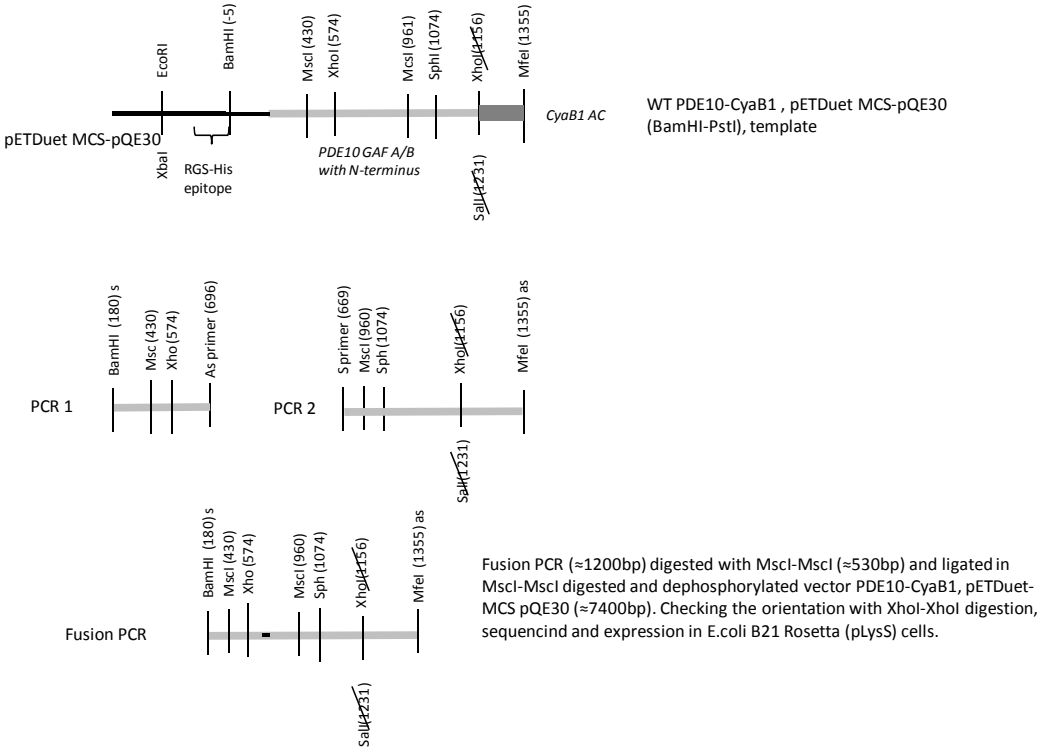


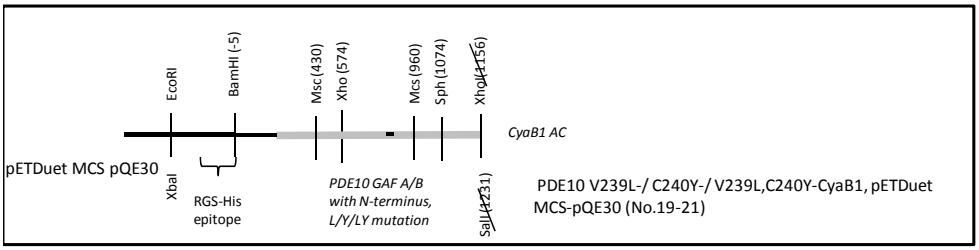


For constructs No.3 V2397L and No.3 C240Y (No.17 and 18) the same way of cloning was used. The only difference is that No.3 was a template and expression vector.

## *PDE10, PDE5 (K298-F341)-CyaB1 AC (No.22)*

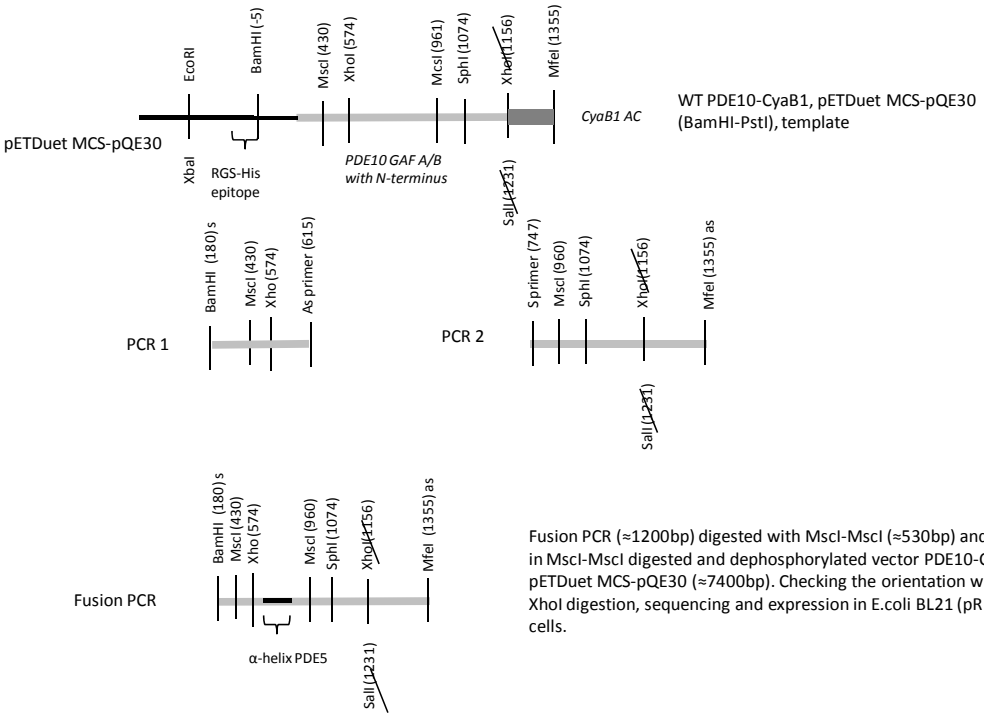


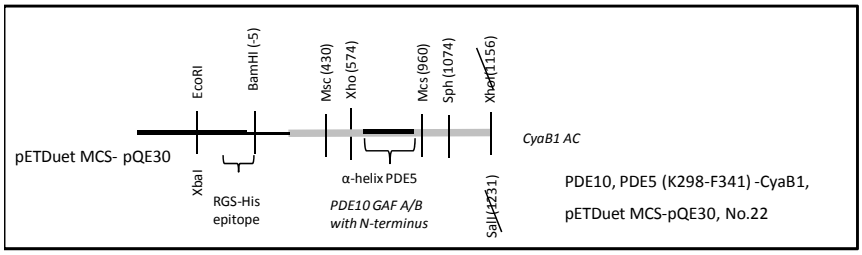

## *PDE5, PDE10 (S218-F261)-CyaB1 AC (No.23)*

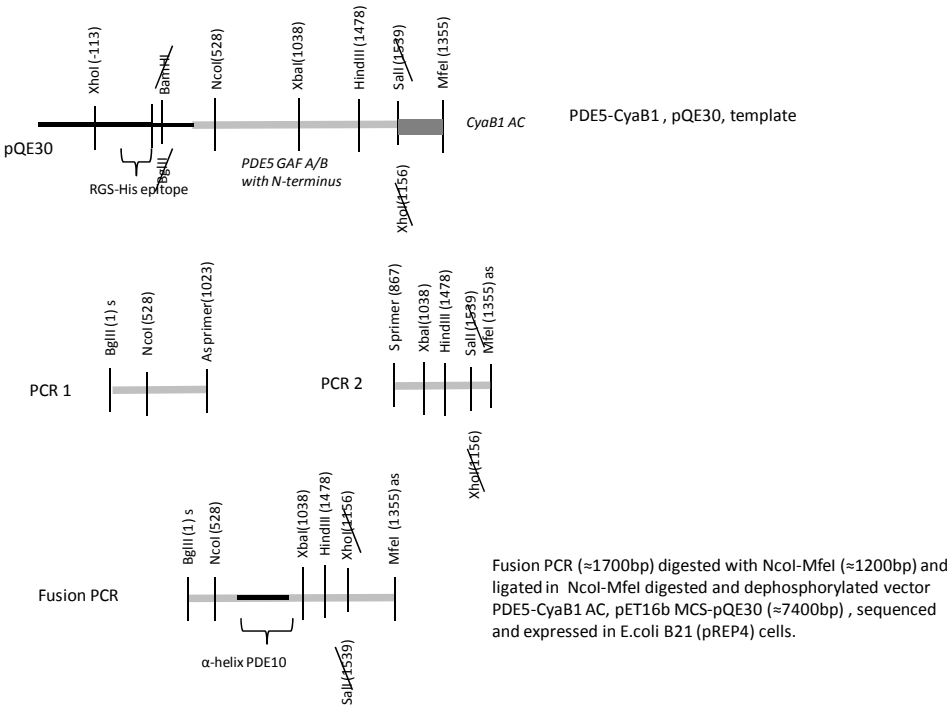


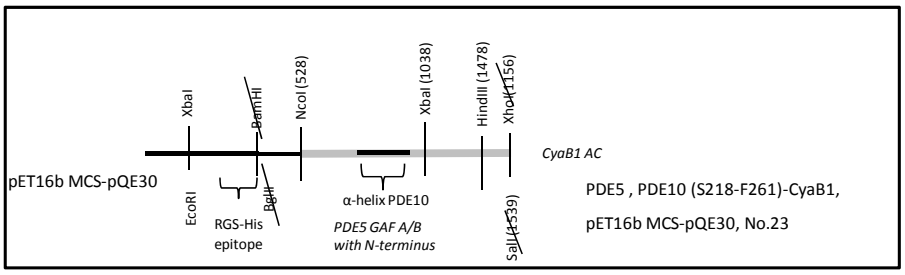

### 3.7.4 PDE1-CyaB1 AC chimeras

#### *PDE1A3 M178-/L206-/M234-CyaB1 AC (A, B and C)*

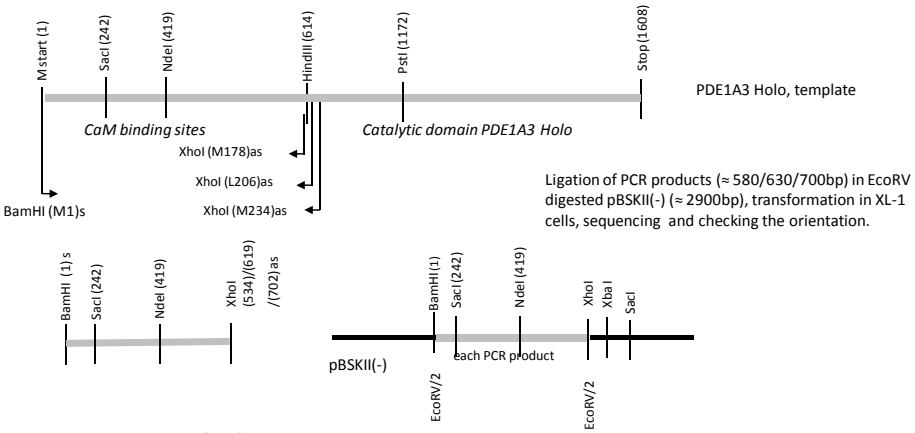


Digestion with BamHI-XhoI (≈534/618/702bp) and ligation in BamHI-XhoI digested, dephosphorylated rPDE2-CyaB1,pET16b-MCSpQE30 (expression vector), transformation in E.coli BL21 (pRep4) cells, sequencing and expression.

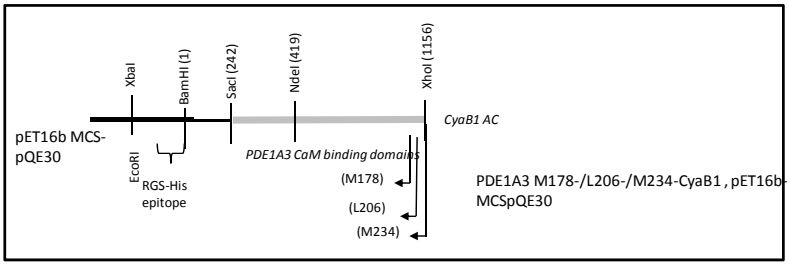


#### *PDE1B1 T182-/A210-/F238-CyaB1 AC (D, E and F)*

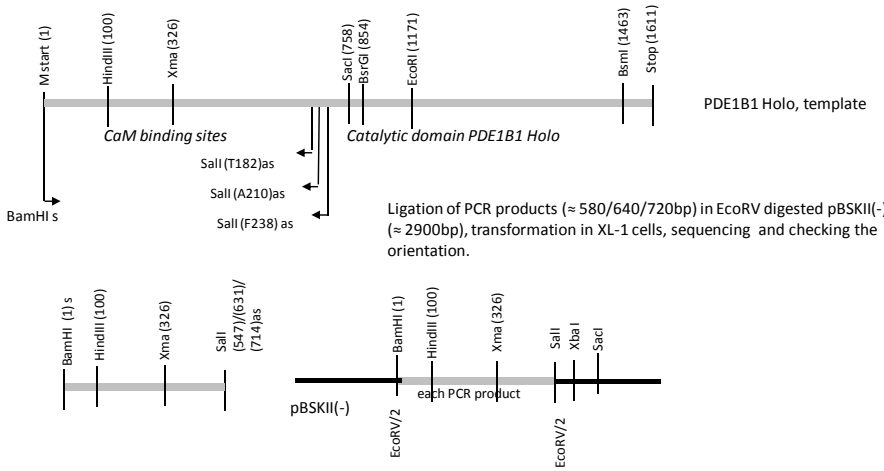


Digestion with BamHI-SalI (≈534/618/702bp) and ligation in BamHI-XhoI digested, dephosphorylated rPDE2-CyaB1,pET16b-MCSpQE30 (expression vector), transformation in E.coli BL21 (pRep4) cells, sequencing and expression.

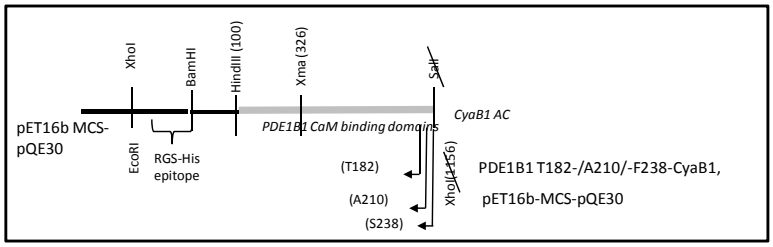

### 3.7.5 PDE4-CyaB1 AC chimeras

#### *PDE4D3-CyaB1 AC chimeras*

*PDE4D3 I/II- and CyaB1 (M1-E48) PDE4D3 -CyaB1 AC*

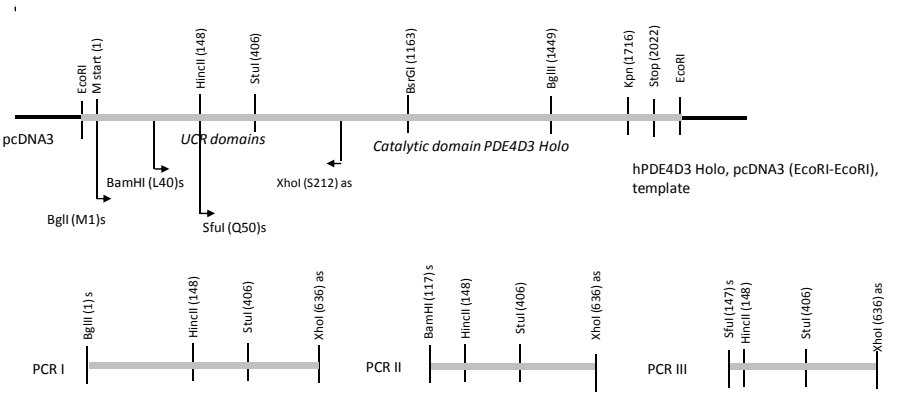


Ligation of PCR products (≈ 640/520/490bp) in EcoRV digested pBSKII(-) (≈ 2900bp), transformation in XL-1 cells, sequencing and checking the orientation.

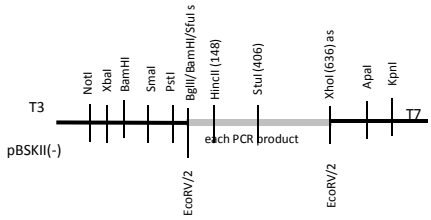


Digestion with NotI-XhoI for I and II (≈650/520) and ligation in NotI-XhoI digested, dephosphorylated WT CyaB1,pEBSKII(-) (≈4300bp), transformation in E.coli XL-1cells; Digestion with SfuI-XhoI for PCR III (≈490) and ligation in SfuI-XhoI digested, dephosphorylated WT CyaB1,pEBSKII(-) (≈4300bp).

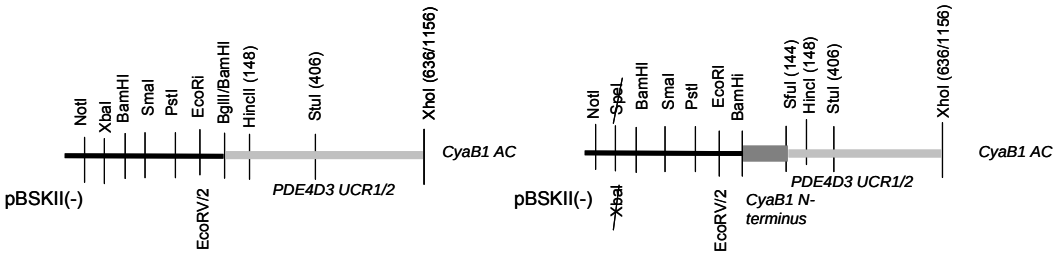


PDE4D3 I/II-CyaB1, pBSKII (-)

CyaB1 (M1-E48) PDE4D3-CyaB1, pBSKII (-)

Digestion with BglI-EcoRV in I (≈1300bp) and BamHI-EcoRV in II and CyaB1 (M1-E48) PDE4D3-CyaB1, pBSKII (-) (≈ 1180bp/1300bp) and ligation in BamHI-EcoRV digested, dephosphorylated vector WT, CyaB1-pQE30 (≈4300), transformation in E.coli BL21 cells, sequencing and expression.

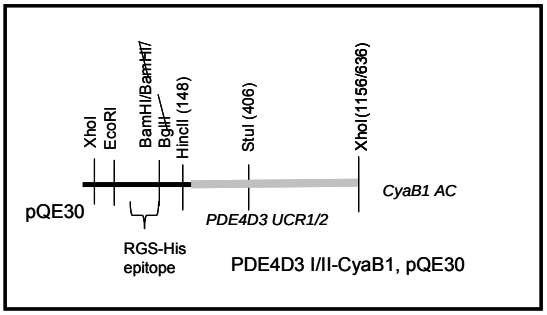


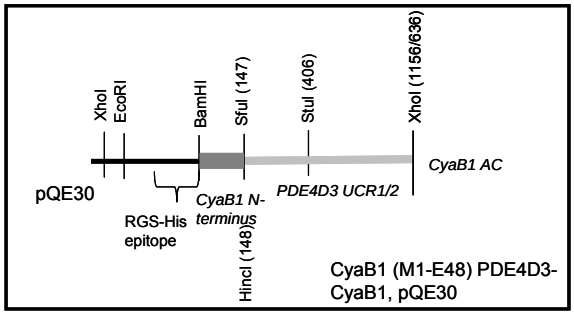

*S54D PDE4D3 III/IV- and CyaB1 (M1-E48) S54D PDE4D3 -CyaB1 AC*

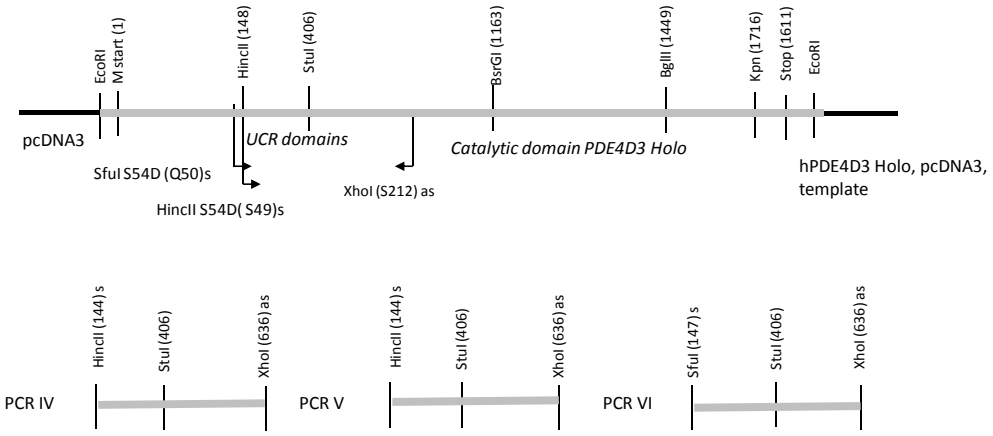


Digestion PCR product IV and V (≈ 500) with HincII-XhoI (≈500bp), ligation in HincII-XhoI digested, dephosphorylated vector PDE4D3 I/II-CyaB1,pBSKII(-), transformation in E.coli XL1 cells, sequencing; digestion PCR product VI with SfuI-XhoI (≈500bp) and ligation in SfuI-XhoI digested, dephosphorylated vector PDE4D3 III-CyaB1,pBSKII(-);

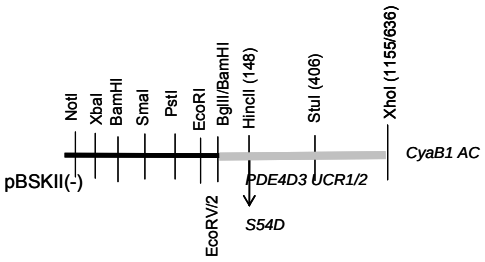


S54D PDE4D3 III/IV-CyaB1, pBSKII (-)

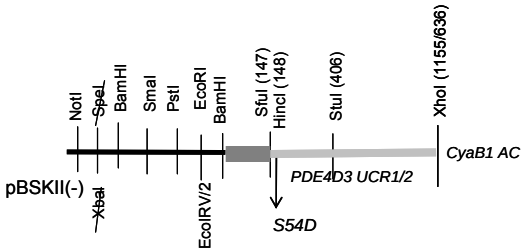


CyaB1 (M1-E48) S54D PDE4D3-CyaB1, pBSKII (-)

Digestion with BglI-EcoRV in III (≈1300bp) and BamHI-EcoRV in IV and CyaB1 (M1-E48) S54D PDE4D3-CyaB1, pBSKII (-) (≈1180bp/1300bp) and ligation in BamHI-EcoRV digested, dephosphorylated vector WT, CyaB1-pQE30 (≈4200), transformation in E.coli BL21 cells, sequencing and expression.

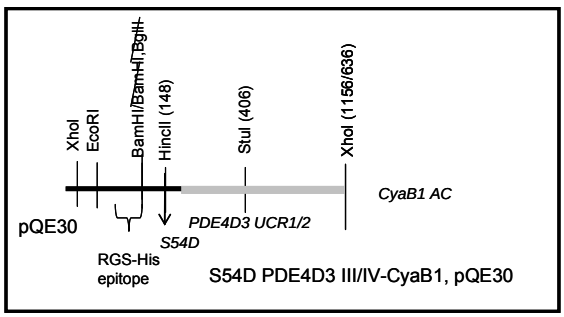


S54D PDE4D3 III/IV-CyaB1, pQE30

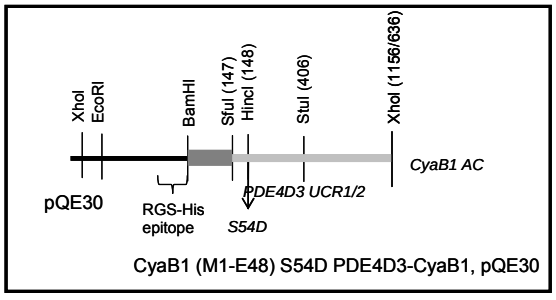


CyaB1 (M1-E48) S54D PDE4D3-CyaB1, pQE30

## *PDE4D3 I/III-CyaB1 AC, pET16b MCS -pQE60*

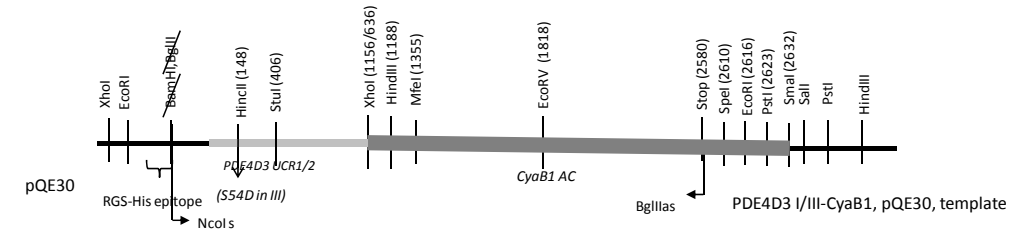


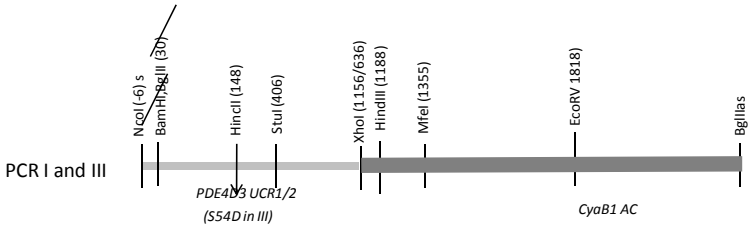


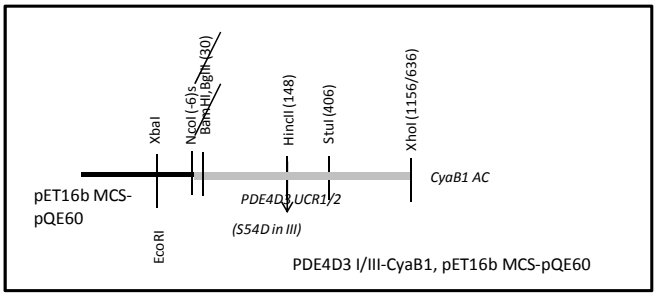


Digestion with NcoI-BglII in PCR I and III (≈ 2060bp) and ligation in NcoI-BamHI digested, dephosphorylated vector pET16b MCS-pQE60 (≈ 5600), transformation in E.coli BL21 (pREP4) cells, sequencing and expression.

## *PDE4D3 I/III-CyaB1 AC, pET16b MCS-pQE30*

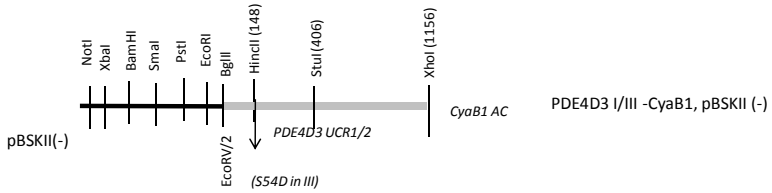


Digestion with BglII –XhoI in PDE4D3 I/III-CyaB1 pBSKII(-) (≈650bp) and ligation in BamHI-XhoI digested, dephosphorylated vector rPDE2-CyaB1,pET16b MCS-pQE30 (≈ 6800), transformation in E.coli BL21 (pREP4) cells, sequencing and expression.

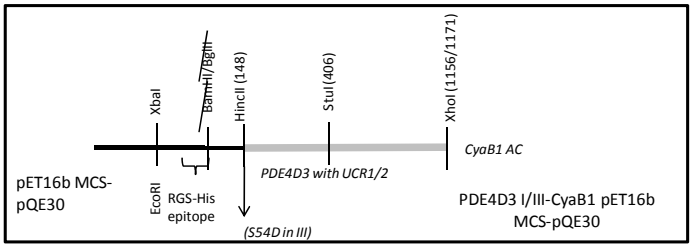

## *PDE4A4-CyaB1 AC chimeras*

### *PDE4A4-CyaB1 AC (V)*

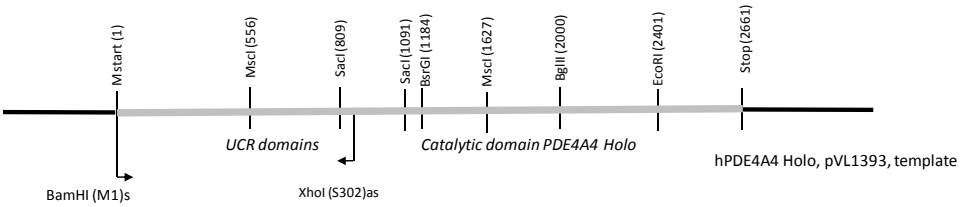


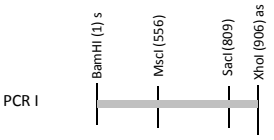


Ligation of PCR products (≈ 920bp) in EcoRV digested pBSKII(-) (≈2900bp), transformation in XL-1 cells, sequencing and checking the orientation.

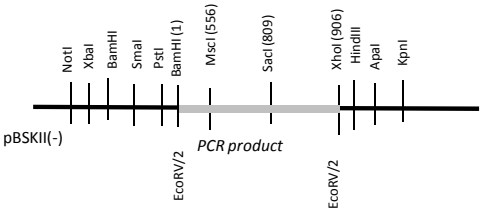


Digestion with NotI-XhoI (≈990) and ligation in NotI-XhoI (≈ 4300) digested, dephosphorylated WT CyaB1,pEBSKII(-), transformation in E.coli XL-1cells, sequencing;

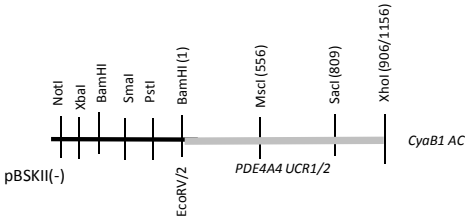


PDE4A4-CyaB1, pBSKII(-), V

Digestion with BamHI-EcoRV (≈1600bp) and ligation in BamHI-EcoRV digested, dephosphorylated vector WT, CyaB1-pQE30 (≈4200), transformation in E.coli BL21 (pREP4) cells, sequencing and expression.

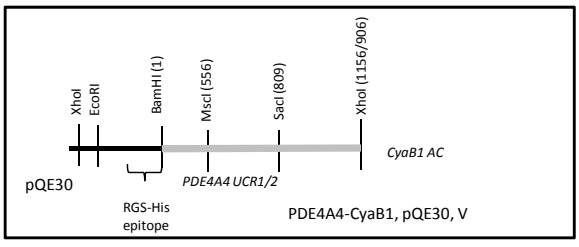

*S145D PDE4A4-CyaB1 AC (VI)*

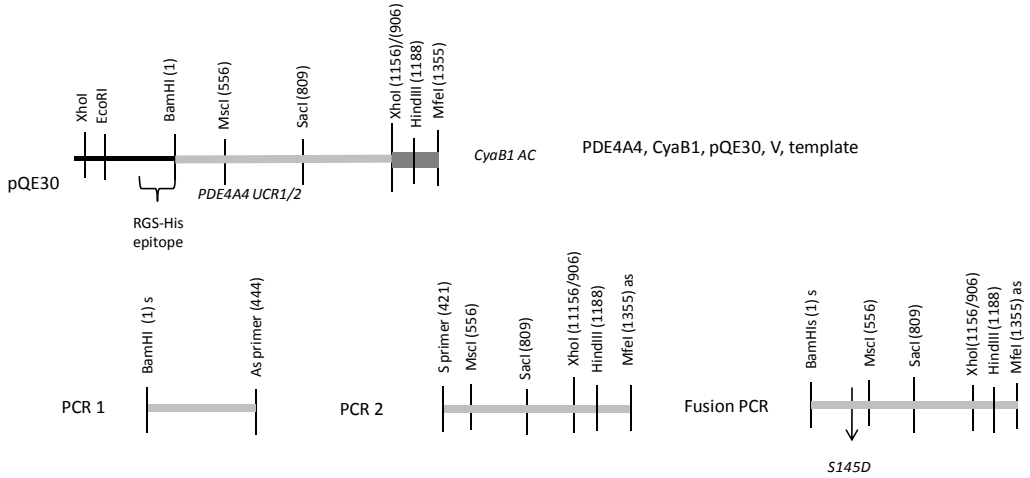


Fusion PCR digested with BamHI-HindIIII (≈ 950bp) and ligated in BamHI-HindIII digested and dephosphorylated (≈ 2900) vector pBSKII(-). Transformation in XL1 E.coli cells and sequencing.

Digestion with BamHI-SacI (≈815) and ligation in BamHI-SacI (≈5000) digested, dephosphorylated PDE4A4 V-CyaB1, pQE30 ,transformation in E.coli BL21 (pREP4) cells, sequencing and expression.

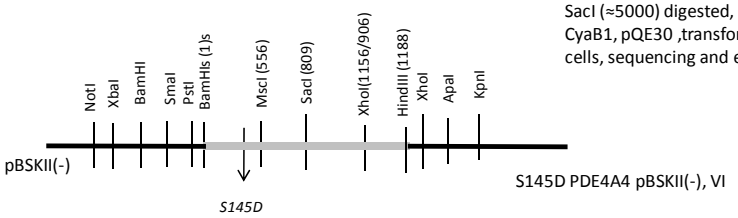


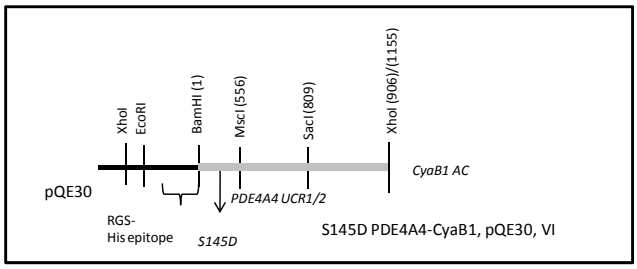

## *PDE4B1-CyaB1 AC chimeras*

### *PDE4B1-CyaB1 AC (VII)*

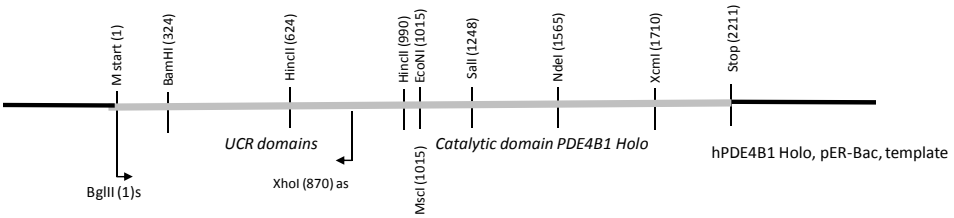


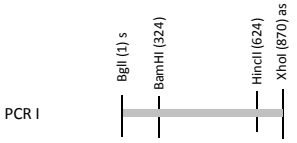


Ligation of PCR products (≈ 880bp) in EcoRV digested pBSKII(-) (≈2900bp), transformation in XL-1 cells, sequencing and checking the orientation.

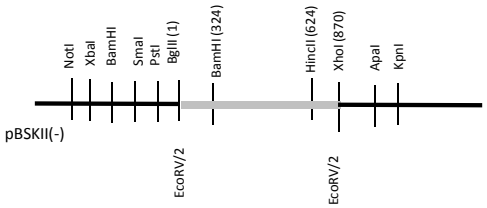


Digestion with NotI-XhoI (≈950) and ligation in NotI-XhoI (≈ 4300) digested, dephosphorylated WT CyaB1, pEBSKII(-), transformation in E.coli XL-1cells, sequencing.

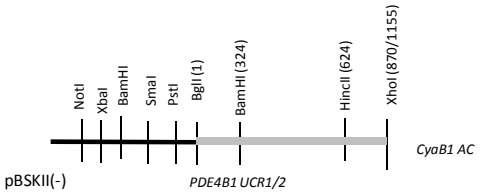


PDE4B1-CyaB1, pBSKII (-), VII

Digestion with BglII-EcoRV (≈1500bp) and ligation in BamHI-EcoRV digested, dephosphorylated vector WT, CyaB1-pQE30 (≈4200), transformation in E.coli BL21 (pREP4) cells, sequencing and expression.

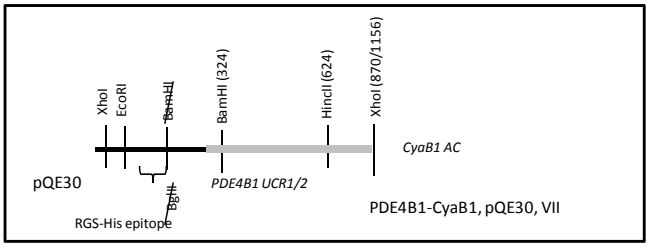

## *S133D PDE4B1-CyaB1 AC (VIII)*

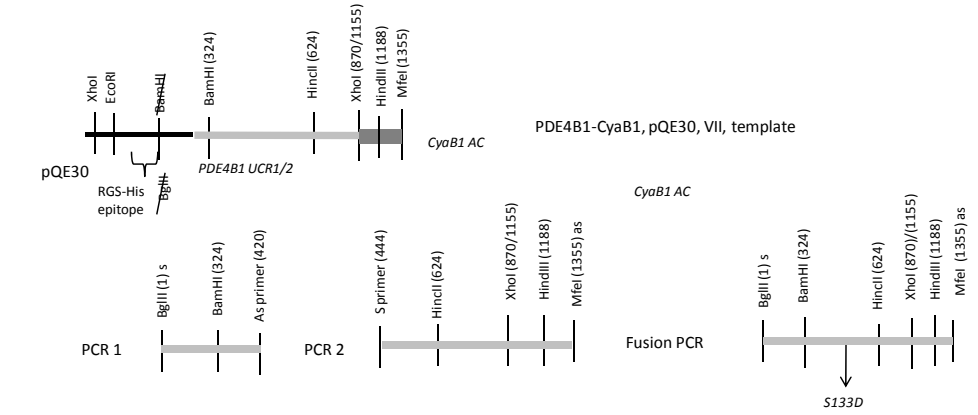


Fusion PCR (≈1085bp) digested with BglII-MfeI (≈1075bp) and ligation in BglII-MfeI digested and dephosphorylated (≈4200) vector PDE4B1-CyaB1,pBSKII(-). Transformation in XL1 E.coli cells and sequencing.

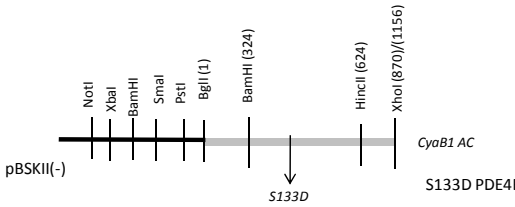


Digestion with BglII-EcoRV (≈1500) and ligation in BamHI-EcoRV ( (≈ 4300) digested, dephosphorylated WT CyaB1, pQE30 ,transformation in E.coli BL21 (pREP4) cells, sequencing and expression.

S133D PDE4B1-CyaB1, VIII, pBSKII (-)

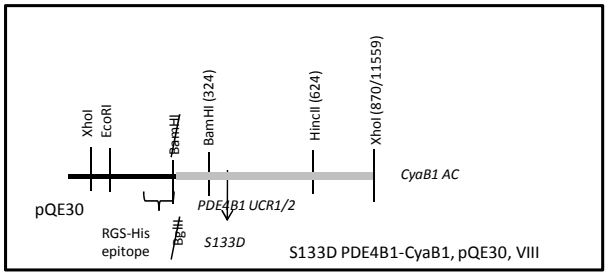

### 3.7.6 Crystal constructs

***PDE5 L136-A517, in pQE70 and in pQE82***

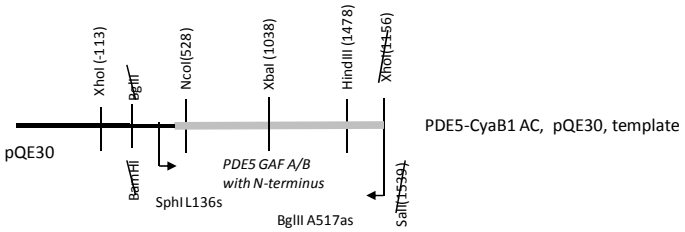


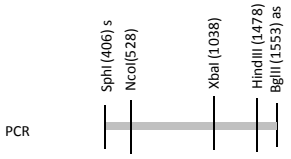


Ligation of PCR product (≈1150bp) in EcoRV digested pBSKII(-) (≈ 2900) transformation in XL-1 cells, sequencing and checking the orientation.

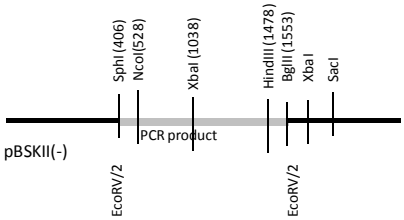


Digestion with SphI-BglII(≈1150bp) and ligation in SphI-BglII digested (≈ 3400bp) , dephosphorylated pQE70 (expression vector), sequncing transformation in E.coli BL21 (pRep4) cells and expression.

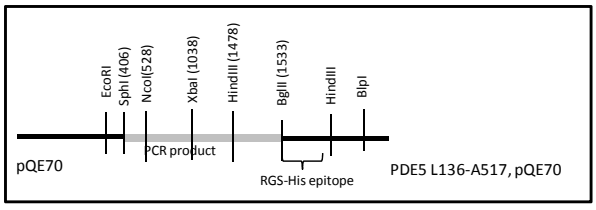


Digestion with SphI-BglII (≈1150bp), Klenow of BglII site and ligation in SphI-HindIII digested (≈3400bp) , dephosphorylated pQE82, Klenow at HindIII site sequencing , transformation in E.coli DH5α cells and than to E.coli BL21 (pRep4) cells , sequencing and expression

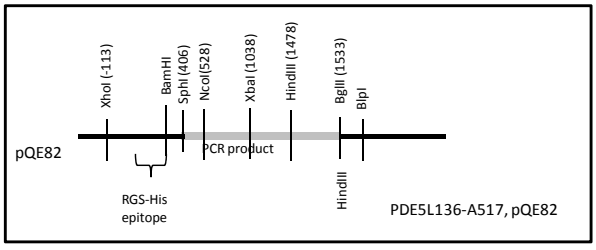

## *PDE4D3 M1-S212*

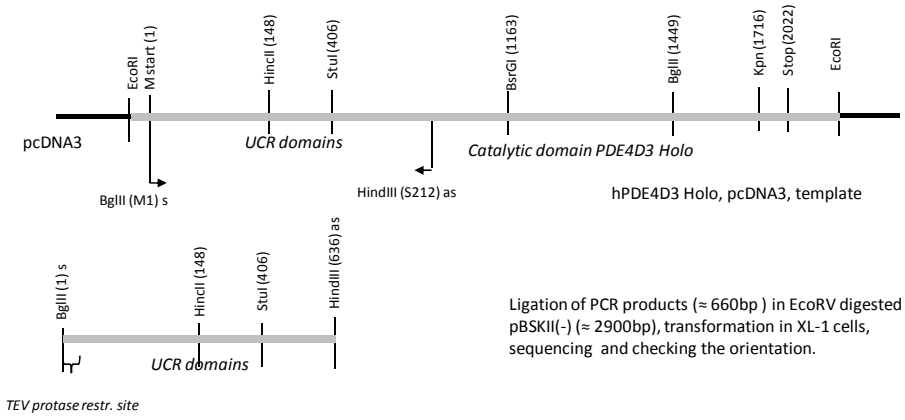


Ligation of PCR products (≈ 660bp ) in EcoRV digested pBSKII(-) (≈ 2900bp), transformation in XL-1 cells, sequencing and checking the orientation.

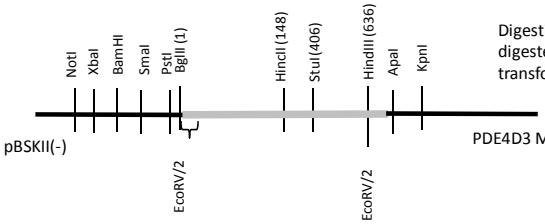


Digestion with BglII-HindIII (≈650bp), ligation in BamHI-HindIII digested, dephosphorylated vector pQE30 (≈3470), sequencing, transformation in E.coli BL21 (pREP4) cells and expression.

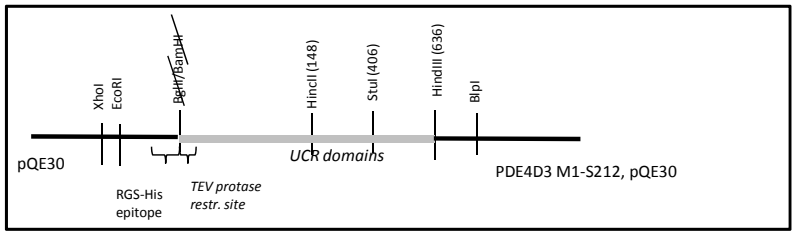

# 4 Results

## 4.1 hPDE5 N-terminus in tandem GAF signaling

In all PDEs with tandem GAF domains an N-termini (approx. 80-220 aa) precede these domains. For PDE5 and PDE11 it has been shown that these N-termini affect regulation [11, 13].

PDE5 has 148 aa long N-terminus. Phosphorylation of Ser-102 (numbering hPDE5) is one way of PDE5 regulation. It increases the affinity for cGMP on the allosteric and catalytic sites (see 1.4.4).

S. Bruder demonstrated that in PDE5-CyaB1 AC chimeras shortenings up to S102 do not change signaling; basal and stimulated activities were similar as in WT PDE5-CyaB1 AC chimeras and cGMP affinity was not much affected. Removal of S102 increased basal activity and reduced cGMP fold stimulation [11].

Three constructs were cloned (Fig. 4.1) with shortenings in predicted flexible regions between α-helices and β-sheets (by *PROTEAN, DNA STAR*):

1) PDE5 (A89-E513)-CyaB1 AC (L386-K859)
2) PDE5 (N91-E513)-
3) PDE5 (G95-E513)-

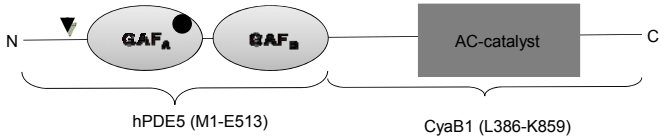


Fig. 4.1: Domain organization of hPDE5-CyaB1 AC chimera
Tandem GAF domain from PDE5 and a catalytic domain of CyaB1 AC; in front of GAF-A is the phosphorylation site (S102); in GAF-A is the cGMP binding site (black circle);

### 4.1.1 Expression and characterization of shortened PDE5-CyaB1 AC chimeras

Three constructs were cloned in pET16 MCS-pQE30, transformed in *E.coli BL-21 (DE3) [pREP4]* and sequenced. Expression was induced with 75 µM IPTG at 16°C. Cells were harvested, washed once, resuspended in lysis buffer and lysed by French Press at 1000 psi. Debris were removed and supernatant was purified with $Ni^{2+}$-NTA in the presence of 15 mM imidazole, 250 mM NaCl and 5 mM $MgCl_2$. After shaking for 3h at 0°C the resin was poured into mini-columns and washed with 5 mM imidazole + 400 mM NaCl, 15 mM imidazole + 400 mM NaCl and 25 mM imidazole + 10 mM NaCl. Proteins were eluted (300 mM imidazole) and dialysed overnight against 35% glycerol (Fig. 4.2). They were assayed

immediately and stored at -20°C. Calculated molecular masses were 100 kDa, (black arrow near SDS-PAGE gel).

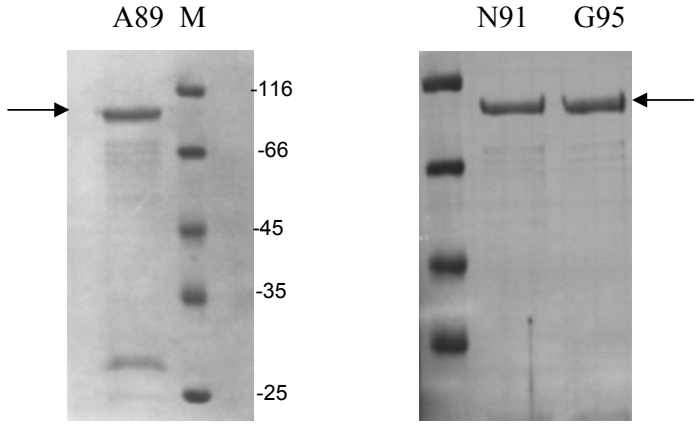


Fig. 4.2: SDS-PAGE gel (12.5%) of PDE5 A89-/N91-/G95-CyaB1 AC

After elution, protein purity was evaluated by the densitometry (see 3.3).

PDE5 A89

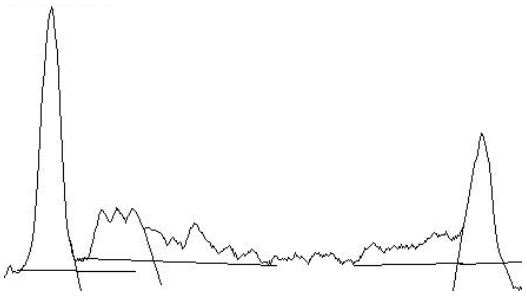

PDE5 N91

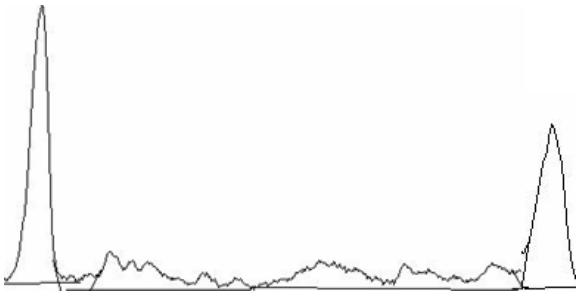

PDE5G95

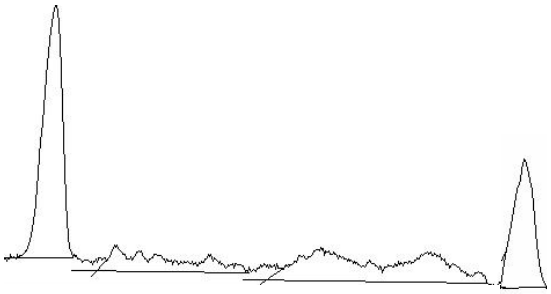

| *Protein* | *AUP* | *% of pure protein* |
|---|---|---|
| *PDE5A81* | 4.302.234 | 37.9 |
| *impurities* | 1.716.012 | 15.1 |
| *impurities* | 1.613.953 | 14.2 |
| *impurities* | 1.505.640 | 13.3 |
| *impurities* | 2.217.698 | 19.5 |
| *PDE5 N91* | 3.869.648 | 37.6 |
| *impurities* | 1.663.731 | 16.2 |
| *impurities* | 2.534.472 | 24.6 |
| *impurities* | 2.217.698 | 21.6 |
| *PDE5 G95* | 4.191.527 | 38.8 |
| *impurities* | 1.329.610 | 12.3 |
| *impurities* | 3.072.087 | 28.4 |
| *impurities* | 2.217.698 | 20.5 |

Table 4.1: Estimation of protein purity (%) by densitometry
The peak on the gel plots with the highest AUP is the signal of the purified protein;

For proteins PDE5 A89-/N91- and G95- estimated purity is similar - approx. 38% (Table 4.1). For protein dependence 0.05 µg to 5 µg of each protein were used (n=4), (Fig 4.3).

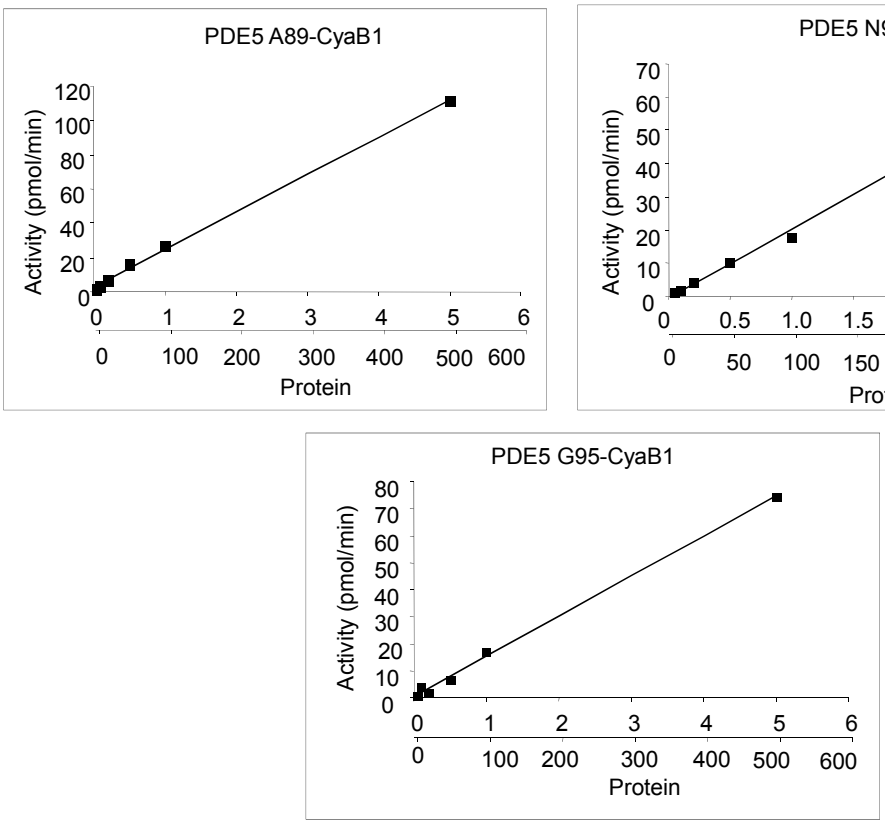


Fig. 4.3: Protein dependence of PDE5 A89-/N91-/G95-CyaB1 AC
On x-axis, upper scale represents µg of protein, lower scale nM protein;

For these constructs concentration response curves with cGMP were determined. All assays were run in quadruplicates (n=4), (Fig. 4.4). Since the estimated protein purities of three proteins were almost identical, specific activities were comparable.

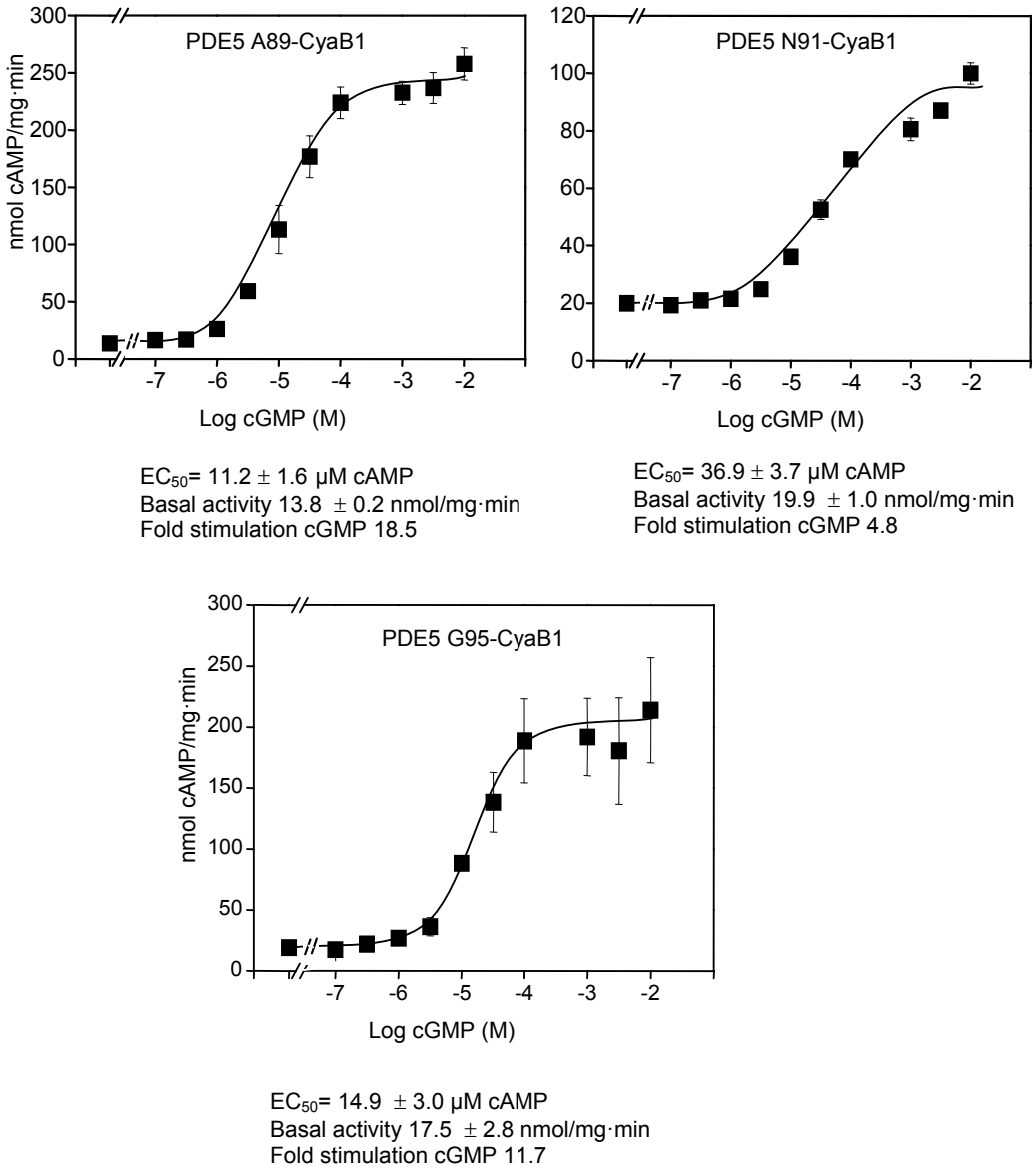


Fig. 4.4: Concentration response curves of PDE5 A89-/N91-/G95-CyaB1 AC
7.7 nM of PDE5 A89, 9.2 nM of PDE5 N91 and 8.5 nM of PDE5 G95 were used in assays;

| *Protein* | *$EC_{50}$ cGMP (µM)* | *Fold activation by cGMP* |
|---|---|---|
| *WT PDE5** | 22.1 ± 1.3 | 6.3 |
| *PDE5 A89* | 11.2 ±1.6 | 18.5 |
| *PDE5 N91* | 36.9 ± 3.7 | 4.8 |
| *PDE5 G95* | 14.9 ± 3.0 | 11.7 |

Table 4.2: Summary: $EC_{50}$ values and cGMP fold stimulation of PDE5 A89-/N91-/G95- and WT PDE5-CyaB1 AC

The three shortened constructs were cGMP activated similar as WT PDE5-CyaB1.

*- WT PDE5-CyaB1 AC assay results (p.83)

## 4.2 Insertion of NAAIRS between hPDE5 GAF-B and CyaB1 AC

All constructs have the same end of PDE5 - E513, which according to the alignment represents the end of the GAF-B domain. CyaB1 AC starts with L386. To test if PDE5 chimeras were recombined optimally, the hexapaptide NAAIRS was inserted inbetween these two parts (Fig. 4.5). This hexapeptide is flexible and reported to adopt any secondary structure [97].

PDE5 (M1-E513) NAAIRS-CyaB1 AC (L386-K859)

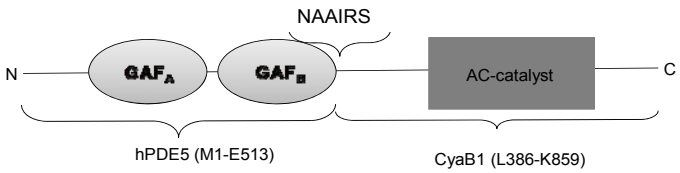


Fig. 4.5: Domain organization of PDE5 NAAIRS-CyaB1 AC; the hexapeptide NAAIRS was inserted at the junction;

### 4.2.1 Expression and characterization of PDE5 NAAIRS-CyaB1 AC

The construct was cloned in pET16b MCS-pQE30, transformed in *E.coli BL-21 (DE3) [pREP4]*, sequenced and expressed. Expression was induced with 25 µM IPTG at 16°C. Protein was purified with $Ni^{2+}$-IDA affinity chromatography in the presence of 7.5 mM imidazole and washed with 35 mM imidazole + 400 mM NaCl, 70 mM imidazole + 400 mM NaCl and 70 mM imidazole + 10 mM NaCl. After protein elution (300 mM imidazole) it was dialysed overnight against 35% glycerol, assayed immediately and stored at -20°C. Calculated molecular mass was 114 kDa (black arrow).

Expression and purification conditions were optimized. Parameters which were explored were: T, IPTG concentration, concentration of imidazole in cell lysis buffer, Ni slurry used in affinity chromatography purification, imidazole concentration in cell wash buffers. The protein was best purified when using $Ni^{2+}$-IDA agarose and higher imidazole concentrations for wash (Fig.4.6).

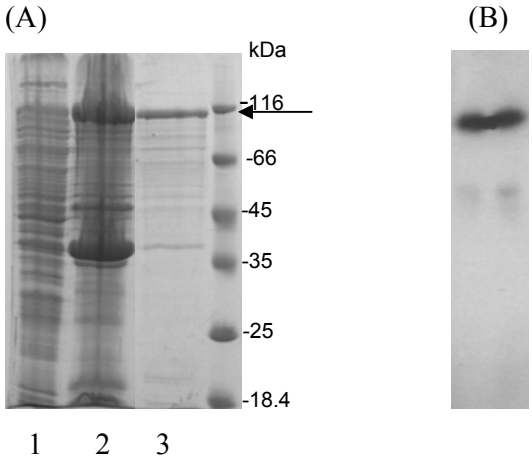


Fig. 4.6: (A) SDS-PAGE gel (12.5%) of PDE5 NAAIRS-CyaB1 AC, (B) Western blot (0.03µg)
Lane 1 supernatant after cell lysis (3µg); lane 2 pellet after cell lysis (4µg); lane 3 eluted protein (5µg);

Protein purity after elution was evaluated by the densitometry (see 3.3), as described with PDE5 shortened constructs (see Table 4.1.). Estimated protein purity was 66%.

For protein dependence 0.03-1 µg of protein was used. (n=4), (Fig. 4.7).

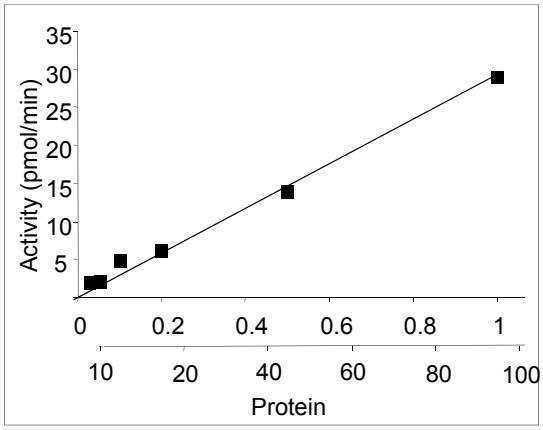


Fig. 4.7: Protein dependence of PDE5 NAAIRS-CyaB1 AC
On x-axis, upper scale represents µg of protein, lower scale nM protein;

In concentration response assays 3 nM protein was assayed with cAMP and cGMP (n=4), (Fig.4.8).

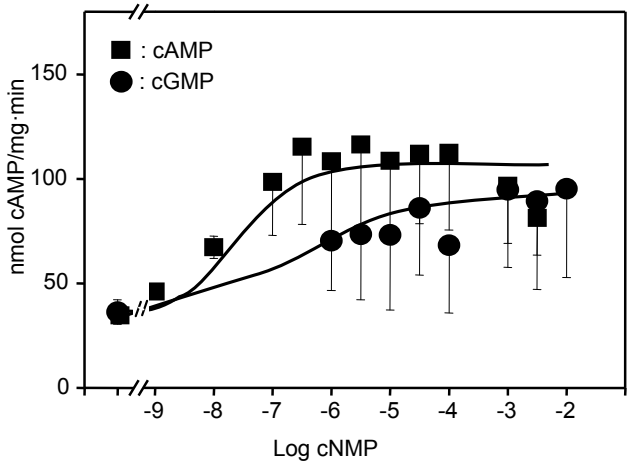


Fig. 4.8: Concentration response curves of PDE5 NAAIRS-CyaB1 AC

| *Protein* | *$EC_{50}$ cGMP (μM)* | *Fold activation by cAMP* | *Fold activation by cGMP* |
|---|---|---|---|
| *WT PDE5* | 22.1 ± 1.3 | - | 6.3 |
| *PDE5 NAAIRS-* | - | 2.5 | 2.0 |

Table 4.3: Summary: $EC_{50}$ values, cAMP and cGMP fold stimulation of PDE5 NAAIRS- and WT PDE5-CyaB1 AC

Due to the minor cGMP stimulating effect on PDE5 NAAIRS-CyaB1 AC, an $EC_{50}$ value could not be calculated (Table 4.3). Insertion of the hexapeptide NAAIRS probably changed the flexibility of the chimera and impaired completely coupling since it was up to 3-fold cAMP stimulated and only 2-fold GMP stimulated.

## 4.3 hPDE10 and hPDE5 α-helical linker in tandem GAF signaling

CyaB1 AC chimeras with only GAF-A of PDE5 are unregulated [9]. What is the structural relationship between the two GAF domains in the tandem, when only one binds a cNMP?

Earlier data from K.Hofbauer demonstrated that specific interdomain interactions occur in GAF chimeras of PDE10 and PDE5 [12] e.g. swapping the linkers between GAF domains of PDE5 and PDE10 (Fig. 4.9) abrogated signaling (Fig. 4.10). Obviously, sequence differences in the linkers provide for highly specific interactions between the two GAFs which are important for intramolecular signal transmission.

The α–helical linker is 36 aa long in all PDE with tandem GAF domains and CyaB1 and 2 ACs.

```
PDE5linker  : GIVLHNAQLYETSLLENKRNQVLLDLASLIFEEQQS    36
PDE10linker : SVAIHQVQVCRGLAKQTELNDFLLDVSKTYFDNIVA    36
```

Fig. 4.9: Sequence alignment of the linker between GAF-A and GAF-B domains of PDE5 and PDE10

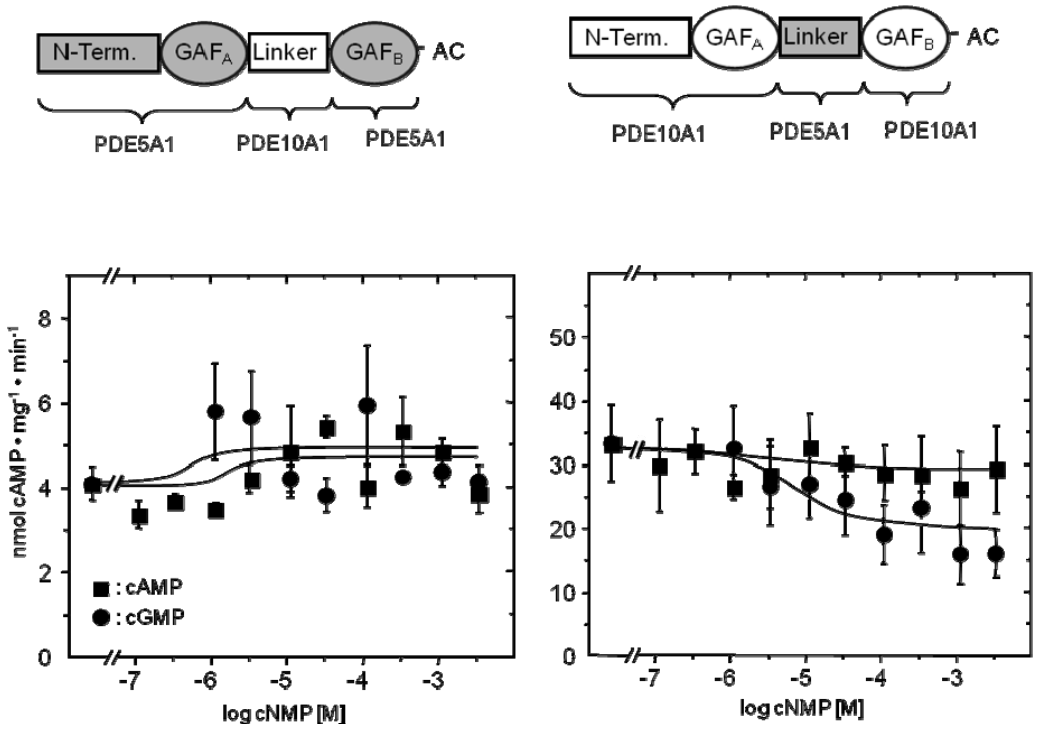


Fig. 4.10: Domain organization and concentration response curves of PDE5 and PDE10 linker chimeras, from [12]

### 4.3.1 Expression and characterization of PDE10, PDE5 (G311-S346)-CyaB1 AC chimeras (No.1-16)

A series of constructs were generated to investigate the molecular basis of linker specificity in PDE5 and 10. These isoforms were selected because in PDE5 **cGMP** effects are mediated via GAF-**A** and in PDE10 **cAMP** effects are mediated via GAF-**B**. Two by two aa from PDE5 linker were introduced in PDE10 linker (Fig. 4.11). Constructs No.1-15 and WT PDE10 were cloned in pETDuet MSC-pQE30, construct No.16 in pRSET-A was from K.Hofbauer. Clones No.1-12 were transformed in *E.coli Rosetta BL21 (pLys*S) and No.13-16 in *E.coli BL-21 (DE3) [pREP4]*.

```
PDE10 (WT)   SVAIHQVQVCRGLAKQTELNDFLLDVSKTYFDNIVA
No.1         GIAIHQVQVCRGLAKQTELNDFLLDVSKTYFDNIVA
No.2         GIVLHQVQVCRGLAKQTELNDFLLDVSKTYFDNIVA
No.3         GIVLHNAQVCRGLAKQTELNDFLLDVSKTYFDNIVA
No.4         GIVLHNAQLYRGLAKQTELNDFLLDVSKTYFDNIVA
No.5         GIVLHNAQLYETLAKQTELNDFLLDVSKTYFDNIVA
No.6         GIVLHNAQLYETSLKQTELNDFLLDVSKTYFDNIVA
No.7         GIVLHNAQLYETSLLETELNDFLLDVSKTYFDNIVA
No.8         GIVLHNAQLYETSLLENKLNDFLLDVSKTYFDNIVA
No.9         GIVLHNAQLYETSLLENKRNDFLLDVSKTYFDNIVA
No.10        GIVLHNAQLYETSLLENKRNQVLLDVSKTYFDNIVA
No.11        GIVLHNAQLYETSLLENKRNQVLLDLAKTYFDNIVA
No.12        GIVLHNAQLYETSLLENKRNQVLLDLASLYFDNIVA
No.13        GIVLHNAQLYETSLLENKRNQVLLDLASLIFDNIVA
No.14        GIVLHNAQLYETSLLENKRNQVLLDLASLIFEEIVA
No.15        GIVLHNAQLYETSLLENKRNQVLLDLASLIFEEQQA
No.16(PDE5)  GIVLHNAQLYETSLLENKRNQVLLDLASLIFEEQQS
```

Fig. 4.11: List of linker clones
Green letters represent conserved aa;

With constructs No.1 and WT PDE10- expression was optimized (Fig. 4.12 and 4.13). Optimized conditions (protein was always eluted with 300 mM imidazole):

- expression temperature: 16°C, 12 h and 24°C 4-6 h
- IPTG concentration: 100 µM and 400 µM
- cell lysis buffer ± 2-Mercaptoethanol
- imidazole concentrations during protein purification (in cell lysis buffer, $Ni^{2+}$ affinity chromatography, in wash buffers)

Construct No.1:

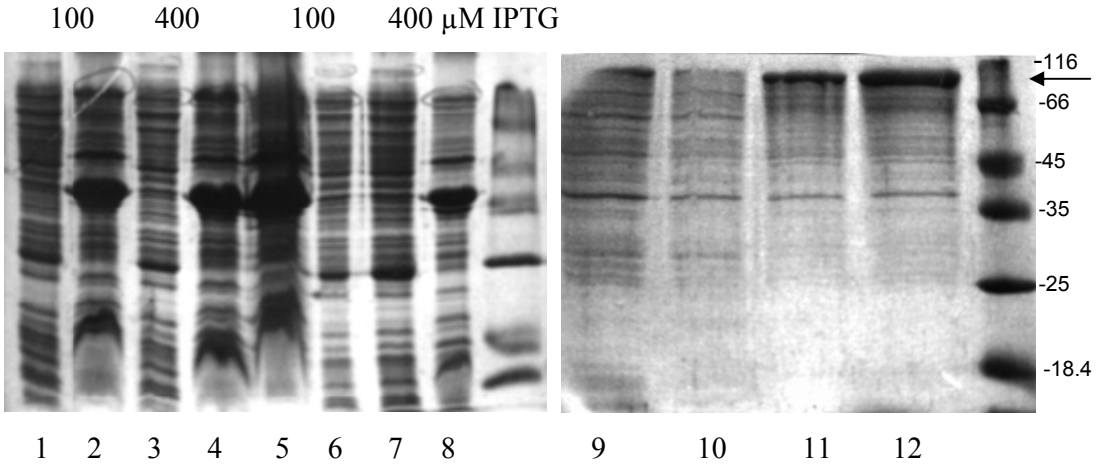


Fig. 4.12: SDS-PAGE gels (12.5%) of No.1;
Expression at 16°C and 24°C, induction with 100 and 400 µM IPTG; purification with $Ni^{2+}$-IDA (25 mM imidazole, 400 mM NaCl, 5 mM $MgCl_2$); lanes 1, 3, 6 and 7 supernatant after cell lysis at 24°C and 16°C induced with 100 µM and 400 µM IPTG (3 µg); lanes 2, 4, 5 and 8 pellet after cell lysis at 24°C and 16°C (4 µg) induced with 100 µM and 400 µM IPTG; lanes 9 and 10 eluted proteins at 24°C induced with 100 µM and 400 µM IPTG; lanes 11 and 12 eluted proteins at 16°C induced with 100 µM and 400 µM IPTG, respectively all washed with 40 mM imidazole + 400 mM NaCl, 50 mM imidazole + 400 mM NaCl and 75 mM imidazole + 10 mM NaCl (2.5 µg);

The yield of protein was better after expression at 16°C, but the purity was not satisfying.

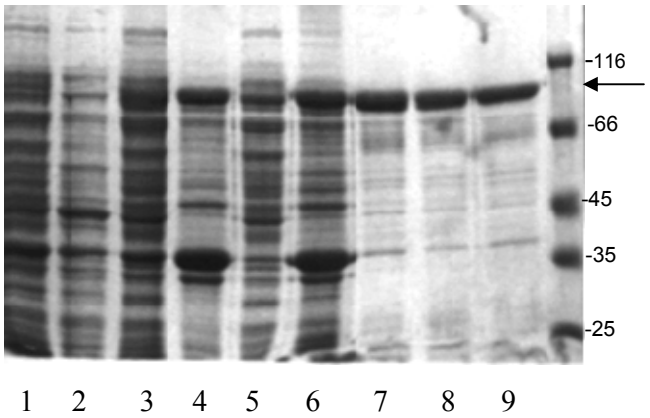


Fig. 4.13: SDS-PAGE gel (10%) of WT PDE10-CyaB1 AC, pETDuet MCS-pQE30
Expression at 16°C , induction with 400 µM IPTG; lane 1 before induction; lane 2 before harvesting; lanes 3 and 5 supernatant after cell lysis (8 µg) with cell lysis buffer ± 2-ME; lanes 4 and 6 pellet after cell lysis (8 µg); lane 7 eluted protein (cell lysis without 2-ME) after $Ni^{2+}$-IDA purification with 25 mM imidazole (400 mM NaCl and 5 mM $MgCl_2$) , washed with 35 mM imidazole + 400 mM NaCl, 55 mM imidazole + 400 mM NaCl and 75 mM imidazole + 10 mM NaCl; lane 8 eluted protein (cell lysis with 2-ME) after $Ni^{2+}$-IDA purification without imidazole (400 mM NaCl and 5 mM $MgCl_2$), washed with 5 mM imidazole + 400 mM NaCl, 10 mM imidazole + 400 mM NaCl and 15 mM imidazole + 400 mM NaCl; lane 9 eluted protein (cell lysis with 2-ME) after $Ni^{2+}$-IDA purification without imidazole (400 mM NaCl and 5 mM $MgCl_2$), washed with 40 mM imidazole + 400mM NaCl, 50 mM imidazole + 400 mM NaCl and 60 mM imidazole + 400 mM NaCl;

The yield of the WT PDE10-CyaB1 AC protein was good and the purity was satisfying. Proteins No.1-16 were expressed and purified using the conditions outlined in the legend of

Fig. 4.13. Cell cultures were induced with 400 µM IPTG and grown overnight at 16°C. Proteins were purified with $Ni^{2+}$-IDA affinity chromatography in the presence of 25 mM imidazole, 400 mM NaCl and 5 mM $MgCl_2$ and washed with 35 mM imidazole + 400 mM NaCl, 55 mM imidazole + 400 mM NaCl and 75 mM imidazole + 10 mM NaCl. After protein elution (300 mM imidazole) they were dialysed overnight against 35% glycerol, assayed immediately and stored at -20°C. Mw were 101 kDa, except for No.16, 104 kDa.

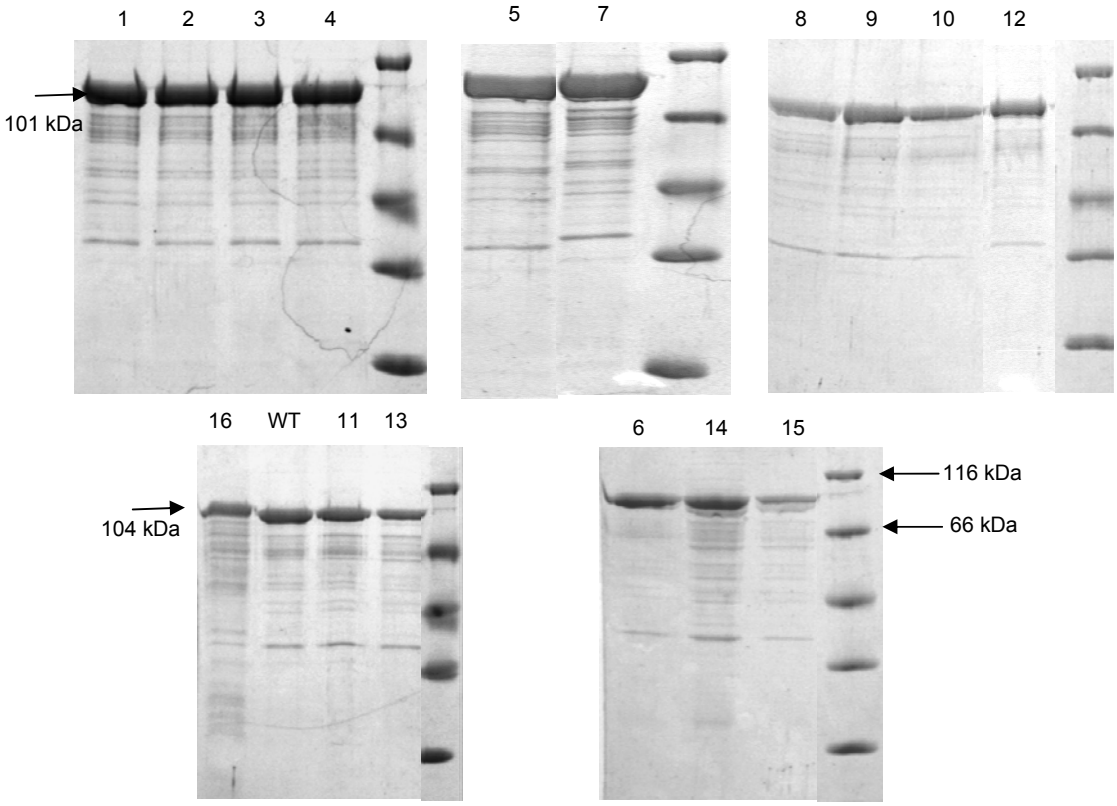


Fig. 4.14: SDS-PAGE gels (12.5%) of No.1-16 and WT PDE10-CyaB1 AC
Constructs No.1, 2, 3, 4, - 3.5 µg; 5, 6, 7, 14, 15 – 3 µg; 8, 9, 10, 12 – 2.5 µg; WT, 11, 13, 16 – 2 µg;

After elution purity of each protein was estimated by the densitometry (Table 4.4), as described (see Table 4.1.).

| *Protein* | *% of pure protein* | *Protein* | *% of pure protein* |
|---|---|---|---|
| *WT PDE10* | 78.7 | *No.9* | 74.8 |
| *No.1* | 76.5 | *No.10* | 84.9 |
| *No.2* | 79.1 | *No.11* | 71.2 |
| *No.3* | 77.4 | *No.12* | 82.5 |
| *No.4* | 81.0 | *No.13* | 73.1 |
| *No.5* | 75.2 | *No.14* | 80.3 |
| *No.6* | 84.1 | *No.15* | 76.5 |
| *No.7* | 74.9 | No.16 | 75.6 |
| *No.8* | 75.1 | | |

Table 4.4: Estimation of protein purity (%) by densitometry

For WT PDE10 and No.1-16 estimated purity is similar 75-85%. Their specific activities were comparable.

Western blottings showed no degradation products (Fig. 4.15).

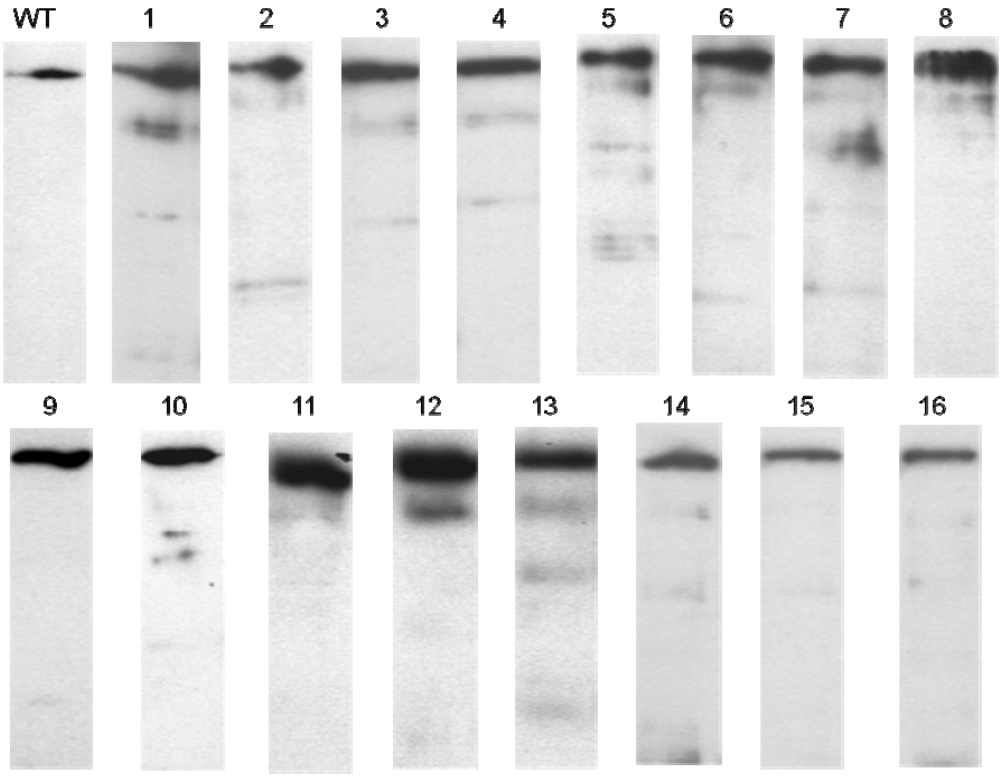


Fig. 4.15: Western blots of No.1 - 16 and WT (0.05–1 µg)
0.5 µg - WT, 3, 4, 5, 6, 9, 11, 12, 13, 15, 16 1 µg - 1, 2, 10; 0.1 µg - 7, 8, 14;

For all constructs concentration response curves with cAMP and cGMP were established (0.1 µg of each protein was assayed, approx. 10 nM), (n=4-8), (Fig. 4.16). Basal activities, 300 µM cAMP and cGMP points were compared (Fig. 4.17 and 4.18).

No.1 GI

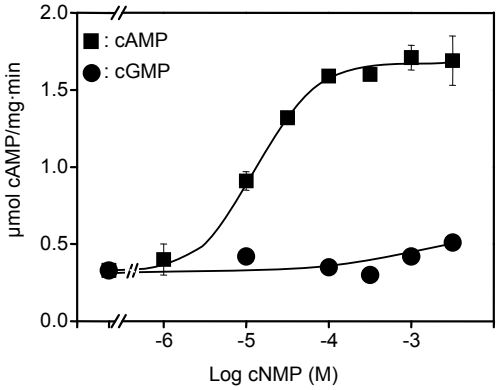


$EC_{50}$= 12.1±1.4 µM cAMP
Basal activity 0.33 ±0.02 µmol/mg·min
Fold stimulation cAMP 5.2

No.2 GIVL

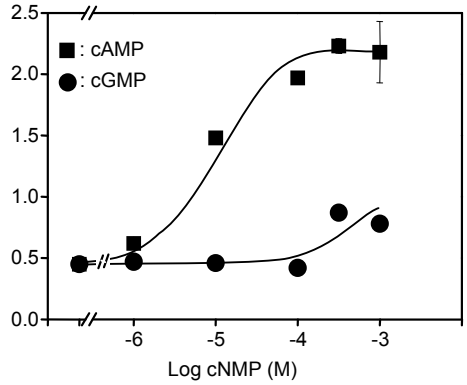


$EC_{50}$= 6.6 ± 0.9 µM cAMP
Basal activity 0.45 ± 0.02 µmol/mg·min
Fold stimulation cAMP 5.0

No.3 GIVLHNA

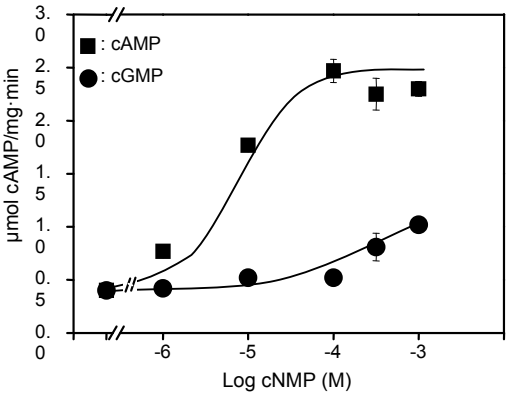


$EC_{50}$= 3.9 ± 0.5 µM cAMP
Basal activity 0.40 ± 0.04 µmol/mg·min
Fold stimulation cAMP 6.3

No.4 GIVLHNAQLY

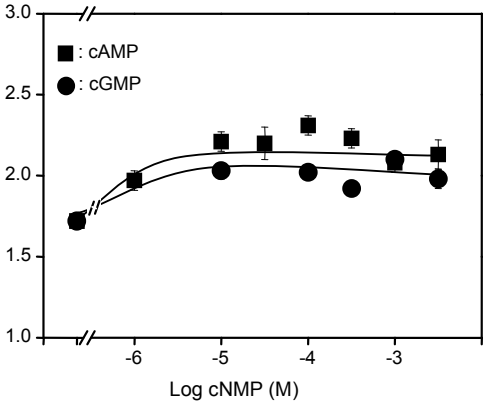


$EC_{50}$= 1.0 ± 0.02 µM cAMP
Basal activity 1.72 ± 0.05 µmol/mg·min
Fold stimulation cAMP 1.2

No.5 GIVLHNAQLYET

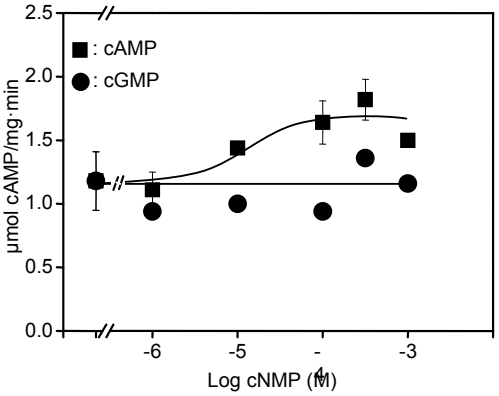


Basal activity 1.18 ± 0.23 µmol/mg·min
Fold stimulation cAMP 1.3

No.6 GIVLHNAQLYETSL

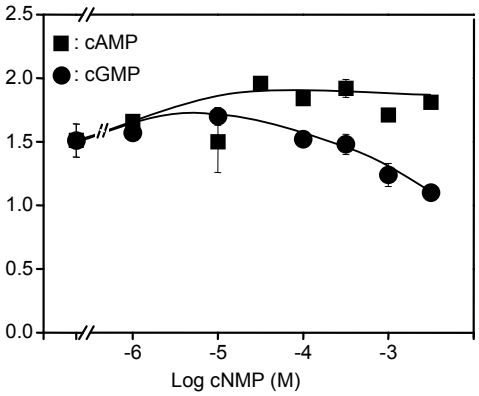


Basal activity 1.51 ± 0.13 µmol/mg·min
Fold stimulation cAMP 1.3

No.7 GIVLHNAQLYETSLLE

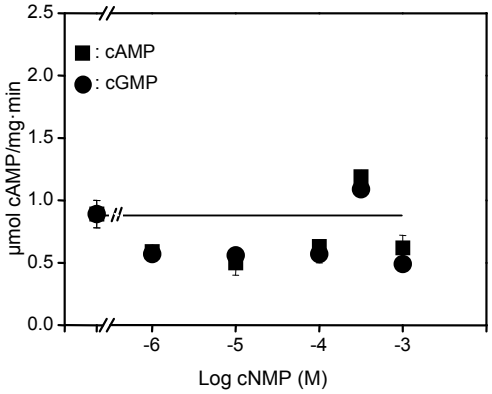


Basal activity 0.89 ± 0.11 µmol/mg·min
Fold stimulation cAMP -

No.8 GIVLHNAQLYETSLLENK

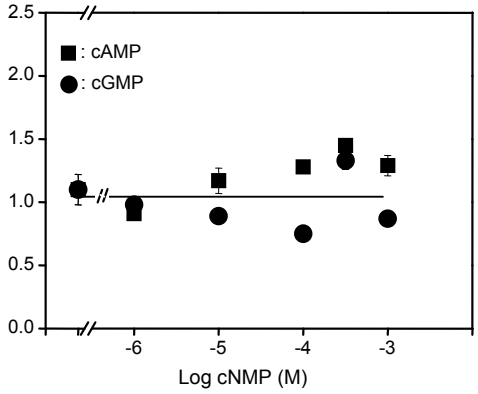


Basal activity 1.1 ± 0.12 µmol/mg·min
Fold stimulation cAMP -

No.9 GIVLHNAQLYETSLLENKRN

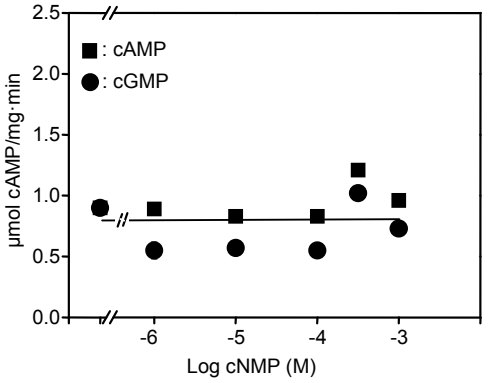


Basal activity 0.90 ± 0.01 µmol/mg·min
Fold stimulation cAMP -

No.10 GIVLHNAQLYETSLLENKRNQV

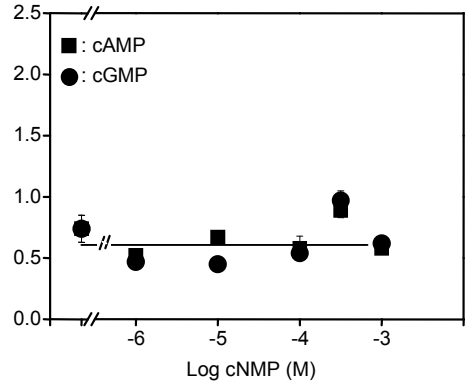


Basal activity 0.74 ± 0.11 µmol/mg·min
Fold stimulation cAMP -

No.11 GIVLHNAQLYETSLLENKRNQVLLDLA

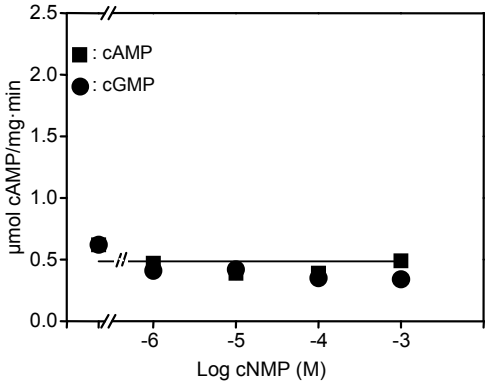


Basal activity 0.62 ± 0.01 µmol/mg·min
Fold stimulation cAMP -

No.12 GIVLHNAQLYETSLLENKRNQVLLDLASL

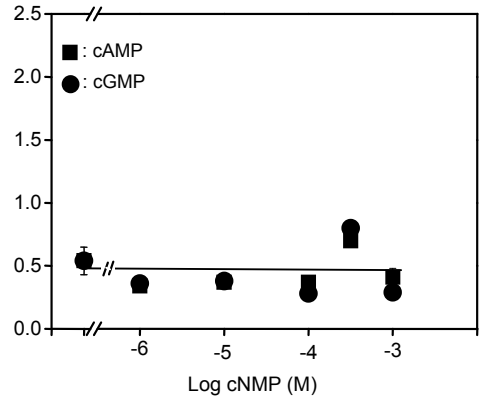


Basal activity 0.54 ± 0.11 µmol/mg·min
Fold stimulation cAMP -

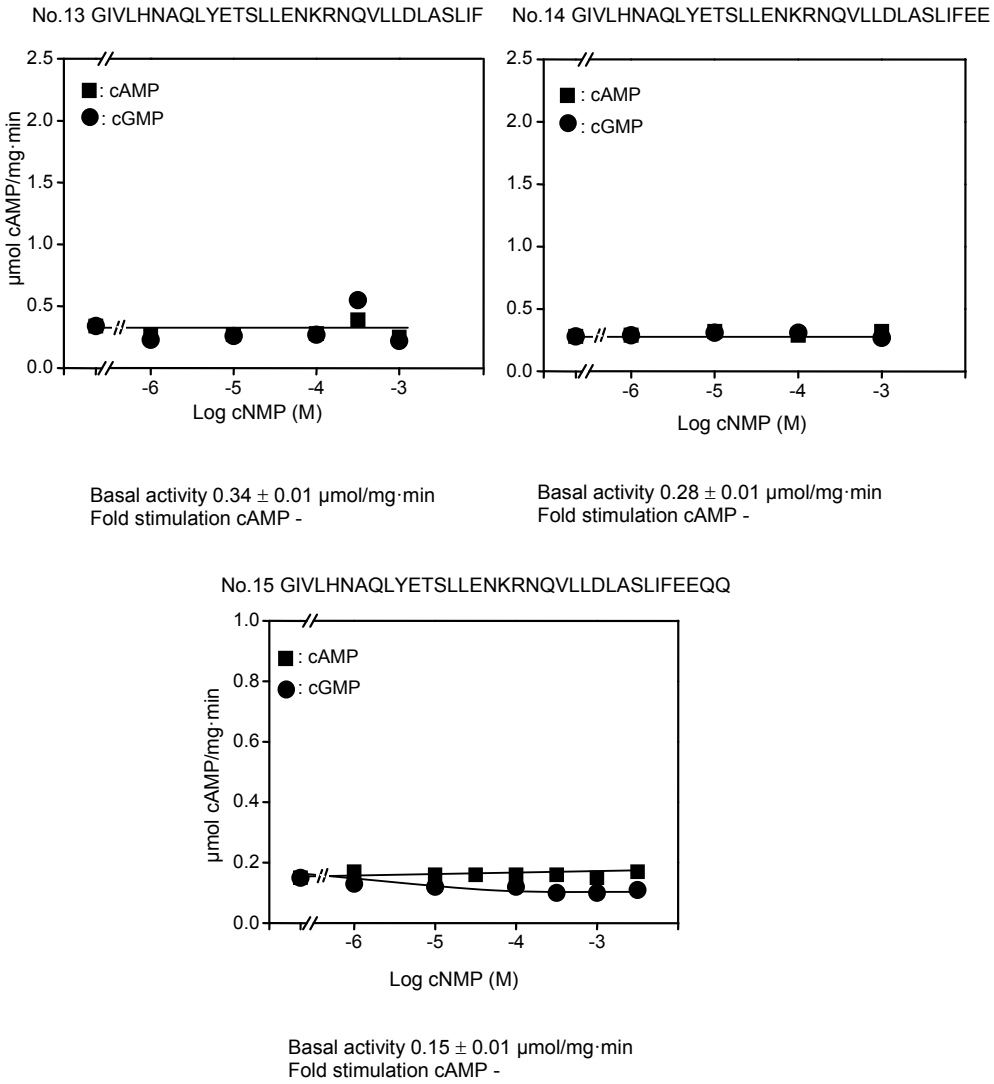


Fig. 4.16: Concentration response curves of No.1-15
No.16 was assayed by K. Hofbauer, Fig. 4.10

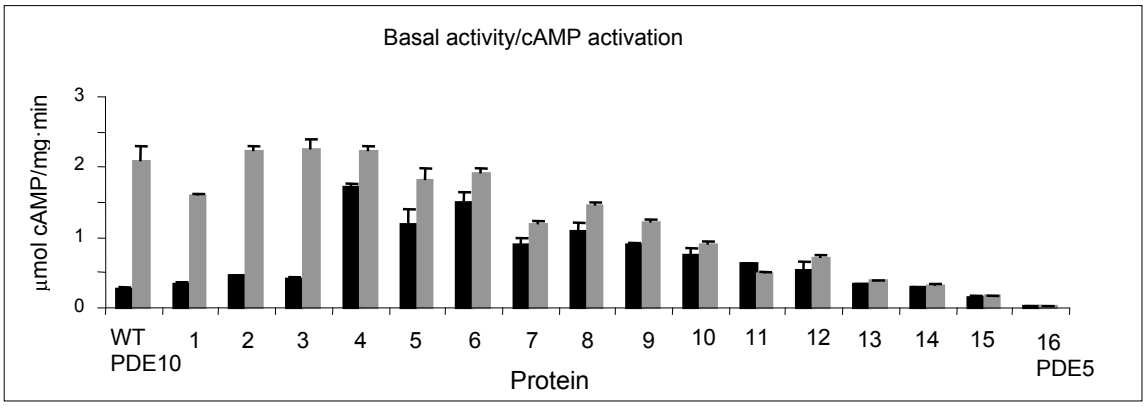


Fig. 4.17: Comparison of AC activities ± 300 µM cAMP; black bars basal activity, grey bars + cAMP

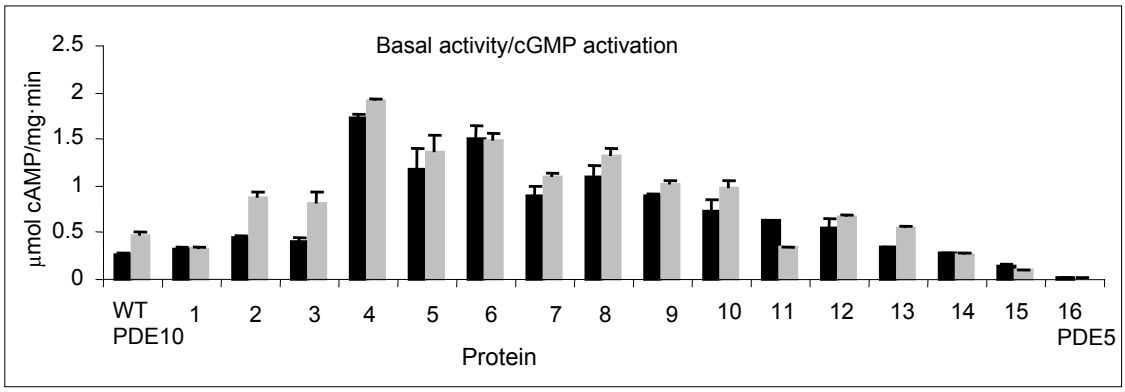


Fig. 4.18: Comparison of AC activities ± 300 µM cGMP; black bars basal activity, grey bars + cGMP

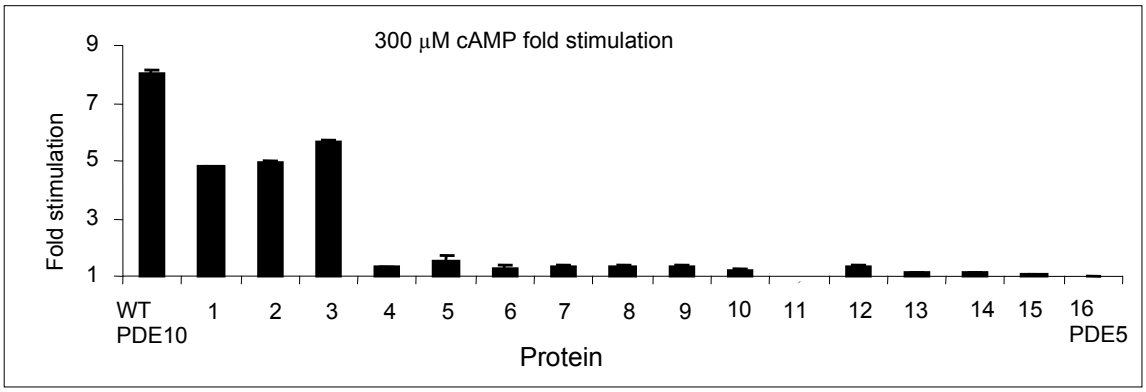


Fig. 4.19: Fold stimulation with 300 µM cAMP

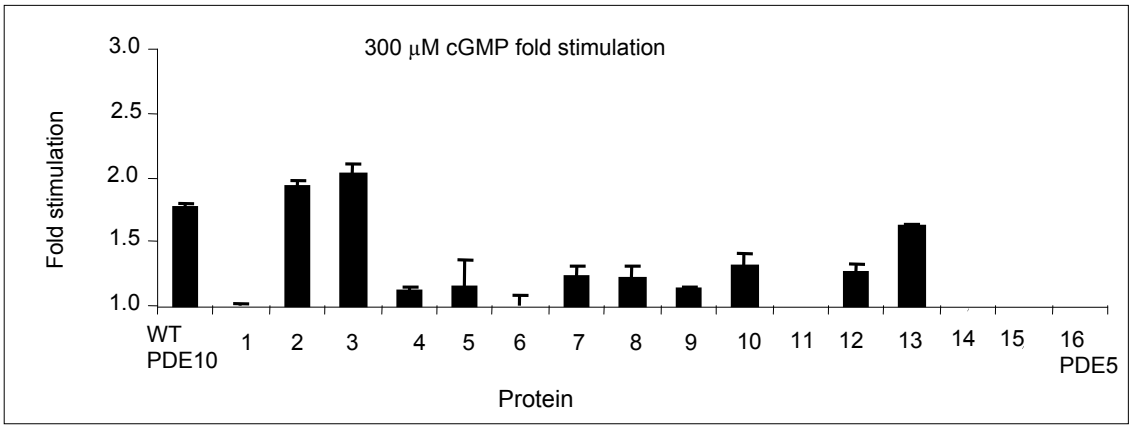


Fig. 4.20: Fold stimulation with 300 µM cGMP

| *Protein* | *$EC_{50}$ (µM cAMP)* | *cAMP stimulation* | *cGMP stimulation* |
|---|---|---|---|
| *WT PDE 10* | 8.1 ± 2.0 | 8.0 | 1.8 |
| *No.1* | 12.1 ± 1.4 | 5.2 | - |
| *No.2* | 6.6 ± 0.9 | 5.0 | 1.9 |
| *No.3* | 3.9 ± 0.5 | 6.3 | 2.0 |
| *No.4* | 1.0 ± 0.02 | 1.2 | - |

Table 4.5: Summary: $EC_{50}$ values, cAMP and cGMP fold stimulation of No.1-4 and WT PDE10-CyaB1 AC
$EC_{50}$ values for No.5-16 could not be determined and No.5-16 were not cAMP and cGMP activated;

Constructs No.1-3 were stimulated with cAMP, the No.4-16 were not any more (Table 4.5). By mutations of V239L and C240Y in construct No.4, cAMP regulation was lost and basal activity was approx. 7 fold higher. In the next experiment single mutations of these aa were introduced in construct No.3.

### 4.3.2 Expression and characterization of chimeras No.17 and 18

To determine which mutation in No.4 was responsible for loss of regulation No.3 with V239 mutated to L (No.17) and No.3 with C240 mutated to Y (No.18) were cloned (Fig. 4.21).

Fig. 4.21: Sequences of the linkers in chimeras No.17 and 18

Constructs were cloned in pETDuet MCS-pQE30, transformed in *E.coli BL-21 Rosetta (pLysS)*, expressed and purified (see 4.3.1), (Fig. 4.22). Mw were 101 kDa.

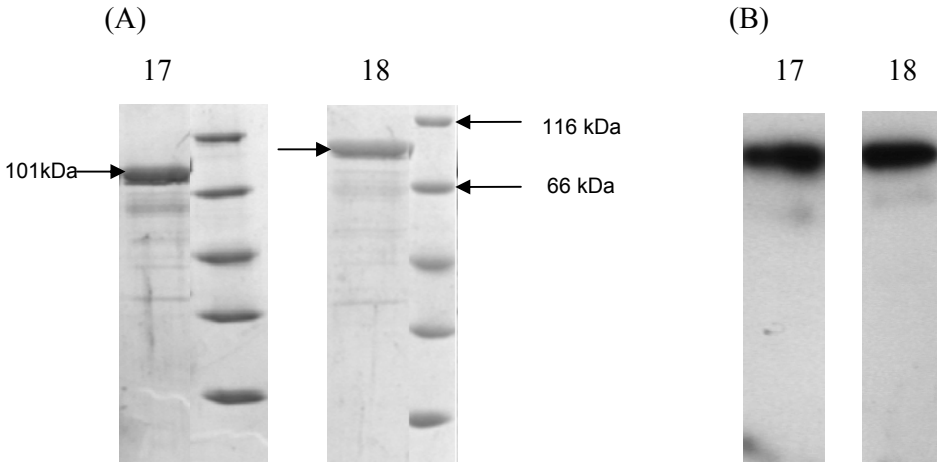


Fig. 4.22: (A) SDS-PAGE gel (12.5%) (3 µg) (B) Western blot (0.5 µg) of No.17 and 18

After elution protein purity was estimated by the densitometry (Table 4.6), as described (see Table 4.1.).

| *Protein* | *% of pure protein* |
|---|---|
| *WT PDE10* | 78.7 |
| *No.17* | 79.1 |
| *No.18* | 74.5 |

Table 4.6: Estimation of protein purity (%) by densitometry

For WT PDE10 and No.17 and 18 estimated purities are similar 75-80%. Their specific activities were comparable.

Concentration response curves with cAMP and cGMP were established (0.1 µg of each protein was assayed, approx. 10 nM, n=4) (Fig. 4.23). Basal activities, 300 µM cAMP and cGMP points were compared (Fig. 4.24 and 4.25).

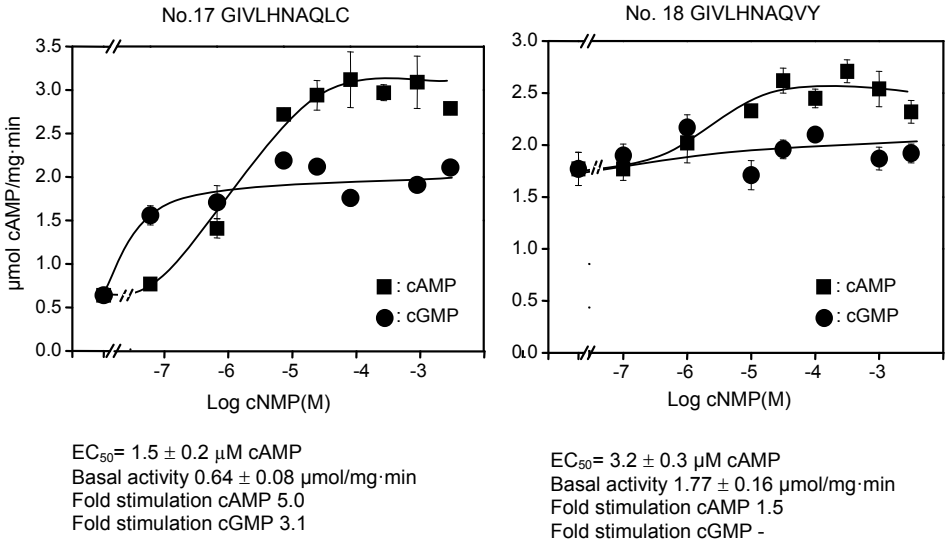


Fig. 4.23: Concentration response curves of No.17 and 18

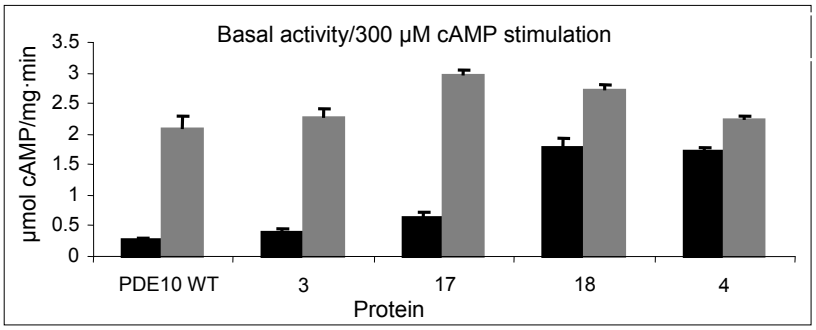


Fig. 4.24: Comparison of AC activities ± 300 µM cAMP; black bars basal activity, grey bars + cAMP

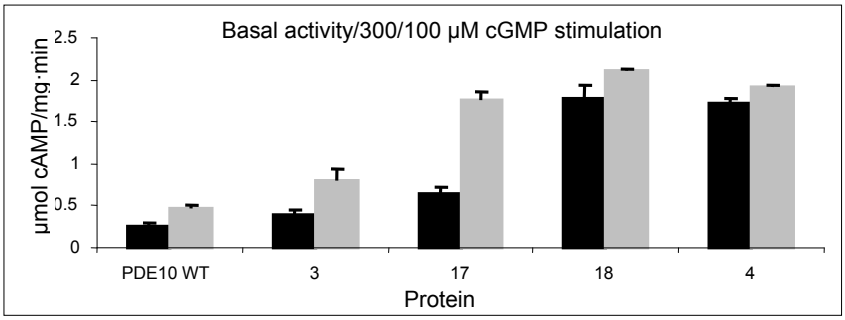


Fig. 4.25: Comparison of AC activities ± 300/100 µM cGMP (for No.17 and 18 ± 100 µM cGMP); black bars basal activity, grey bars + cGMP

(A) (B)

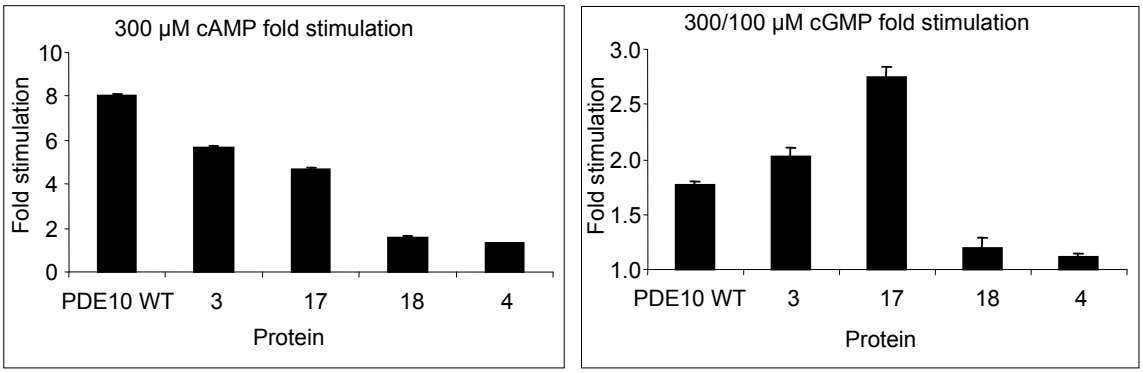


Fig. 4.26: Fold stimulation with (A) 300 µM cAMP (B) 300 µM cGMP (100 µM for No.17 and 18)

| *Protein* | *$EC_{50}$ (µM cAMP)* | *cAMP fold stimulation* | *cGMP fold stimulation* |
|---|---|---|---|
| *WT PDE10* | 8.1 ± 2.0 | 8.0 | 1.8 |
| *No.3* | 3.9 ± 0.5 | 6.3 | 2.0 |
| *No.17* | 1.5 ± 0.2 | 5.0 | 3.1 |
| *No.18* | 3.2 ± 0.3 | 1.5 | - |
| *No.4* | 1.0 ± 0.02 | 1.2 | - |

Table 4.7: Summary: $EC_{50}$ values, cAMP and cGMP fold stimulation of No.3, 4, 17, 18 and WT PDE10-CyaB1 AC

Construct No.17 was cAMP activated and had similar properties as No.3. Construct No.18 lost cAMP activation and was similar to No.4 (Table 4.7).

### 4.3.3 Expression and characterization of chimeras No.19-21

To check the contribution of V239 and C240 to regulation of the catalytic domain, two single mutations V239L (No.20) and C240Y (No.21) and a double mutation (No.19) were introduced in the PDE10 linker (Fig. 4.27).

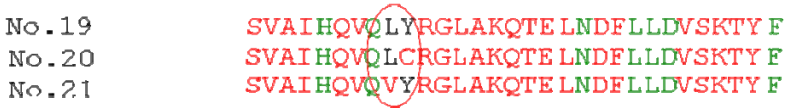


Fig. 4.27: Sequences of the linkers in proteins No.19, 20 and 21

Constructs were cloned in pETDuet MCS-pQE30, transformed in *E.coli Rosseta BL21 (pLysS)*, expressed and purified (see 4.3.1), (Fig. 4.28). Mw were 101 kDa.

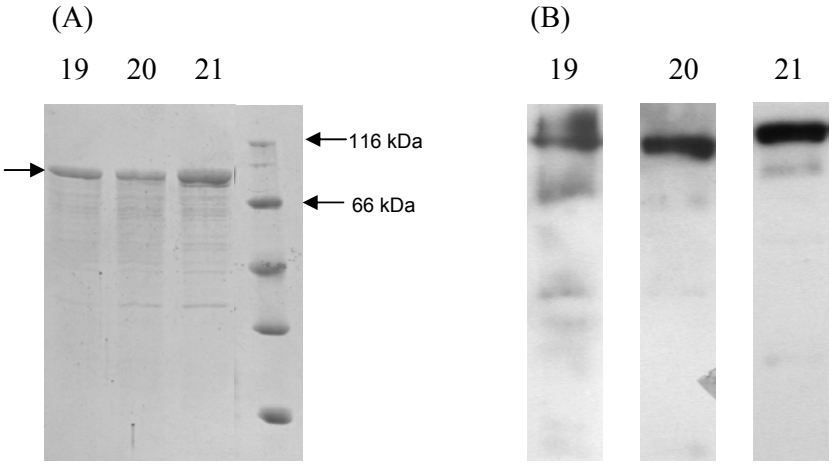


Fig. 4.28: (A) SDS-PAGE gel (12.5%) (2 µg) (B) Western blots of 50-100 ng of No.19-21

After elution the purity of the proteins was estimated by the densitometry (Table 4.8), as described (see Table 4.1.).

| *Protein* | *% of pure protein* |
|---|---|
| *WT PDE10* | 78.7 |
| *No.19* | 83.3 |
| *No.20* | 78.0 |
| *No.21* | 78.9 |

Table 4.8: Estimation of protein purity (%) by densitometry

For proteins WT PDE10 and No.19-21 estimated purity was similar and their specific activities were comparable.

Concentration response curves with cAMP and cGMP were established (0.1 µg of each protein was assayed, approx. 10 nM, n=4) (Fig. 4.29). Basal activities, 300 µM cAMP and 100 µM cGMP points were compared (Fig. 4.30 and 4.31).

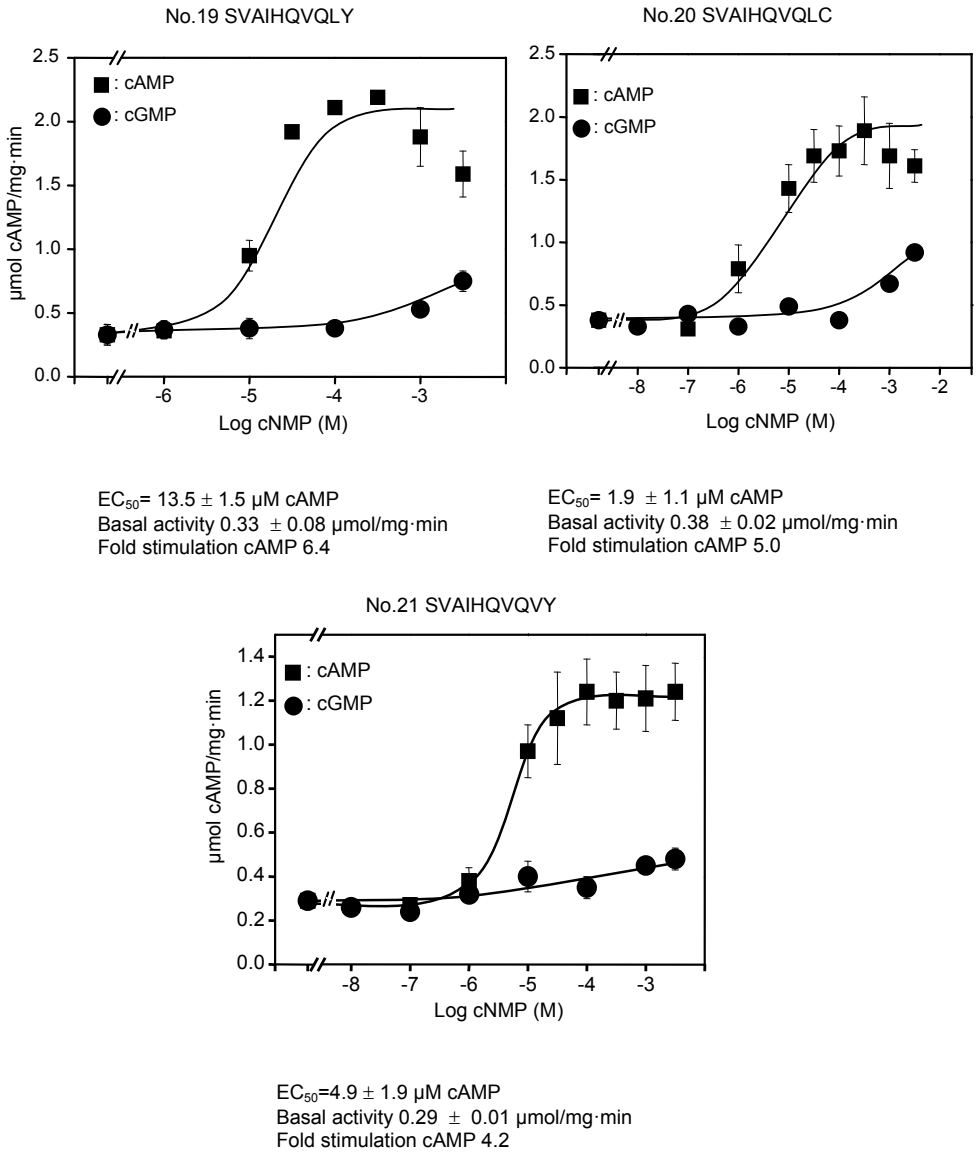


Fig. 4.29: Concentration response curves of No.19-21

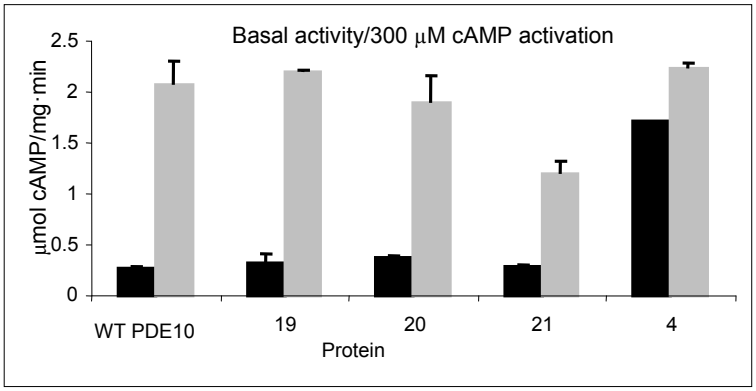


Fig. 4.30: Comparison of AC activities ± 300 µM cAMP; black bars basal activity, grey bars + cAMP

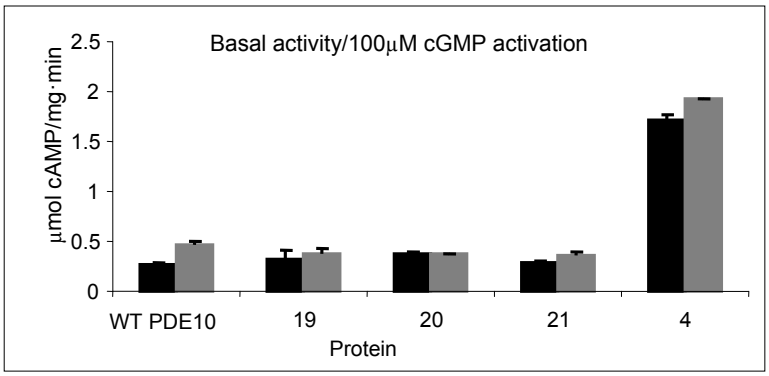


Fig. 4.31: Comparison of AC activities ± 100 μM cGMP; black bars basal activity, grey bars + cGMP

(A) (B)

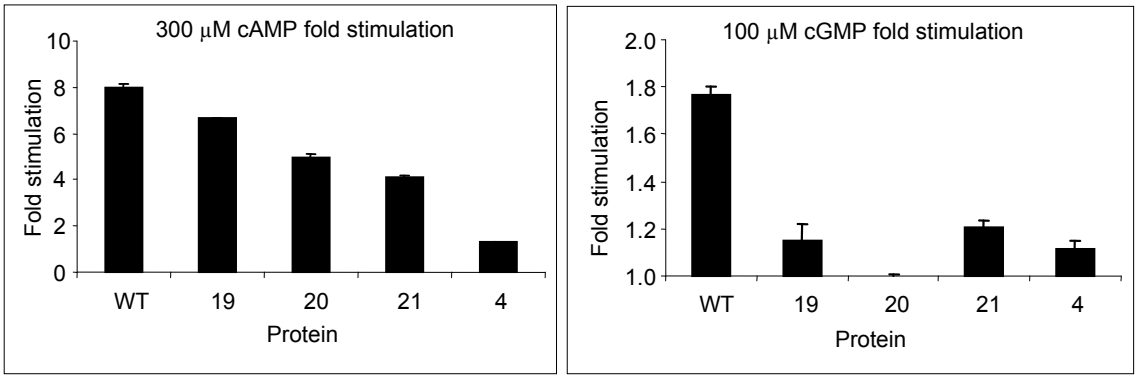


Fig. 4.32: Fold stimulation with (A) 300 μM cAMP (B) 100 μM cGMP

| *Protein* | *$EC_{50}$ (μM cAMP)* | *cAMP stimulation* | *cGMP stimulation* |
|---|---|---|---|
| *WT PDE10* | 8.1 ± 2.0 | 8.0 | 1.8 |
| *No.4* | 1.0 ± 0.02 | 1.2 | - |
| *No.19* | 13.5 ± 1.5 | 6.4 | - |
| *No.20* | 1.9 ± 1.1 | 5.0 | - |
| *No.21* | 4.9 ± 1.9 | 4.2 | - |

Table 4.9: Summary: $EC_{50}$ values, cAMP (300 μM) and cGMP (100 μM) fold stimulation of No.4, 19, 20, 21 and WT PDE10-CayB1 AC

Constructs No.19, 20 and 21 are cAMP activated (Table 4.9). At high cGMP concentration (1 or 3 mM) there is 2-2.5 fold stimulation.

### 4.3.4 Expression and characterization of chimeras No.22 and 23

In 2009 the crystal structure of near full length PDE2 (aa 215-900) was published [33]. The tandem GAF domain contained no ligand. PDE2 crystallized as a parallel dimer in which both GAF domains as well as linker helices are involved in the dimer interface. Contacts between catalytic domains stabilize the structure (Fig. 1.4).

In that structure α-helix between GAF-A and GAF-B starts 13 aa before starting aa in No.1-16 and it is shorter for 5 aa comparing to 36 aa long linker used before (see Fig. 4.9). Therefore 44 aa α-helices were exchanged between PDE10 and PDE5 (Fig. 4.33). Parallely, WT PDE10- and WT PDE5 chimeras were assayed.

Fig. 4.33: Sequence alignment of a full length α-helical linker of hPDE2, hPDE5 and hPDE10
Red arrow shows the beginning of the α-helix in constructs No.1-16;

PDE10, PDE5 (K298-F341)-CyaB1 (No.22) was cloned in pETDuet MCS-pQE30, transformed in *E.coli BL-21 (DE3) [pREP4]*, expressed and purified (see 4.3.1). Mw was 101 kDa (Fig. 4.34).

PDE5, PDE10 (S218-F261)-CyaB1 (No.23) was cloned in pET16b MSC-pQE30, transformed in *E.coli BL-21 (DE3) [pREP4]*. The expression and purification of this protein was optimized. The best conditions were: overnight expression at 16°C, induction with 75 µM IPTG, purification with $Ni^{2+}$-NTA in the presence of 15 mM imidazole, 250 mM NaCl and 5 mM $MgCl_2$, wash buffers containing 7.5 mM imidazole + 400 mM NaCl, 15 mM imidazole + 400 mM NaCl and 25 mM imidazole + 10 mM NaCl. Mw was 113 kDa.

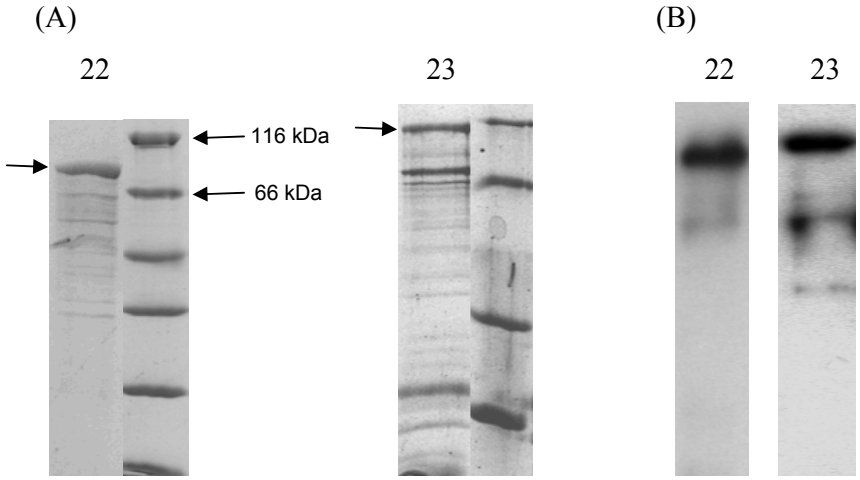


Fig. 4.34: (A) SDS-PAGE gel (12.5%) (3µg) (B) Western-Blots of No.22 and 23 (100 ng)

WT PDE10-CyaB1 AC, pETDuet MCS-pQE30 was transformed in *E.coli BL-21 Rosseta (pLysS)*, expressed and purified (see 4.3.1). Mw was 101 kDa.

WT PDE5-CyaB1 AC, pET16b MCS-pQE30 (from S. Bruder) was transformed in *E.coli BL-21 (DE3) [pREP4]*. Expression and purification conditions were: overnight expression at 16°C, induction with 75 µM IPTG, purification with $Ni^{2+}$-IDA in the presence of cell lysis buffer, containing 7.5 mM imidazole, wash buffers with 7.5 mM imidazole + 400 mM NaCl, 15 mM imidazole + 400 mM NaCl and 25 mM imidazole + 10 mM NaCl. Mw was 113 kDa (Fig. 4.35).

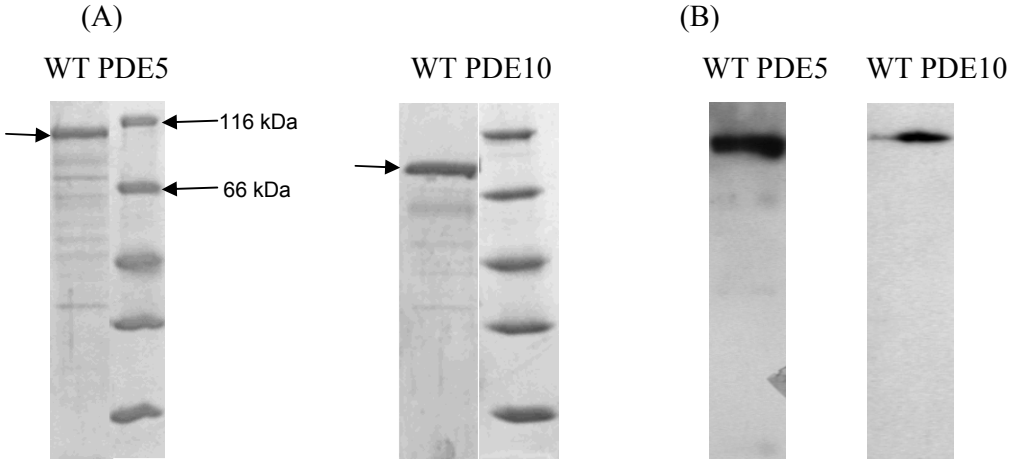


Fig. 4.35: (A) SDS-PAGE gel (12.5%) (3 µg), (B) Western blots of WT PDE5- and WT PDE10-CyaB1 AC (500 and 50 ng, respectively)

After elution protein purity was estimated by the densitometry (Table 4.10), as described (see Table 4.1.).

| *Protein* | *% of pure protein* |
|---|---|
| *WT PDE10* | 78.7 |
| *No.22* | 73.4 |
| *WT PDE5* | 48.4 |
| *No.23* | 35.9 |

Table 4.10: Estimation of protein purity (%) by densitometry

Proteins No.22 and 23 had similar purities as their WTs.

For all four constructs concentration response curves with cAMP and cGMP were established (0.1 µg of each protein was assayed, approx 10 nM, n=4), (Fig. 4.36-4.38).

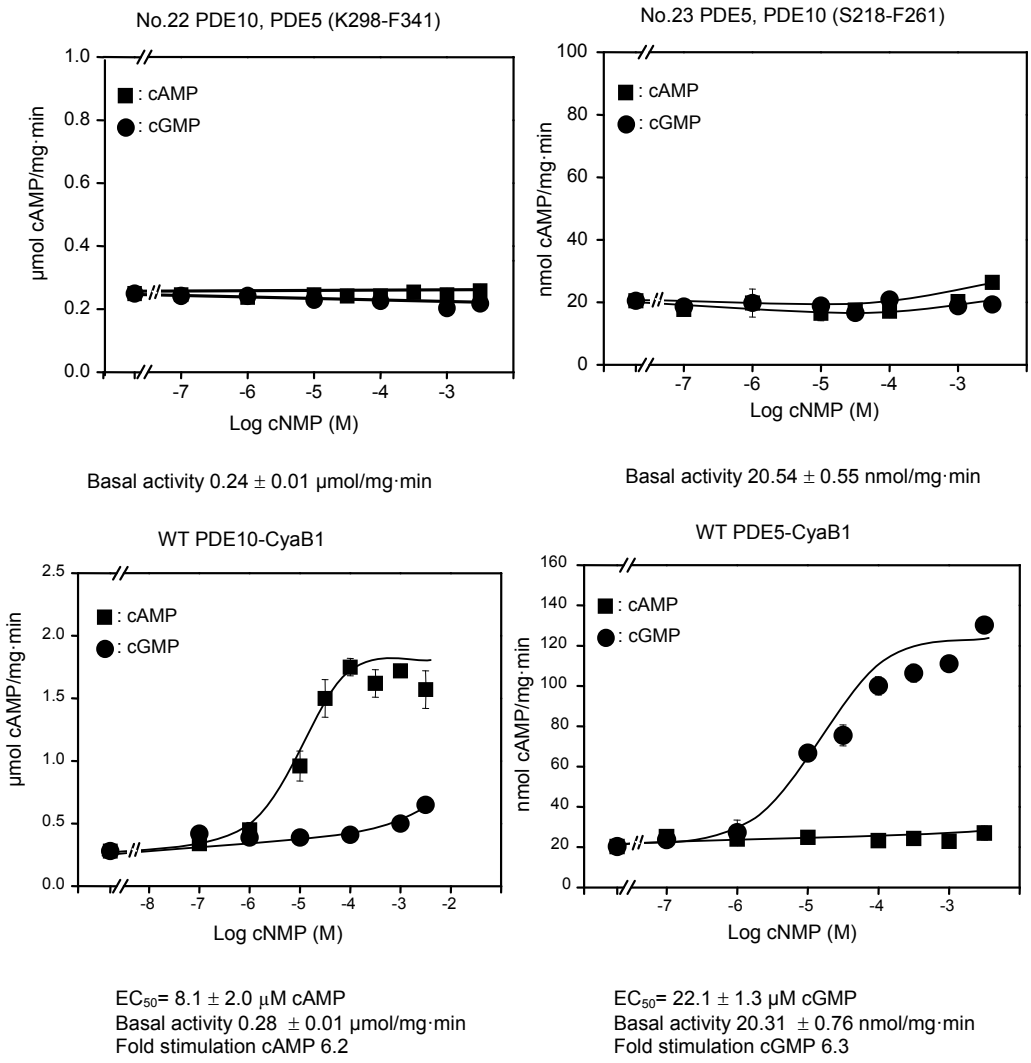


Fig. 4.36: Concentration response curves of No.22 and 23, WT PDE5- and WT PDE10-CyaB1 AC

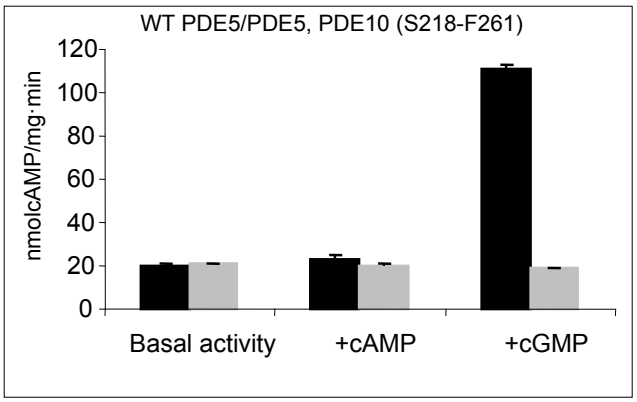


Fig. 4.37: Comparison of AC activities ± 1 mM cAMP/ cGMP; black bars WT PDE5, grey bars PDE5, PDE10 (S218-F261);

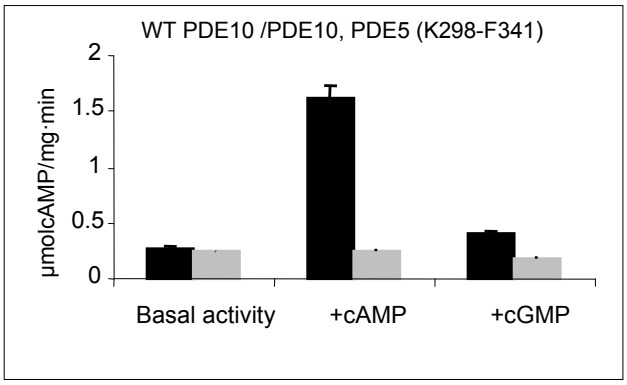


Fig. 4.38: Comparison of AC activities ± 1 mM cAMP/ cGMP; black bars WT PDE10, grey bars PDE10, PDE5 (K298-F341)

| *Protein* | *$EC_{50}$ (µM cAMP)* | *Fold cAMP stimulation* | *Fold cGMP stimulation* |
|---|---|---|---|
| *PDE10 WT* | 8.1 ± 2.0 | 6.2 | 1.6 |
| *No.22* | - | - | - |
| *PDE5 WT* | 22.1 ± 1.3 | - | 6.3 |
| *No.23* | - | 1.3 | - |

Table 4.11: Summary**:** $EC_{50}$ values and fold cAMP and cGMP stimulation No.22 and 23, WT PDE5-and WT PDE10-CyaB1 AC

Chimeras with 44 aa α-helical linker exchange in PDE5 and PDE10 could not be regulated by their respective ligands cAMP/cGMP ($EC_{50}$ values for No.22 and 23 could not be determined), (Table 4.11).

## 4.4 Tandem CaM-binding domains in signaling: hPDE1-CyaB1 AC chimeras

Calcium-calmodulin dependent PDE1 family consists of three gene families PDE1A, B and C, each containing several isoforms with unique N-termini (Fig. 4.39). The N-termini possess two CaM-binding domains and a short autoinhibitory region inbetween (see 1.4.1).

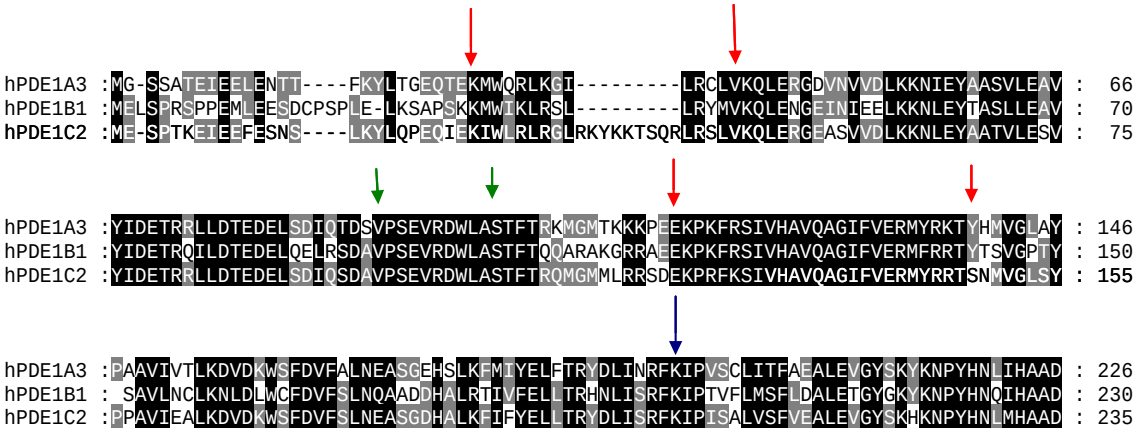


Fig. 4.39: Sequence alignment of the N-terminal regulatory domains of PDE1A3, B1 and C2
Sequences between red arrows are CaM1 and CaM2 binding sites, respectively; the sequence between green arrows is an autoinhibitory sequence; the catalytic domain starts at the blue arrow.

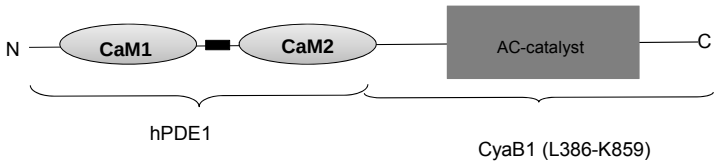


Fig. 4.40: Domain organization of PDE1-CyaB1 AC chimeras

N-terminal tandem CaM-binding domains from PDE1A3 and B1 (CaM1 and CaM2) were attached to the catalytic domain of AC CyaB1 AC (L386-K859), (Fig. 4.40, p.117). The question is whether these constructs can be stimulated by CaM similarly as chimeras with the tandem GAFs from PDE 2, 5, 10 and 11 by cGMP/cAMP.

Chimeras with the tandem CaM-binding domains from hPDE1A3:

A: PDE1A3 (M1–M178)-CyaB1 AC (L386-K859)

B: PDE1A3 (M1–L206)-

C: PDE1A3 (M1–M234)-

Chimeras with the tandem CaM-binding domains from hPDE1B1:

D: PDE1B1 (M1–T182)-

E: PDE1B1 (M1–A210)-

F: PDE1B1 (M1–F238)-

### 4.4.1 Expression and characterization of PDE1A3- and PDE1B1-CyaB1 AC chimeras

Constructs were cloned into PET16 MCS-pQE30, transformed in *E.coli BL-21 (DE3) [pREP4]*, sequenced and expressed. Expression of proteins D, E and F was induced with 100 µM IPTG at 16°C. Proteins were purified with $Ni^{2+}$-IDA in the presence of 400 mM NaCl and 2/5 mM $MgCl_2$, washed with cell lysis buffer ± 20 mM imidazole and eluted (300 mM imidazole). Mw of these proteins were 76 kDa, 79 kDa and 83 kDa for D, E and F, respectively (Fig. 4.41).

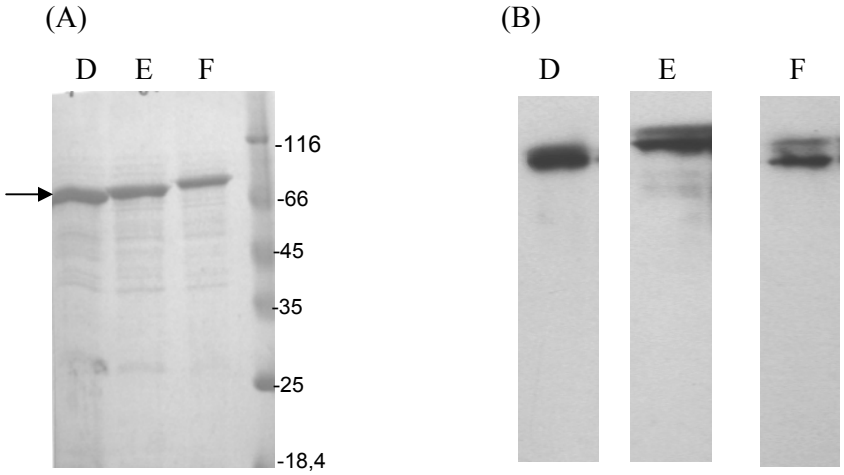


Fig. 4.41: (A) SDS-PAGE gel (12.5%) of PDE1B1-CyaB1 AC constructs D, E and F (2 µg) (B) Western blots (0.2 µg)

To purify better A, B and C proteins, expression conditions were varied:

- temperature: 12°C and 22°C
- concentration of IPTG: 10µM, 1µM and 0,1µM,
- $Ni^{2+}$ -IDA affinity chromatography in the presence of 10 mM imidazole, and
- different wash conditions: 15 and 30 mM imidazole + 400 mM NaCl and 50 mM imidazole + 10 mM NaCl

The yields of proteins were better after expression at 12°C (not shown), but the purity was unsatisfactory. In next experiments concentration of IPTG was reduced to 0.1 µM and expression temperature remained at 12°C. Proteins were purified with $Ni^{2+}$-IDA agarose in the presence of 400 mM NaCl , 5 mM $MgCl_2$ and 10 mM imidazole, washed with 20 mM imidazole + 400 mM NaCl and 20 mM imidazole + 50 mM NaCl and than eluted (300 mM imidazole). Mw of these proteins were 75 kDa, 79 kDa and 82 kDa for A, B and C, respectively. Proteins were dialyzed overnight against 35% glycerol, assayed immediately and stored at -20°C. Western blots showed no degradation products (Fig. 4.42).

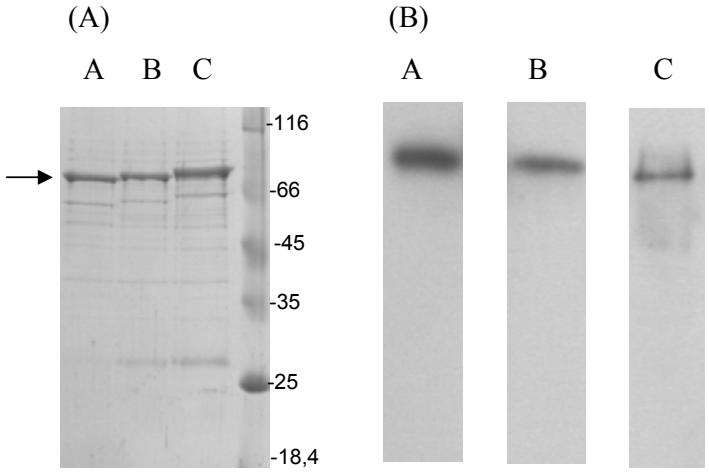


Fig. 4.42: (A) SDS-PAGE gel (12.5%) of PDE1A3-CyaB1 constructs A, B and C (3 µg) (B) Western-Blot (0.2 µg)

After elution protein purity was estimated by densitometry (see 3.3, Table 4.12), as described (see Table 4.1.).

| *Proteins* | *% of pure protein* |
|---|---|
| *A* | 75.8 |
| *B* | 68.4 |
| *C* | 71.2 |
| *D* | 76.9 |
| *E* | 77.5 |
| *F* | 78.7 |

Table 4.12: Estimation of protein purity (%) by densitometry

The purity of these six proteins was similar 68-78 %.

**Preparation of calmodulin (CaM) from pig brain**

Prior to AC assays, CaM was purified (Fig. 4.43) from pig brain according to [98]. It involved precipitation with $(NH_4)_2SO_4$, isoelectric point precipitation of CaM at pI 4.1, heat treatment, hydrophobic interaction chromatography on Phenyl Sepharose (see 3.4) and dialysis.

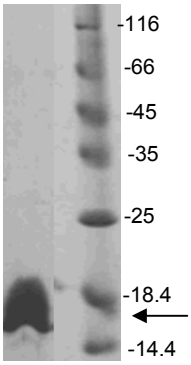


Fig. 4.43: SDS-PAGE gel (15 %) CaM 17 kDa (10 µg), (black arrow)

For constructs PDE1A3- and PDE1B1-CyaB1 AC concentration response curves were determined in two ways (n=4-6): in the presence of increasing concentrations of $Ca^{+2}$ at 3 µM CaM and at increasing concentrations of CaM at 30 µM $Ca^{+2}$ (Fig. 4.44 and 4.45, Table 4.13).

*Construct A: PDE1A3 (1-178)*

(A) (B)

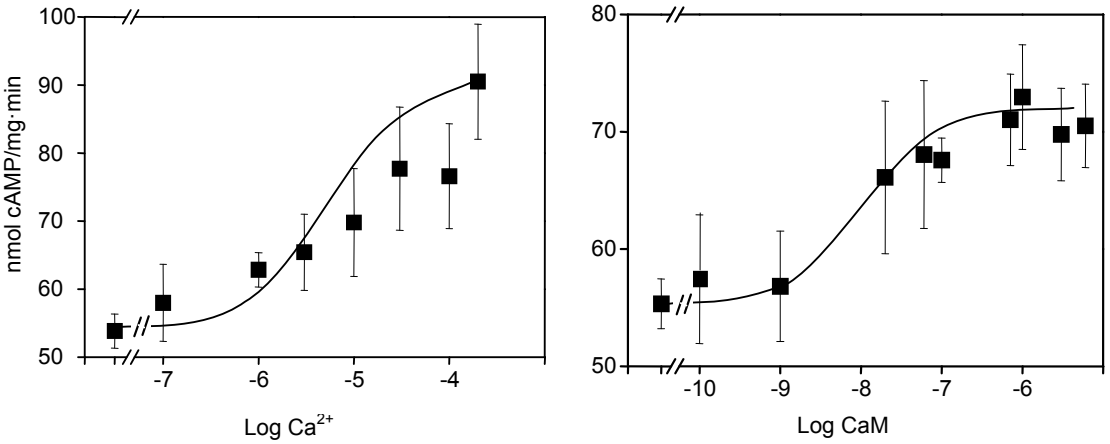


*Construct B: PDE1A3 (1-206)*

(A) (B)

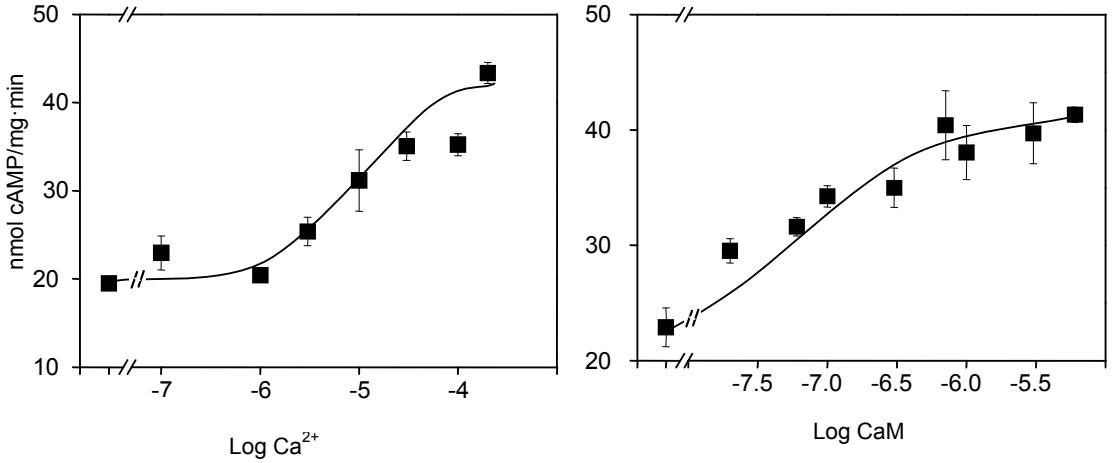

*Construct C: PDE1A3 (1-234)*

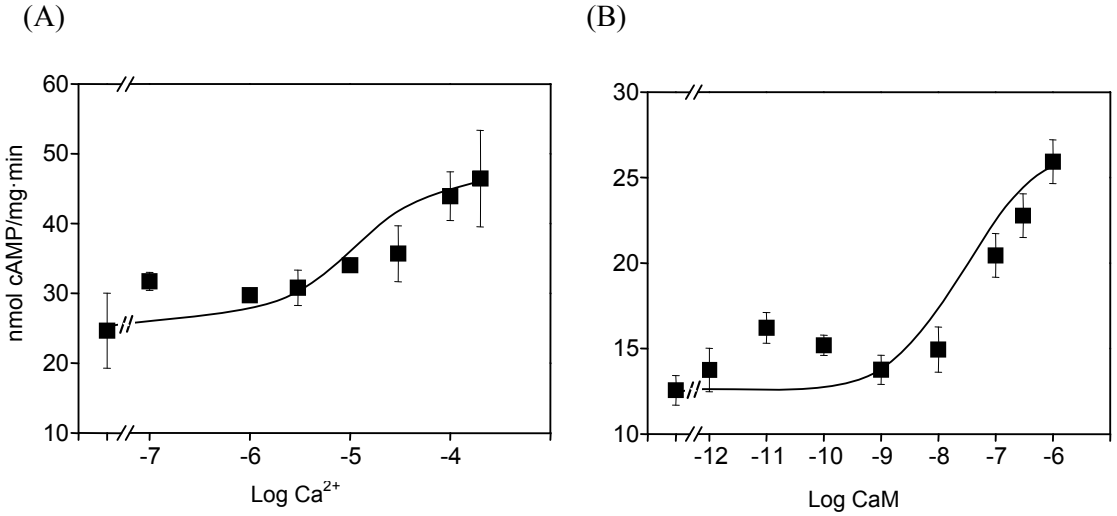


Fig. 4.44: Concentration response curves of constructs A, B and C
(A) A, B and C (15-20 nM) stimulation with $Ca^{+2}$ at 3 µM CaM; (B) stimulation with CaM at 30 µM $Ca^{+2}$;

*Construct D: PDE1B1 (1-182)*

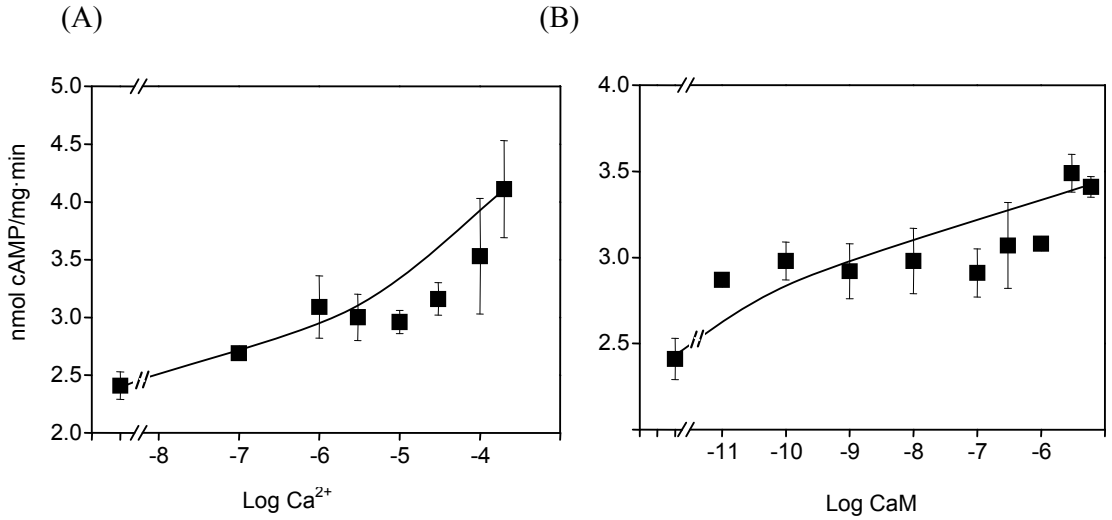

*Construct E: PDE1B1 (1-210)*

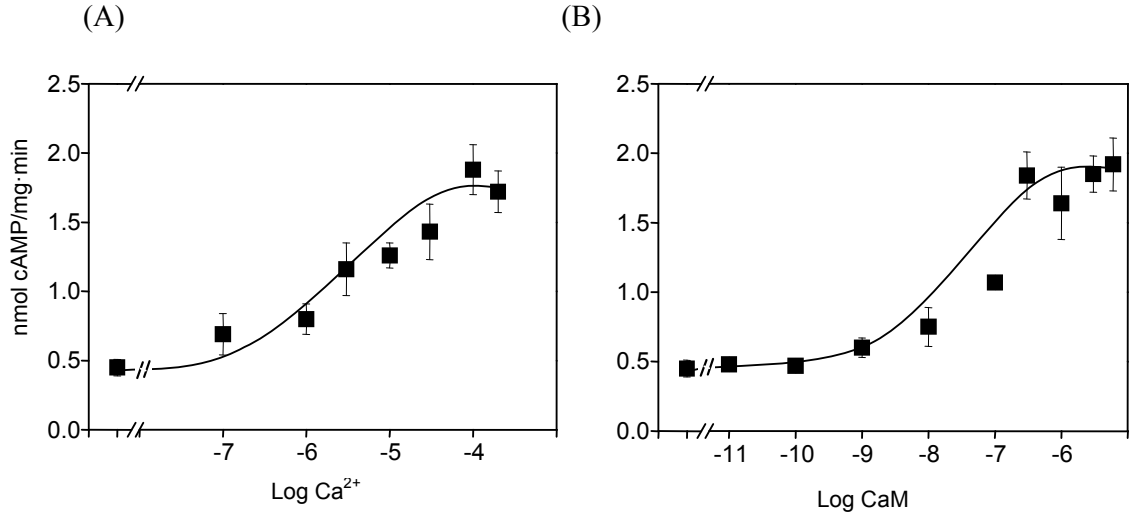


*Construct F: PDE1B1 (1-238)*

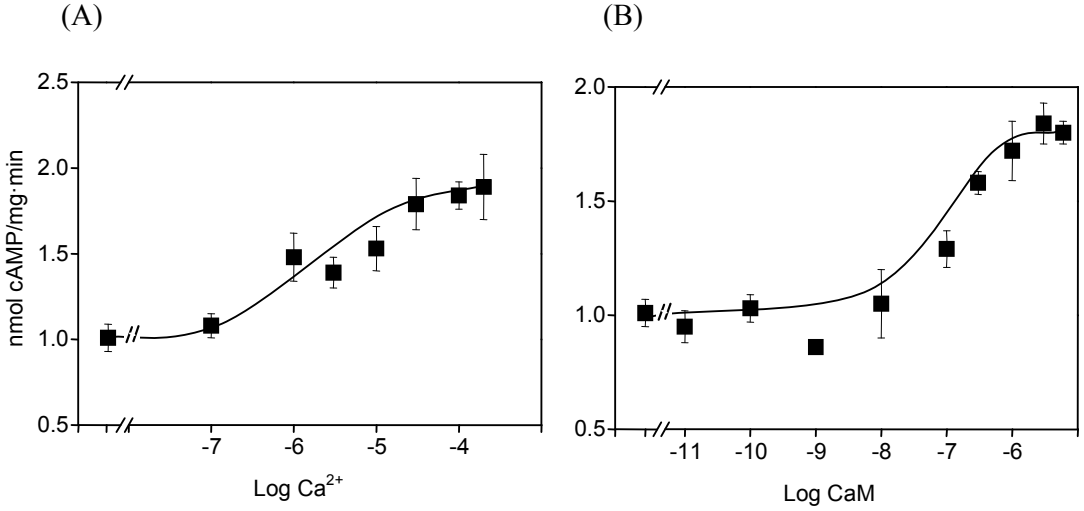


Fig. 4.45: Concentration response curves of constructs D, E and F
(A) D, E and F (40-60 nM) stimulation with $Ca^{+2}$ at 3 µM CaM; (B) stimulation with CaM at 30 µM $Ca^{+2}$;

In each test, three controls were run (there was no significant difference between these three values in tests).

- with no additions,+ 50 µM EGTA + 3 µM CaM and + 50 µM EGTA

| | *A3(1-178) A* | *A3(1-206) B* | *A3(1-234) C* | *B1(1-182) D* | *B1(1-210) E* | *B1(1-238) F* |
|---|---|---|---|---|---|---|
| *with $Ca^{2+}$* | 1.6 | 2.2 | 1.9 | 1.7 | 4.2 | 1.9 |
| *with CaM* | 1.3 | 1.8 | 2.1 | 1.4 | 4.4 | 1.8 |

Table 4.13: Fold stimulation PDE1A3- and PDE1B1-CyaB1 AC chimeras

## 4.5 Tandem UCR domains in signaling: hPDE4-CyaB1 AC chimeras

PDE4 is a cAMP specific, rolipram inhibited PDE family. Four genes encode this family - PDE4A, B, C and D. In each gene family there are multiple variants, mainly due to differences at the N termini, (Fig. 4.46). Long variants have tandem regulatory UCR domains (UCR1 + UCR2). The long isoforms can be phosphorylated by PKA at a Ser located at the beginning of UCR1 which increases catalytic activity (60-250%). Although there is no homology between UCR1 and UCR2, UCR1s and UCR2s from different isoforms show strong conservation (see 1.4.3).

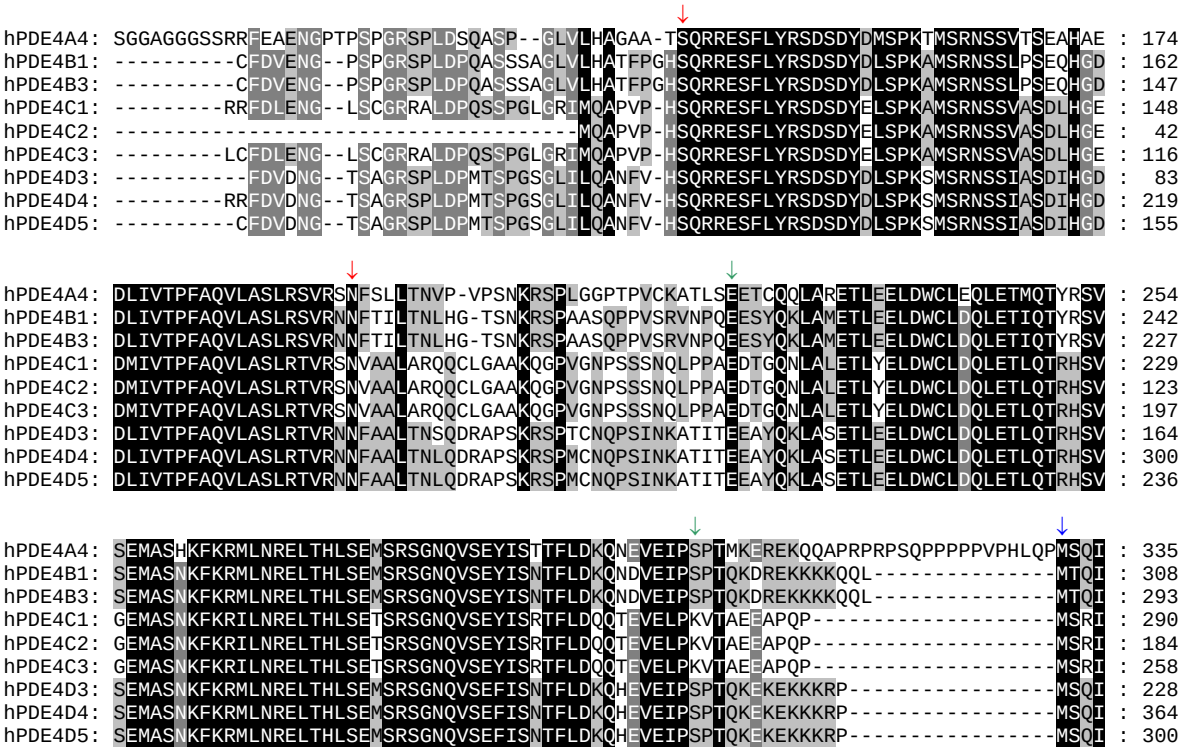


Fig. 4.46: Sequence alignment of PDE4 long isoforms
UCR1 is the sequence between red arrows, UCR2 is the sequence between green arrows; catalytic domains start from the blue arrow;

Three different long isoforms PDE4A4, B1 and 4D3 were used. Their N-terminal regulatory domains with tandem UCR1/2 were attached to the reporter CyaB1 AC, (Fig. 4.47, p.117).

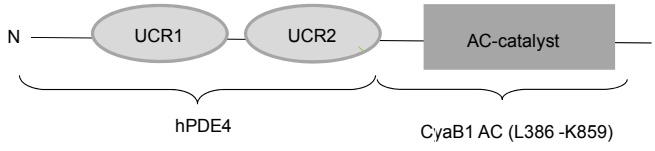


Fig. 4.47: Domain organization of PDE4-CyaB1 AC chimeras

### 4.5.1 Expression and characterization of hPDE4D3-CyaB1 AC chimeras

PDE4D3 has a 49 aa long N-terminus ahead of tandem UCR domains. Following chimeras PDE4D3-CyaB1 AC were generated:

I PDE4D3 (M1-S212)-CyaB1 AC (L386-K859)

II PDE4D3 (L40-S212)-

Constructs III and IV corresponded to I, II with phosphomimetic mutation of Ser-54 to Asp:

III **S54D** PDE4D3 (M1-S212)-

IV **S54D** PDE4D3 (L40-S212)-

The question is whether these mutations activate the reporter enzyme similarly as phosphorylation of PDE4 long isoforms.

Constructs were cloned in pQE30, transformed in *E.coli BL-21 (DE3) [pREP4]* and sequenced. Since all four proteins ended mainly in inclusion bodies, a great number of experiments were carried out with different expression and purification conditions to obtain soluble recombinant proteins: the temperature was varied from 16°C to 30°C, IPTG concentration from 100 to 500 μM, purification with $Ni^{2+}$-NTA or $Ni^{2+}$-IDA and imidazole concentrations at different purification steps.

Constructs were recloned in pET16 MCS-pQE60 (C-terminal His-tag) and pET16 MCS-pQE30 (N-terminal His-tag) which resulted in more soluble protein, yet purification was more difficult. The Western blots showed degradation products.

The best expression and purification conditions were: expression with 100 μM IPTG at 16°C, protein purification with $Ni^{2+}$-NTA in the presence of 40 mM imidazole, 400 mM NaCl and 5 mM $MgCl_2$ and wash step with 60 mM imidazole + 400 mM NaCl and 60 mM imidazole + 10 mM NaCl. They were eluted (300 mM imidazole) and dialyzed against 35% glycerol 2-3 h and assayed immediately, (Fig. 4.48).

Mw of these proteins were: I / III 79 kDa, II / IV 75 kDa.

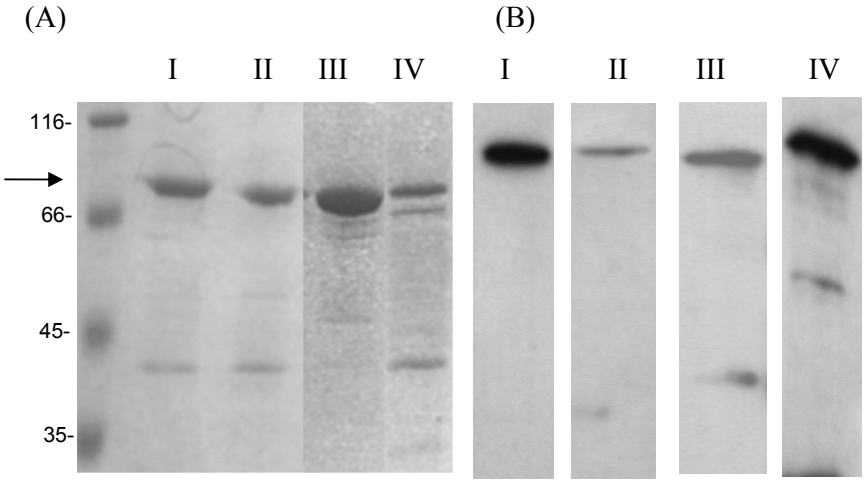


Fig. 4.48: (A) SDS-PAGE gel (15%) PDE4D3-CyaB1 constructs I-IV (2 µg) (B) Western blots (0.5µg)

Protein purity was estimated by the densitometry (see 3.3) as described (see Table 4.1.). Estimated purity for I, II and III proteins was similar 70-80% and for IV was 43% (Table 4.14).

| *Protein* | *% of the pure protein* |
|---|---|
| *I* | 73.2 |
| *II* | 70.6 |
| *III* | 82.4 |
| *IV* | 43.2 |

Table 4.14: Estimation of protein purity (%) by densitometry

For protein dependence 0.05 µg to 5 µg of protein I and II was used (Fig. 4.49).

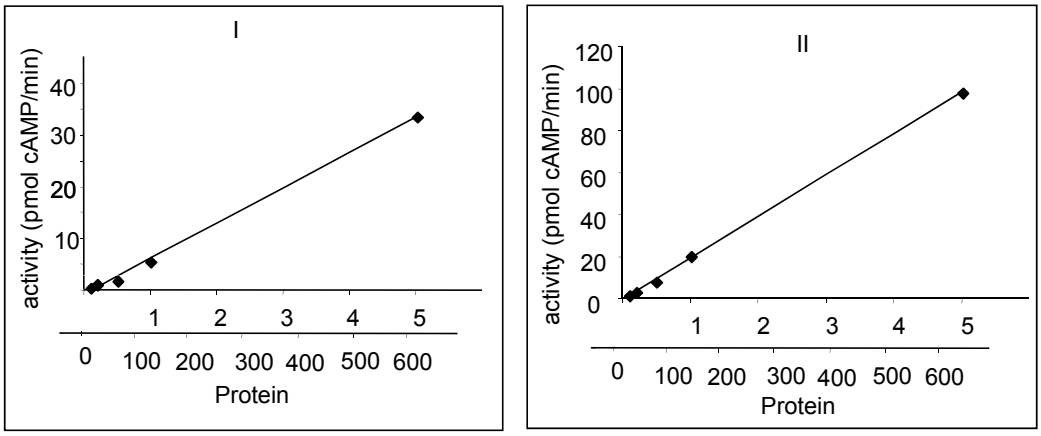


Fig. 4.49: Protein dependence of PDE4D3-CyaB1 AC, constructs I and II
On x-axis, upper scale represents µg of protein, lower scale nM protein;

| *Protein* | *Specific activity (nmol/mg·min)* | *Protein* | *Specific activity (nmol/mg·min)* |
|---|---|---|---|
| *I* | 5.7 ± 0.7 | *III* | 17.2 ± 1.8 |
| *II* | 18.9 ± 1.6 | *IV* | 0.3 ± 0.06 |

Table 4.15: Specific activities of proteins I-IV (1 μg of protein was assayed)

Protein I and III have similar purity and their specific activities were comparable. Protein with phosphomimetic mutation shows 3-fold activation over the unmutated protein I (Table 4.15). Since proteins I and III were poorly expressed, one more expression was carried out in which higher concentrations of imidazole were used during $Ni^{2+}$-NTA purification (50 mM) and wash (75 mM). Proteins were dialyzed overnight against 35% glycerol to remove imidazole which can influence the AC assay, (Fig. 4.50). Protein purity was estimated by the densitometry (Table 4.16).

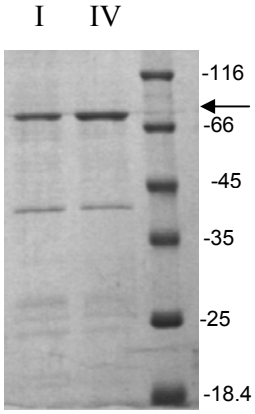


Fig. 4.50: SDS-PAGE gel (15%) of PDE4D3-CyaB1 AC constructs I and III (1.5 and 2.5 μg)

| *Protein* | *% of the pure protein* | *Specific activity (nmol/mg·min)* |
|---|---|---|
| *I* | 50.8 | 22.7 ± 1.4 |
| *III* | 56.3 | 87.2 ± 5.3 |

Table 4.16: Estimation of protein purity (%) by densitometry and specific activities of I and III

Protein III was 3.8-fold activated over I, i.e. the similar result as in a previous experiment, (Table 4.16).

Phosphatidic acid stimulates long PDE4 (60-200%) probably by binding to the N-terminal part of UCR1 domain [62, 63] and in the same manner as PKA phosphorylation. 45 μM phosphatidic acid did not stimulate constructs I and II (Fig. 4.51).

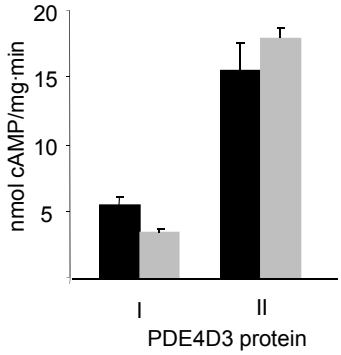


Fig. 4.51: The effect of phosphatidic acid on constructs I and II (black bars are I and II, grey bars + 45 μM PA)

### 4.5.2 Expression and characterization of hPDE4A4-CyaB1 AC chimeras

PDE4A4 is a long isoform which contains an N-terminal regulatory domain of 140 aa in front of the tandem of UCR domains. Two construct were generated:

V PDE4A4 (M1-S302)-CyaB1 AC (L386-K859)

VI **S145D** PDE4A4 (M1-S302)- with phosphomimetic mutation

Constructs in pQE30 were transformed in *E.coli BL-21 (DE3) [pREP4]*, sequenced, expressed and purified.

As with PDE4D3 constructs, proteins V and VI were mostly in inclusion bodies. Therefore expression conditions were varied. These optimizations did not improve the yield and purity of recombinant proteins.

Expression and purification conditions were: induction with 100 μM IPTG at 16°C, purification with $Ni^{2+}$-IDA in the presence of 40 mM imidazole, 400 mM NaCl and 5 mM $MgCl_2$ and wash with 60 mM imidazole + 400 mM NaCl, and 60 mM imidazole + 10 mM NaCl. Most protein remained in inclusion bodies. Mw was 88.6 kDa (Fig. 4.52).

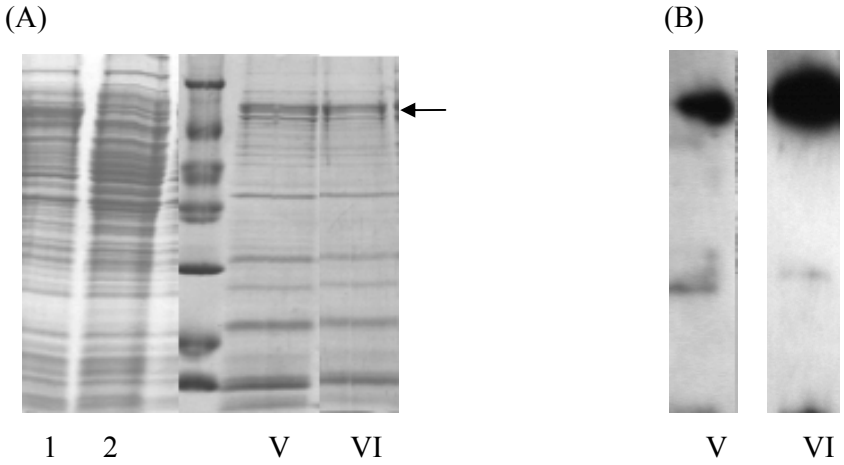


Fig. 4.52: (A) SDS-PAGE gel (12.5%) of V and VI (3 µg) (B) Western blots (1µg)
Lanes 1 and 2 homogenate after cell lysis of V and VI (2 µg);

1µg assay of each protein was tested. (1µg/100 µl corresponds to 110 nM protein, but due to impurities the estimated amount of recombinant protein by densitometry is < 10%). Both proteins were assayed under the standard conditions (Fig. 4.53; n=6). Western blots were analyzed by densitometry and specific activities were calculated accordingly.

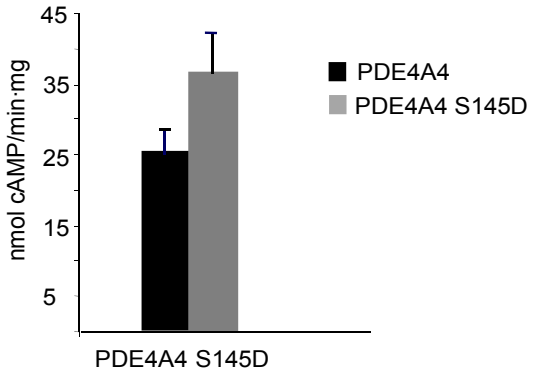


PDE4A4 26.6 ± 1.2

PDE4A4 S145D 38.5 ± 5.7

Fig. 4.53: Specific activities (nmol/mg·min) of V and VI (n=6)

Protein VI shows 1.5-fold higher activity than V.

To establish pH dependence for V and VI, different buffer systems pH (4-10) were used, (Fig. 4.54). The optimum pH was between 7 and 9. For all experiments pH 7.5 was used. Isoelectric point of these proteins is 6.2.

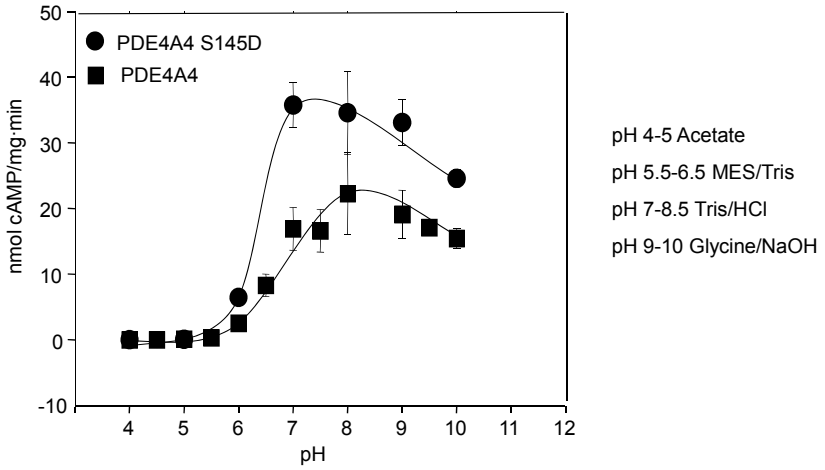


Fig. 4.54: pH dependence of V and VI (100 nM, including impurities)

Here the stimulation of about 2-fold of protein with S145D over the unmutated protein can bee seen at pH 7.

For further purification proteins V and VI were applied to an anion-exchange column (see 3.4). During sample preparation for chromatography it was noticed that recombinant protein aggregated and was pelleted after short centrifugations. Therefore proteins were purified from 3.2 L cell culture, dialyzed overnight in 35% glycerol and centrifuged at 49,200×g first for 10 min and than for 1h. Most of the protein was in the supernatant, yet the material with the highest specific activity was in the pellet (pellet were resuspended in dialysis buffer and assayed). Similar to previous experiments, protein with S145D had a 1.3-1.5 higher activity than V. The same experiment was repeated once again, this time proteins were dialysed in 10% glycerol and centrifuged at 49,200×g for 1h, (Fig. 4.55), to obtain more protein in pellet.

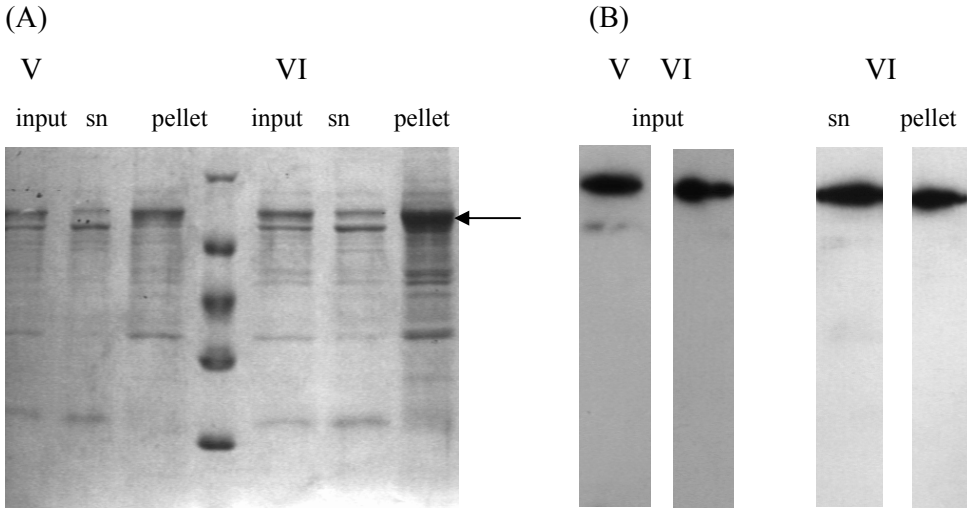


Fig. 4.55: (A) SDS-PAGE gel (12.5 %) V and VI in input, supernatant and pellet after 1h centrifugation at 49,200×g in 10% glycerol (3 µg), (B) Western blots of (1-2 µg)

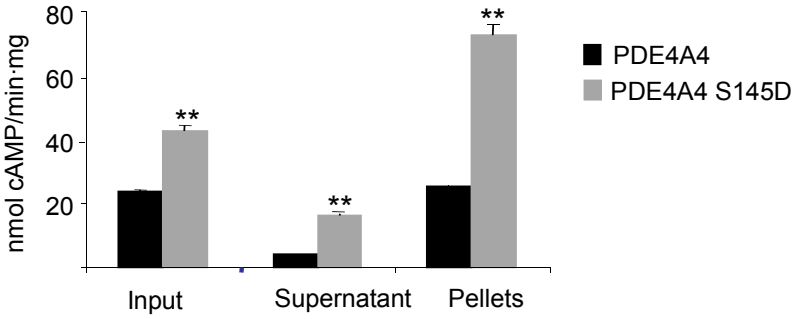


PDE4A4: Input 23.3 ± 0.7 (n=2) PDE4A4 S145D: Input 42.4 ± 2.1

Supernatant 3.8 ± 0.3 Supernatant 16.3 ± 0.7

Pellets 25.2 ± 0.3 Pellets 72.3± 3.6

Fig. 4.56: Specific activities (nmol/mg·min) of V and VI in input, supernatant and pellet after 1h centrifuge at 49,200×g in 10% glycerol, (n=4)

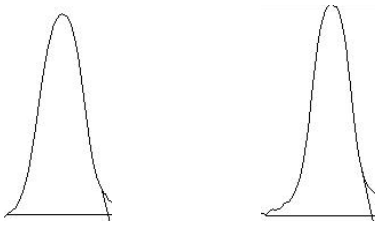

V input VI input

Fig. 4.57: AUPs of Western blot signals (2 µg) of V and VI in input (same exposure time and background)

| *Protein* | *Area under the peak* | *Protein (%)* | *Protein in test(µg)* | *Spec.act (nmol/min·mg)* | *Corrected spec.act.(1µg) (nmol/min·mg)* | *Fold stimulation* |
|---|---|---|---|---|---|---|
| *V* | 7.570.397 | 100 | 1 | 23.3 | 23.3 | |
| *VI* | 7.379.518 | 97 | 0.97 | 42.4 | 43.7 | 1.9 |

Table 4.17: Corrected specific activities of 1µg of V and VI in input according to the densitometry of Western blots

Specific activities of mutated protein VI were up to 4.3-fold in input, supernatant and pellet (Fig. 4.56). Western blot signals of protein V and VI in input were almost the same (Fig 4.57). Stimulation of VI over V was 1.9-fold (Table 4.17).

In the final experiment the expression temperature was decreased to 12°C, as an attempt to obtain more pure protein (Fig. 4.58).

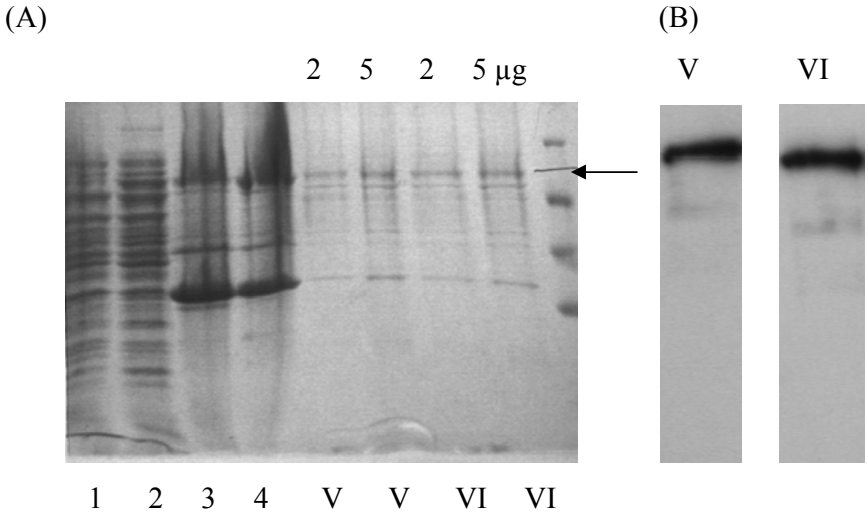


Fig. 4.58: (A) SDS-PAGE gel (12.5 %) of V and VI (2 and 5 µg) (B) Western blots of 2 µg
Lanes 1 and 2 supernatants after cell lysis (3 µg); lanes 3 and 4 pellets after cell lysis (4 µg) for V and VI, respectively;

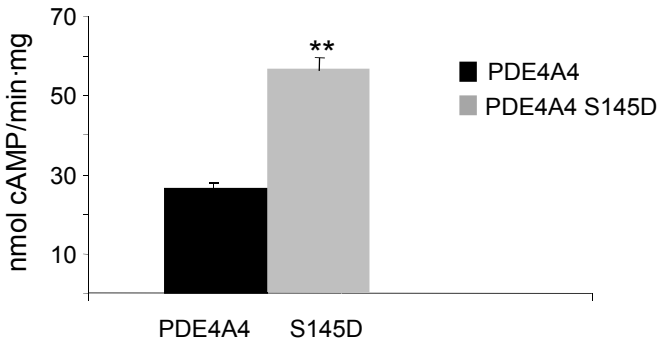


PDE4A4 26.3 ± 1.8

PDE4A4 S145D 56.2 ± 3.3

Fig. 4.59: Specific activities (nmol/mg·min) of V and VI after expression at 12°C (n=4)

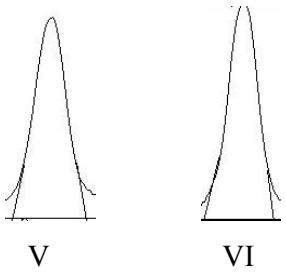


Fig. 4.60: AUPs of Western blot signals (1 µg) of V and VI in input (same exposure time and background)

| *Protein* | *Area under the peak* | *Protein (%)* | *Protein in test(µg)* | *Spec.act (nmol/min·mg)* | *Corrected spec.act. (1µg) (nmol/min·mg)* | *Fold stimulation* |
|---|---|---|---|---|---|---|
| *V* | 6.579.790 | 98 | 0.98 | 26.3 | 26.8 | |
| *VI* | 6.680.376 | 100 | 1 | 56.2 | 56.2 | 2 |

Table 4.18: Corrected specific activities of 1 µg of V and VI according to densitometry of Western blots after expression at 12°C

Western blot signals of protein V and VI were almost identical (Fig. 4.60). Stimulation of VI over V was 2-fold, (Fig. 4.59, Table 4.18).

### 4.5.3 Expression and characterization of hPDE4B1-CyaB1 AC chimeras

PDE4B1 is another long isoform, which contains a 128 aa long N-terminal ahead of the tandem UCR domain.

Two constructs were made:

VII PDE4B1 (M1-S290)-CyaB1 AC (L386-K859)

VIII **S133D** PDE4B1 (M1-S290)-

The constructs were cloned in pQE30, transformed in *E.coli BL-21 (DE3) [pREP4]*, sequenced, expressed and purified.

Expression and purification conditions were: induction with 40 µM IPTG at 16°C, purification with $Ni^{2+}$-IDA in the presence of 400 mM NaCl and 5 mM $MgCl_2$ and wash with cell lysis buffer ± 20 mM imidazole. Mw was 87.5 kDa, (Fig. 4.61).

1µg assay of each protein was tested (Fig. 4.62). (1µg/100 µl corresponds to 110 nM protein, but due to impurities the estimated amount of recombinant protein by densitometry is < 10%). Their Western blot signals were compared by densitometry and specific activities recalculated accordingly (Fig. 4.63).

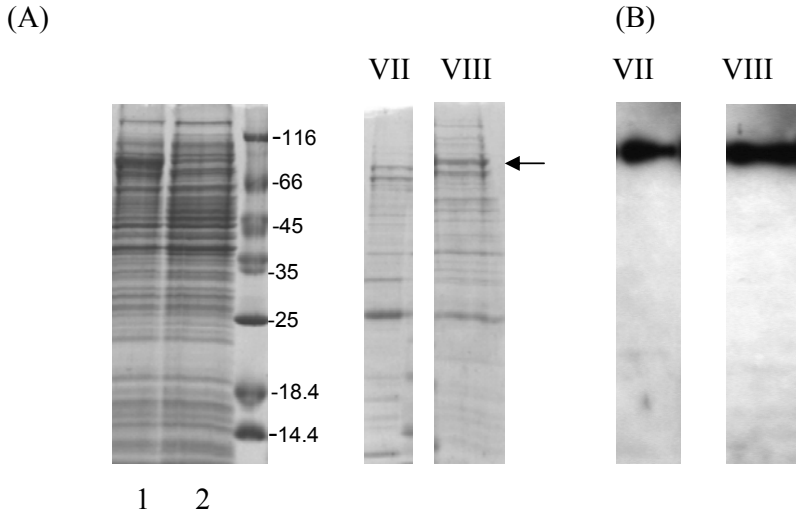


Fig. 4.61: (A) SDS-PAGE gel (12.5%) of VII and VIII, (B) Western blots (1 µg)
(A) Lanes 1 and 2 are homogenates after cell lysis (2µg);

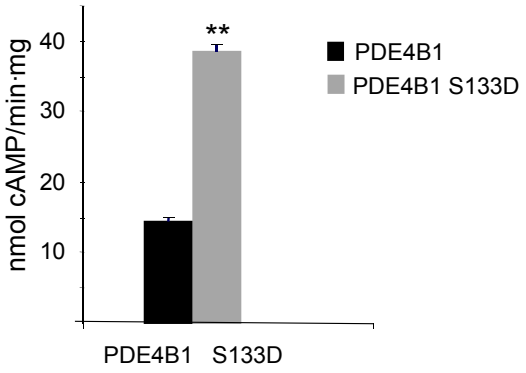


PDE4B1 14.3 ± 0.6

PDE4B1 S133D 38.4 ± 1.0

Fig. 4.62: Specific activities of (nmol/mg·min) VII and VIII (n=6)

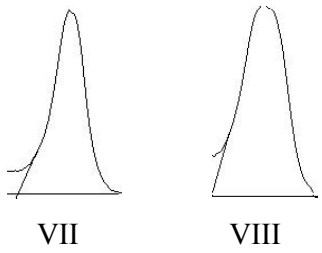


Fig. 4.63: AUPs of Western blot signals (1 µg) of VII and VIII (same exposure time and background)

| *Protein* | *Area under the peak* | *Protein (%)* | *Protein in test(µg)* | *Spec.act (nmol/min·mg)* | *Corrected spec.act.(1µg) (nmol/min·mg)* | *Fold stimulation* |
|---|---|---|---|---|---|---|
| *VII* | 5.829.104 | 80 | 0.8 | 14.3 | 17.9 | |
| *VIII* | 9.051.054 | 100 | 1 | 38.4 | 38.4 | 2.1 |

Table 4.19: Calculated specific activities of 1µg (including impurities) of VII and VIII according to densitometry of Western blots

The Western blot signal of protein VII was approx. 80 % of VIII, therefore VIII was 2.1-fold stimulated over VII (Table 4.19).

# 5 Discussion

PDEs are modular enzymes characterized by a conserved C-terminal catalytic domain and a more variable N-terminal domain involved in regulation of enzyme activity, interactions with other proteins and subcellular localization. PDE isoforms originate from 11 gene families [22-24]. Despite functional and structural diversity of N-terminal regulatory domains most PDEs are generally activated upon phosphorylation at the N-terminus or occupancy of respective ligand binding sites. Also, PDEs are dimers and dimerization is mediated through highly conserved interfaces, probably an important property of PDEs conserved in evolution. Although characterizing different domains of PDEs helped our understanding of cellular signaling processes in intracellular compartments (microdomains), the exact mechanisms of PDE regulation are not yet understood sufficiently.

In the last few years several structures of PDE N-termini have been solved: PDE10 GAF-B, PDE2 GAF A+B, PDE6 GAF-A, PDE5 GAF-A and most recently the structure of PDE2 with catalytic and regulatory domains [30-33, 43]. These structures gave important insights into these protein`s organization and in regulation of activity.

In mammals, GAF domains are presented in PDE2, 5, 6, 10 and 11, usually as tandem domains, GAF A+B. Ligand for GAF domains of PDE2, 5, 6 and 11 is cGMP and for PDE10 cAMP. They allosterically activate the catalytic domain by binding to one GAF domain in the tandem. cAMP and cGMP serve concurrently as allosteric activators and substrates in these PDEs, which impedes studies of catalytic regulation.

Cyanobacterial ACs CyaB1 and CyaB2 have an N-terminal tandem GAF domain with a similar sequence as mammalian tandem GAF domains. Allosteric activator of CyaB1 AC catalytic domain is cAMP. Mutational studies showed that the tandem GAF domains from mammalian PDEs and cyanobacterial ACs are related despite the huge evolutionary distance [9, 11, 43].

Tandem GAF domains from PDE2, 5, 10 and 11 can substitute that from CyaB1 AC and regulate CyaB1 AC activity [7, 9-13] indicating that the mechanism of regulation is conserved. Producing chimeras with different N-terminal GAF domains from PDE2, 5, 10 and 11 with CyaB1 AC as a reporter enzyme helped to better understand this regulatory mechanism. All biochemical studies which have been done using CyaB1 as a reporter assume that signaling in these chimeras is similar as signaling in mammalian PDEs.

## 5.1 Role of hPDE5 N-terminus in tandem GAF signaling

The PDE5 tandem GAF domain has been intensively characterized. Different PDE5 GAF domain constructs had highly different affinities for cGMP (range of 70-fold) [3, 37, 41, 74]. It is possible that N-terminal truncations in different constructs have contributed to this effect. Initially it was shown that the 197 aa long N-terminus ahead of GAF-A of PDE11 affects cyclic nucleotide signaling, since the removal of 176 aa and more increased basal activity and cGMP affinity [13].

PDE5 has a 148 aa long N-terminus ahead of tandem GAF domains. Phosphorylation of S102 increases cGMP affinity [74-76]. PDE5-CyaB1 AC chimera was activated 6.3-fold by cGMP binding to the GAF-A, an $EC_{50}$ was 22.1 ± 1.3 µM cGMP with a basal activity of 20.3 ± 0.1 nmol cAMP/mg·min (Fig. 4.36). By removal of aa up to the phosphorylation site basal activity remained low, cGMP affinity was largely unaffected and activation by cGMP was higher. Removal of 102 aa i.e. including S102 and more increased basal activity up to 25-fold, reduced cGMP activation and decreased $EC_{50,}$ thus influencing cGMP affinity [11, 100]. Significant 16 fold drop of cGMP $EC_{50}$ occurred upon truncations at I72 and I101, although they were still cGMP activated. To locate the position possibly important for this increase of cGMP affinity 89, 91 and 95 aa were removed from the N-terminus. The basal activities of these chimeras remained low and cGMP activated the enzyme (Fig. 4.4, Table 4.2). The chimera which was shortened by 89 aa was 18.5-fold activated, similar as a chimera shortened by 87 aa [11]. Basal activities were similar to WT PDE5-CyaB1 AC from 13.8 ± 0.2 to 20.0 ± 1.0 nmol cAMP/mg·min. Affinity for cGMP was also similar to the WT construct, 11.2 ± 1.6 µM for A89 shortening and 14.9 ± 3.0 µM for G95 shortening. cGMP $EC_{50}$ for N91 shortening was higher (36.9 ± 3.7 µM cGMP).

148 aa long PDE5 N-terminus has an important role in signaling. Shortenings at A89, N91, and G95 confirmed previous result in which removal of 101 aa had mild effect on the function and probably the structure of the N-terminus, thus stabilizing the inactive conformation of the enzyme.

Obviously, the interactions between N-terminus and GAF domains in PDE5 are important for the regulation of the signal transmission, since removal of first 109 aa released CyaB1 AC from inhibition.

## 5.2 Role of the linker between GAF-A and B in hPDE5 and 10

PDE10 GAF-**B** binds **cAMP** and PDE5 GAF-**A cGMP** as an allosteric activator. This fact was used for preparing a variety of chimeras in which different segments of the tandem GAF domains from PDE5 and 10 were permutated (N-terminus, GAF-A, GAF-B and the linker between GAF-A and B) [12, 99]. Chimeras with GAF-A from PDE5 and GAF-B from PDE10 were cAMP stimulated via GAF-B, irrespective of the N-terminus in front of GAF-A. GAF-A from PDE5 was not functional and had a structural role only. However, chimeras in which only 36 aa long α-helical linker between PDE10 and PDE5 was switched, could not be activated, (Fig. 4.10). This result indicated that very specific domain interactions occur within GAF tandems in which this particular linker region plays an important role.

To determine which aa from the linker are responsible for the loss of regulation, two by two aa were changed in the PDE10 linker into the corresponding aa of the PDE5 linker (constructs No.1-16, Fig. 4.11, p. 117). WT PDE10-CyaB1 AC was 6.2-8.1-fold activated by cAMP, had a basal activity of 280 nmol cAMP/mg·min and an $EC_{50}$ value of 8.1 ± 2.0 μM cAMP (Fig. 4.36).

Constructs No.1-3 with mutations within the first 8 aa (two of them are conserved, Fig. 4.11) were regulated by cAMP, with basal activities and cAMP affinities comparable with the WT. Constructs No.4-16 could not be cAMP regulated (Fig. 4.16-20, Table 4.5). No.4-10 were fully active, with high basal activities. Constructs No.11-15 had basal activities gradually declining. No.16 had the lowest basal activity of only 14 nmol cAMP/mg·min. Low cGMP activation occurred in No.2 and 3 (1.9 and 2.0-fold, respectively at high cGMP concentrations), perhaps due to the fact that cGMP can slip into the cAMP binding pocket [12].

The most striking fact was that V239L and C240Y mutations in construct No.4 caused a 7-fold increase in basal activity, an 8-fold decrease of cAMP $EC_{50}$ concentrations in comparison with WT and essentially a loss of cAMP regulation. It seems that No.4 was in a kind of "on" state, fully active due to disinhibition of the AC at the N-terminus. Possibly, the mutations in the linker caused a conformational change towards the "active state" of the enzyme and had the same effect as cAMP activation of WT PDE10 –forming the CyaB1 AC catalytic cleft and allowing substrate to bind. Concomitantly the flexibility between N-terminal domains and the catalytic center was changed causing a kind of disengagement between GAF domains and loss of cAMP regulation. In No.5-10 mutants the same effect may prevail, although their basal activities were slightly lower than No.4. In these constructs subtle interactions within

tandem GAFs which hold the enzyme in the "off" state could be disrupted allowing full enzyme activity.

The crystal structure of PDE2 showed that the linker between GAF-A and B is extensively involved in dimerzation and thus plays an important role in the regulation of activity. There are indications that the domain organization of PDE5 is the same as in PDE2 [33]. Mutations in No.4-16 could alter this dimerization interface and cause the conformational change of the regulatory/catalytic domains, i.e. loss of regulation.

In the next experiments, mutations of V239L or C240Y in construct No.3 (No.17 and 18, Fig. 4.21) should indicate whether both aa or only one of them are responsible for the increase in basal activity and loss of regulation in No.4. One assumed that mutation of valine into another hydrophobic aa such as leucine will not influence regulation, but that a cystein mutation into an aromatic tyrosine could do so. Results of threading (Prof. Böckler) using the crystal structure of PDE2 for modelling of the PDE10 structure showed that leucine and tyrosine may substitute for alanine and phenylalanine present in PDE2, without causing steric clashes or the secondary and tertiary structure changes.

No.17 was 5-fold cAMP stimulated, with basal activity similar as WT (0.6 ± 0.1 µmol cAMP/mg·min). cGMP stimulation was 3.1-fold, similar as No.3. No.18 was not cAMP regulated and had a high basal activity (1.8 ± 0.2 µmol cAMP/mg·min) similar as No.4. Both constructs had similar cAMP affinities 1.5 ± 0.2 µM and 3.2 ± 0.3 µM, respectively, for No.17 and 18 (Table 4.7, Fig 4.23-26). As speculated, the mutation of cysteine to tyrosine in No.3 was responsible for the dramatic changes observed in No.4.

To investigate whether mutations of V239L and C240Y have the same effect in WT PDE10-CyaB1 AC, three new constructs were generated: V239L, C240Y - No.19, V239L - No.20 and C240Y - No.21 (Fig. 4.27). These three constructs were cAMP regulated with activation factors of 6.4 for No.19, 5.0 for No.20 and 4.2 for No.21. Their basal activities were similar as WT (0.29 - 0.38 µmol cAMP/mg·min) and the cAMP $EC_{50}$ concentrations were 13.5 ± 1.5 µM (No.19), 1.9 ± 1.1 µM (No.20) and 4.9 ± 1.4 µM (No.21), (Fig. 4.29-32, Table 4.9). Obviously these mutations did not change cAMP regulation.

In 2009, the crystal structure of a near the full length of PDE2 (aa 215-900) was solved (see Fig. 1.4). That was the first PDE crystal structure with both regulatory and catalytic domains, without a ligand at GAF-B, according to which the α-helical linker between GAF-A and B is longer than deduced from the structure of the PDE2 tandem GAF (Fig 4.33). In the novel structure the linker is 44 aa long and consists of three segments: α5-helix from GAF-A, LH1 linker and α1-helix from GAF-B [33]. To confirm the importance of this linker in the

regulation of the catalytic activity, the complete α-helices were exchanged, K298-F341 from PDE5 to PDE10 (No.22) and S218-F261 from PDE10 to PDE5 (No.23). Both constructs lost the regulation with their respective allosteric activators cAMP/cGMP. Their basal activities were similar as WT PDE10/WT PDE5 (Fig. 36-38, Table 4.11). No.22 had the tendency to be inhibited by cGMP, similar as No.16. These results confirmed that the origin of α-helical linker plays an important role in the regulation of intramolecular signal transmission and that very subtle interactions occur in the dimers.

## 5.3 Tandem CaM-binding domains from hPDE1 in regulation of CyaB1 AC activity

As mentioned above, N-terminal domains have an important role in the regulation of most PDE activities. Homologies between different PDE families suggest that this property is evolutionarily conserved among all PDEs. Is it possible that other N-terminal regulatory tandem domains couple with the CyaB1 AC? This would indicate similarities in the mechanisms of PDE regulation at large.

PDE1 family contains N-terminal tandem CaM-binding domains (CaM1 and CaM2). CaM binding to these domains stimulates enzymatic activity up to 4-fold, probably through a conformational change which releases the inhibition of the enzyme (see 1.4.1) [50, 51]. A similar mechanism of activation was suggested for other CaM binding proteins such as CaM kinase II, myosin light chain kinase or calcineurin [51].

Calmodulin is a small acidic protein which changes its conformation by $Ca^{2+}$ binding to four binding sites. It was identified as an activator of PDE activity in the 1970s, prior to the advent of molecular cloning techniques [44].

Six chimeras were generated: A, B and C of PDE1A3 and D, E and F of PDE1B1 (p.117). They differ in their lengths at the C-terminal parts which are attached to the reporter enzyme. Expression and purification of PDE1A3 constructs under the same conditions as PDE1B1 constructs left impurities, possible degradation products detected by Western blotting (not shown). Proteolysis of PDE1As has been already described [48, 49, 51]. According to these reports, the cleavage site is in the CaM2 binding site region; the inhibitory domain is cleaved off and the enzyme is irreversibly activated in the absence of CaM. It is suggested that this could be the long-term mechanism of PDE1A activation. After the decreasing the expression temperature to 12°C and the IPTG concentration to 0.1 μM, these impurities were not anymore detected by Western blotting.

All six constructs were assayed in two ways (Fig. 4.44 and Fig. 4.45):

-at 3 μM calmodulin with increasing concentrations of $Ca^{2+}$

-at 30 μM $Ca^{2+}$ with increasing concentrations of calmodulin

These concentrations of $Ca^{2+}$ and calmodulin cover the physiological range of their concentrations.

PDE1A3 constructs had basal activities from 12.6-53.8 nmol cAMP/mg·min. Construct C had a maximal stimulation of 2.1-fold at 3 μM calmodulin and 200 μM $Ca^{2+}$. Constructs A and B were maximally 1.6 (2.2) fold activated, respectively.

PDE1B1 constructs had lower basal activities from 0.4-2.4 nmol cAMP/mg·min. Construct E was maximally stimulated 4.4-fold at 6 μM calmodulin and 30 μM $Ca^{2+}$. D and F were 1.7 and 1.9 fold stimulated, respectively, at 3 μM calmodulin and 200 μM $Ca^{2+}$ (Table 4.13).

Although tandem CaM binding domains structurally and functionally differ from tandem GAF domains, chimeras PDE1A3-CyaB1 AC and PDE1B1-CyaB1 AC were activated by CaM.

## 5.4 Tandem UCR domains from hPDE4 in regulation of CyaB1 AC activity

PDE4s have tandem regulatory UCR domains in front of the catalytic domain. In the long PDE4 isoforms, UCR1 and UCR2 interact with each other through electrostatic interactions and this module is important for the regulation of enzyme activity [59]. PKA phosphorylation of the serine in the RRESF motif located at the N-terminus of UCR1 activates long isoforms 60-250% [29, 56, 57]. Long PDE4s are dimers and UCR1 and 2 are involved in the dimerization interface [60]. They are also responsible for different interactions with other proteins, intracellular targeting and localization of the enzyme [66]. Restricted cAMP signaling in cellular compartments is best studied on this family of PDEs [29].

To investigate whether the tandem UCR1/2 domains from different long isoforms (PDE4D3, -A4 and -B1) can regulate the reporter enzyme CyaB1 AC by phosphomimetic mutation of the respective serine in the RRESF motif, constructs I-VIII were generated (p.117). All PDE4-CyaB1 AC proteins were partially purified. To improve the yield of the soluble proteins, a great number of expressions were carried out, in which different expression and purification condition were tried: cloning in vector systems with another promoter (pET vectors), expression temperature, IPTG concentration, imidazole concentration during cell lysis and affinity chromatography purification, $Ni^{2+}$ slurry used for purification ($Ni^{2+}$-NTA or $Ni^{2+}$-IDA), imidazole and sodium gradient concentrations during wash steps, the amount of elution buffer; for purification of PDE4A4 constructs an anion exchange chromatography was

attempted. Under all examined conditions, most of the protein remained in inclusion bodies. One of the reasons for that could be the fact that UCR domains have a great affinity to many proteins, making aggregates which can not be separated. Nevertheless, Western blotting signals of all chimeras showed no degradation products and they were used for densitometric evaluations of the protein purity (see 3.3).

### 5.4.1 hPDE4D3 tandem UCR domains in regulation of CyaB1 AC activity

Construct I had the complete N-terminal domain of PDE4D3, II was N-terminally truncated by 40 aa and III and IV had the phosphomimetic mutation of S54. Construct III was 3-3.8-fold more active than the unmutated I. This was similar to the reported fold activation of PDE4D3 holoenzyme by PKA phosphorylation of this serine residue [57]. The truncated construct II had a 3-4 higher basal activity which dropped almost 63 fold with the S54D mutation, (the purity of IV was 30% lower according to densitometry) indicating the role of N-terminus ahead of the UCR1 in signal transmission (Tables 4.15 and 4.16). It is possible that removal of 40 aa released the inhibition of the catalytic domain through a conformational change and shifted the catalytic domain toward a more compact state. A similar effect was demonstrated for PDE5 and PDE11 N-termini [11, 13].

Construct I and II were also altered by replacing the N-terminus by the respective 48 aa from CyaB1. Activity of the S54D protein was 2-fold higher than the unmutated construct (data not shown).

It was reported that phosphatidic acid activates PDE4 long isoforms 0.7-3-fold [62, 63]. This stimulatory action is probably charge mediated, since the N-terminus of UCR1 is polar, carrying a net positive charge (attracts negatively charged phosphatidic acid) and C-terminal of UCR1 is apolar. It is suggested that the mechanisms of phosphatidic acid and PKA activation of long PDE4 isoforms are the same – placing of a negative charge at N-terminus of UCR1, which supposedly causes the same conformational change resulting in PDE4 activation. 45 μM phosphatidic acid did not stimulate constructs I or II (Fig. 4.51).

### 5.4.2 hPDE4A4 tandem UCR domains in regulation of CyaB1 AC activity

PDE4A4 is a long isoform with the S145 phosphorylation site corresponding to PDE4D3 S54. To check whether PDE4A4 is stimulated upon phosphomimetic mutation, chimeras with full length of the UCR tandem (V) and the same one with a S145D mutation were generated (VI). As mentioned above, because of the insufficient purity and the impossibility to analyze the

available SDS-PAGE gels by densitometry, many experiments were carried out to improve protein purity.

In the first experiment, mutated protein was only 1.3-fold more active (Fig. 4.53). This was not very convincing, since both proteins contained many impurities and SDS-PAGE gels and Western blotting could not be evaluated by densitometry (Fig. 4.52).

pH optimum for both of the proteins was between 7 and 8.5 and at that pH protein with S145D mutation had 1.8-2 fold higher activity then the unmutated (Fig. 4.54).

Next, anion exchange chromatography was employed. Samples were dialyzed in equilibration buffer containing 10% glycerol, centrifuged to remove insoluble proteins and fines and chromatographed. No protein bands were visible on SDS-PAGE or Western blotting and there was no AC activity in different fractions. However, even with short centrifugations a small amount of the recombinant protein was pelleted which was clearly seen on Western blotting. Several experiments were carried out to get 1) more soluble protein into the supernatant and purify it by anion exchange chromatography or 2) more recombinant protein in the pellet by longer centrifugation (higher speed). Apparently both trials were unsuccessful. Most of the protein was in supernatant, although the highest specific activity was in the pellet. The next experiment was an attempt to obtain more protein in the pellet by centrifuging the sample in 10% glycerol for 1h at 49,200×g. The values for specific activities were higher for the S145D mutant in all three fractions (uncorrected values showed 1.8-fold activation in input, 4.3 in supernatant and 2.9 in pellet, Fig. 4.56). Densitometric evaluation of the Western blotting of input indicated that mutated PDE4A4 chimera was stimulated 1.9 fold over the unmutated one (Table 4.17). Western blotting of supernatant and pellets of unmutated protein, even after three attempts could not be obtained.

In the final experiment the expression temperature was decreased to 12°C as an attempt to improve the yield of soluble and pure protein and in the hope of a reduced expression of impurities at this temperature. Western blotting signals evaluated by densitometry confirmed 2-fold stimulation of protein by the phosphomimetic mutation (Fig. 4.59 and Table 4.18).

### 5.4.3 hPDE4B1 tandem UCR domains in regulation of CyaB1 AC activity

PDE4B1 is another long PDE4 isoform with the S133 phosphorylation site at the beginning of UCR1 corresponding to PDE4D3 S54. Chimeras with full length of UCR tandem (VII) and with S133D mutation (VIII) were cloned. Their Western blotting signals were evaluated by densitometry and demonstrated a 2.1 fold stimulation of the S133D protein (Fig. 4.62 and Table 4.19).

Long PDE4 isoforms PDE4A4, -B1 and -D3 in chimeras with CyaB1 AC can be regulated via phosphomimetic mutation of serine in the RRESF motif located at the beginning of UCR1. Activation was in the range 2.1-3.8 fold, possibly physiologically important.

## 5.5 Crystallization of hPDE5 GAF domains

Crystal structures of GAF domains from PDE2 (GAF A+B with bound cGMP), CyaB2 AC (GAF A+B with bound cAMP), PDE10 (GAF-B with bound cAMP) and most recently the crystal structure of the PDE2 tandem GAF domain and the catalytic domain as well as the NMR structure of PDE5 GAF-A with bound cGMP revealed similar conformation of all GAF domains [30-33, 43]: a six-stranded antiparallel β-sheet which is sandwiched between 2-4 α-helices involved in the dimerization interface and a mixture of short α-helices and loops which contains the cNMP binding pocket on each side (Fig. 1.3 and Fig. 1.4).

The structure of near full length of PDE2 gave an the insight into the possible mechanism of PDE regulation [33] (Fig. 1.4). According to this structure, PDE2 (aa 215-900) is a dimer with a linear, extended organization of GAF-A and GAF-B and the catalytic domains connected by a long, crossing α-helix. A dimer interface extends over the entire molecule. The two catalytic sites in dimer are occluded in the unliganded state through the dimeric contacts from H-loops which pack against each other and prevent substrate access. Upon cGMP binding into a flexible pocket in GAF-B, it becomes ordered and shifts the orientation of helices involved in the dimerization. Rotation of one of them causes the movement of GAF-B/catalytic domain linker which rotates the catalytic domains. The H-loop dimer interface breaks and the H-loops swing out, open the catalytic centre and enable substrate access. Thus, the rotation of the catalytic domain promotes enzyme activation. This mechanism could be a general mechanism of regulation of the PDE activity from their different N-terminal domains.

Cryo-electron micrography of full-length PDE5 and 6 show a similar domain organization as PDE2. The structure of a PDE5 tandem GAF domain or PDE5 holoenzyme would be of great importance for understanding of protein regulation.

Attempts to crystallize PDE5 tandem GAF domain were unsuccessful.

## 5.6 Possible pharmacological meaning of PDEs N-tandem domains

PDEs are considered for a long time to be attractive therapeutic targets for the treatment of many diseases. Different splice variants have specific functions in a variety of tissues. Deletions of individual promoters of distinct isoforms were associated with different phenotypes.

The highest levels of PDE5 are found in vascular smooth muscle, Purkinje neurons of cerebellum, pancreas, lung, platelets and kidney. PDE5 inhibitors sildenafil, tadalafil and vardenafil are used in the treatment of erectile dysfunction and pulmonary hypertension (most recently of neonates), and currently are tested for other pathological conditions [77-82]. PDE5 inhibitors have an effect only in the presence of NO or atrial natriuretic peptide (ANP) which stimulate GC and increase cGMP levels. In the presence of NO, PDE5 inhibitors reduce platelet aggregation and secretory function. PDE5 regulates cGMP levels in cardiac tissue in rodents during cardiac hypertrophy induced by high blood pressure. Transfer of this mechanism of regulation to human hypertension and heart failure would be of great importance [23, 24].

PDE10 is expressed in the striatum of brain, in testis and thyroid. Localization in striatum suggests a role in modulating striatal pathways and control of motor and behavioural functions. PDE10 inhibitors could have a role for treatment of psychiatric disorders [24, 85, 87]. In transgenic mice with Huntinton`s disease the PDE10 mRNA level was decreased and the change of cyclic nucleotide signaling could cause the loss of neuronal function in this disease. High levels of PDE10 are found in developing spermatocytes.

Different isoforms of PDE1 are localized in the CNS and PNS, sperm, testis, some cells of the immune system such as macrophages and T lymphocytes, heart and blood vessels. Some isoforms are localized in individual cells of the same cell type, like PDE1B expression is only in some Purkinje neurons. PDE1B knock-out mice had increased locomotor activity and reduced learning and memory capacity. Their role in immune cell activation is suggested [22]. PDE1A has a role in regulating the contraction of vascular muscle and sperm function. PDE1C is a regulator of smooth muscle proliferation in humans. PDE1C2 is expressed only in olfactory sensory neurons, regulating the cAMP signal in response to different odorants. CaM stimulated PDE1 isoforms are involved in mechanisms of integration of cell signaling pathways mediated by diverse second messengers, cNMPs and $Ca^{2+}$ [24, 45-52].

PDE4 selective inhibitors and knock-out mice studies gave a lot of information about the localization and role of different isoforms. PDE4D knock-out mice had reduced cholinergic

stimulation in bronchial airways causing the muscle dilatation as well as reduced hyperreactivity to allergens. PDE4D deficiency also promoted heart failure and cardiomyopathy (especially of PDE4D3). That was explained by PDE4D3 association with the ryanodine Ca-channel in cardiac tissue. PDE4D3 is bound to different proteins such as AKAPs (AKAP 450 and muscle-specific AKAP) which determines the localization of cAMP pools in the cell. PDE4B knock-out mice prevented generation of TNF-alpha from lipopolysaccharides in monocytes and macrophages. PDE4B inhibitors can be used as anti-inflammatory agents in asthma, psoriasis and arthritis. A decrease of the short PDE4D7 variant is significantly associated with an increased incidence of stroke and PDE4B1 and 3 and schizophrenia via interaction with DISC1 (disrupted in schizophrenia 1 locus) [71]. Rolipram is a typical PDE4 inhibitor which is an antidepressant, anti-inflammatory agent and vascular smooth muscle dilatator. It has very strong emetic side effects probably due to PDE4D3 inhibition in the area postrema of brain. The new generation of PDE4 inhibitors seems that reduce the emetic side effect. Rofumilast has been approved in July 2010 for treatment of COPD. It was suggested that PDE4 inhibitors can be used as memory-enhancing agents in Alzheimer´s and Parkinson disease as well in some neurodegenerative disease states [29, 54, 64, 66-68].

All PDE inhibitors known to date have been designed as competitive inhibitors of the active site. The high similarities in the catalytic domains cause side effects by inhibition of the other PDEs. However, small molecules could be designed to target regulatory domains. There are more than 100 expressed splice variants of all 11 families PDEs. Their unique N-terminal regulatory domains may be attractive drug targets. For example GAF domains in humans are identified only in PDEs, suggesting that synthesis of specific molecules that bind to GAF domains of hPDEs could be possible. The other unique N-terminal domains can be used for similar investigations. In that way cyclic nucleotide signaling could be controlled very specifically.

## 5.7 Open questions and outlook

More than 100 isoforms of PDEs catalyse hydrolysis of cAMP and/or cGMP, thus playing an important role in the control of cyclic nucleotide signaling.

In this work N-terminal regulatory tandem domains of different PDEs were analysed:

- tandem GAF domains from PDE5 and PDE10: the role of N-terminal part ahead of GAF-A in PDE5 and the role of linker region between GAF-A and GAF-B in PDE10 and PDE5

- tandem UCR domains from different long isoforms PDE4D3, -A4 and -B1
- tandem CaM-binding domains from PDE1A3 and -B1.

These domains structurally and functionally differ but have the same property of regulation of PDE activity by phosphorylation, binding small molecules and specifying the subcellular localization.

The test system in which CyaB1 AC was used as a reporter, helped in characterization of hPDE tandem GAF domains, indicating conservation of regulatory mechanisms from N-terminal domains through evolution.

The N-terminus ahead of GAF-A domain in PDE5 has a significant role in intramolecular signaling [11]. It is possible that the N-terminus with the GAF tandem affects the overall structure and accessibility of the cGMP binding pocket. Since short constructs were fully active and not cGMP affected, limited *in vivo* proteolysis at the N-terminus might be an additional way of PDE5 regulation. To gain further molecular insights it would be of great importance to elucidate the structure of a PDE5.

PDE10 is the only PDE with a tandem GAF domains activated by cAMP binding to GAF-B [10]. It seems that the α-helical linker region between GAF-A and GAF-B is important for signal transmission, since the complete α-helical linker exchange in PDE10 and PDE5 abrogated signaling. The reason for that could be sequence specific differences in the linkers which determine interactions within GAF tandem and influence signaling. This was confirmed by series of mutants in which aa from the PDE5 linker were step-wise introduced into the PDE10 linker. The most striking effect was caused by mutations of two aa in construct No.3, V239L and C240Y (No.4): loss of cAMP regulation, an increase of basal activity and a decrease of cAMP $EC_{50}$ concentration. Further mutational studies demonstrated that C240Y in No.3, but not V239L, was responsible for this effect. It would be interesting to examine what contributes to enzyme activation and loss of regulation in No.3 C240Y in comparison with No.3: is the hydroxyl group or the aromatic ring of tyrosine important? How does this tyrosine influence the flexibility of chimeras? Since V239L and C240Y mutants in the PDE10 linker were still cAMP stimulated, obviously C240Y mutation works together with other mutated aa(s) from PDE5 in front of it, causing enzyme activation and loss of regulation. These aa could be valine instead of alanine 233 and/or asparagine instead of glutamine 236. Mutated aa could also be involved in some new interactions in secondary or tertiary structure. Further mutational studies are currently undertaken to investigate this region.

The mutations in the linker might cause a conformational change in which interactions within tandem GAF domains are disrupted, resulting in forming of the catalytic cleft and substrate access as well as flexibility change between tandem GAF domains and the catalytic domain which abrogated cAMP regulation. The conformational change could occur through the altered dimerization interface.

For a complete understanding of regulatory mechanisms of PDE10 as well as for elucidation of the physiological role, generation of selective inhibitors would be helpful. Most inhibitors that inhibit other PDEs are poor inhibitors of PDE10, but non-selective inhibitors such as papaverine and dipyridamole inhibit PDE10. A structure of a PDE10 holoenzyme would also help in developing inhibitors and understanding the mechanism of signal transmission from GAF domains to the catalytic domain. It seems that the specific domain interactions are decisive for signaling in all PDEs with tandem GAF domains.

Upon CaM binding to PDE1 tandem CaM-binding domains, the conformational change from the N-terminus transmits the signal to the catalytic domain and activates it. Chimeras of PDE1A3 and -B1 with the reporter could be activated by CaM. This was surprising since CaM binding domains are structurally and functionally different from GAF domains. This indicates that mechanisms of regulation were established very early in the evolution.

Different long isoforms of PDE4D3, A4 and B1 in chimeras with the reporter have serine in the RRESF motif mutated to aspartate. This is a phosphomimetic mutation since the negative charge from aspartate mimics the negative charge of the phosphoryl group. All chimeras were activated over the corresponding unmutated proteins. In PDE4D3, removal of the N-terminal 40 aa ahead of UCR1 resulted in 3-4 fold higher basal activities which suggests that PDE4 N-terminals could also play a role in the regulation of signaling, already demonstrated for PDE5 and PDE11. Knowing a possible ligand for UCR1/2 tandem domains would also be helpful in understanding these mechanisms.

Crystal structures of PDE1 CaM binding domains and PDE4 UCR1/2 domains are not available up to now. They would be of great importance in elucidating the mechanisms of regulation.

# 6 Summary

α-helical linker regions between tandem GAF domains in PDE5 and 10 are essential for intramolecular signal transmission through subtle interactions between upstream and downstream GAF domains. Mutations within the first ten aa of the linker region S231-A366 of PDE10 into corresponding aa of PDE5 resulted in enzyme activation and loss of cAMP regulation. C240Y mutation was identified as one of them responsible for this effect and probably for the specific interactions within GAF tandem domains.

Beside tandem GAF domains from PDE2, 5, 10 and 11, N-terminal tandem domains from PDE1 – CaM-binding domains and PDE4 – UCR domains can regulate CyaB1 AC. PDE1A3-CyaB1 AC chimera was 2.1 and PDE1B1-CyaB1 AC was 4.4-fold stimulated by CaM, what is similar to the already reported values for CaM stimulation of these holoenzymes. PDE4A4-, B1- and D3- CyaB1 AC chimeras were activated by phosphomimetic mutation of serine from the phosphorylation motif at the beginning of UCR1, 2, 2.1, and 3.8-fold, respectively, similarly as the reported activation of the holoenzymes by serine phosphorylation.

Successful substitutions of tandem GAF domain from cyanobacterial AC by different tandem domains of human PDEs indicates that molecular mechanisms which regulate enzyme activity upon modifications from N-terminal domains are conserved and similar in all PDEs and established early in the evolution. Recently solved crystal structure of near full length hPDE2 helped in elucidating this mechanism. It is possible that N-terminal domains of different PDEs regulate access to the substrate binding pocket as the way of regulation catalytic activity.

# Appendix

***List of constructs (all constructs contain CyaB1 AC L386-K859 at the C-terminus):***

Shortened hPDE5-CyaB1 AC:

```
PDE5 (A89-E513)-
PDE5 (N91-E513)-
PDE5 (G95-E513)-

PDE5 NAAIRS-
```

Mutations in hPDE10 and hPDE5 linker domain (mutated aa in linker are underlined):

```
No.1  GIAIHQVQVCRGLAKQTELNDFLLDVSKTYFDNIVA-
No.2  GIVLHQVQVCRGLAKQTELNDFLLDVSKTYFDNIVA-
No.3  GIVLHNAQVCRGLAKQTELNDFLLDVSKTYFDNIVA-
No.4  GIVLHNAQLYRGLAKQTELNDFLLDVSKTYFDNIVA-
No.5  GIVLHNAQLYETLAKQTELNDFLLDVSKTYFDNIVA-
No.6  GIVLHNAQLYETSLKQTELNDFLLDVSKTYFDNIVA-
No.7  GIVLHNAQLYETSLLETELNDFLLDVSKTYFDNIVA-
No.8  GIVLHNAQLYETSLLENKLNDFLLDVSKTYFDNIVA-
No.9  GIVLHNAQLYETSLLENKRNDFLLDVSKTYFDNIVA-
No.10 GIVLHNAQLYETSLLENKRNQVLLDVSKTYFDNIVA-
No.11 GIVLHNAQLYETSLLENKRNQVLLDLAKTYFDNIVA-
No.12 GIVLHNAQLYETSLLENKRNQVLLDLASLYFDNIVA-
No.13 GIVLHNAQLYETSLLENKRNQVLLDLASLIFDNIVA-
No.14 GIVLHNAQLYETSLLENKRNQVLLDLASLIFEEIVA-
No.15 GIVLHNAQLYETSLLENKRNQVLLDLASLIFEEQQA-
No.16 GIVLHNAQLYETSLLENKRNQVLLDLASLIFEEQQS-
No.17 GIVLHNAQLCRGLAKQTELNDFLLDVSKTYFDNIVA-
No.18 GIVLHNAQVYRGLAKQTELNDFLLDVSKTYFDNIVA-
No.19 SVAIHQVQLYRGLAKQTELNDFLLDVSKTYFDNIVA-
No.20 SVAIHQVQLCRGLAKQTELNDFLLDVSKTYFDNIVA-
No.21 SVAIHQVQVYRGLAKQTELNDFLLDVSKTYFDNIVA-
No.22 PDE10, PDE5 (K298-F341)-
WT PDE10-
No.23 PDE5, PDE10 (S218-F261)-
WT PDE5-
```

hPDE1-CyaB1 AC chimeras:

```
A: PDE1A3 (M1–M178)-
B: PDE1A3 (M1–L206)-
C: PDE1A3 (M1–M234)-
D: PDE1B1 (M1–T182)-
E: PDE1B1 (M1–A210)-
F: PDE1B1 (M1–F238)-
```

hPDE4-CyaB1 AC chimeras:

I-PDE4D3 (M1-S212)-
II-PDE4D3 (L40-S212)-
III-**S54D** PDE4D3 (M1-S212)-
IV-**S54D** PDE4D3 (L40-S212)-
V- PDE4A4 (M1-S302)-
VI- **S145D** PDE4A4 (M1-S302)-
VII- PDE4B1 (M1-S290)-
VIII- **S133D** PDE4B1 (M1-S290)-

***Sequences used in this study:***

*CyaB1 AC*
gi: 15553049
Acc. nb.: D89623
GeneID (CyaB1): 1105863
*Human PDE10A1*
gi: 4894715
Acc. nb.: AAD32959
GeneID (PDE10A): 10846
*Human PDE10A2*
gi: 5902441
Acc. nb.: AB026816
GeneID (PDE10A): 10846
*Human PDE5A1*
gi: 61744434
Acc. nb.: NM_001083
GeneID (PDE5A): 8654
*Human PDE1A3*
gi: 51102294
Acc. nb.: NM_001003683
GeneID (PDE1A): 5136
*Human PDE1B1*
gi: 24431942
Acc. nb.: NM_000924
GeneID (PDE1B): 5153
*Human PDE4D3*
gi: 157277986
Acc. nb.: NM_006203
GeneID (PDE4D3): 5144
*Human PDE4A4*
gi: 162329607
Acc. nb.: NM_001111307
GeneID (PDE4A4): 5141
*Human PDE4B1*
gi: 82799485
Acc. nb.: NM_001037341
GeneID (PDE4B1): 5142

1. **Katayama, M., and M. Ohmori**. 1997. Isolation and characterization of multiple adenylate cyclase genes from the cyanobacterium Anabaena sp. strain PCC 7120. *J Bacteriol* **179**, 3588-93.
2. **Kasahara, M., and M. Ohmori**. 1999. Activation of a cyanobacterial adenylate cyclase, CyaC, by autophosphorylation and a subsequent phosphotransfer reaction. *J Biol Chem* **274**, 15167-72.
3. **Ho, Y. S., L. M. Burden, and J. H. Hurley**. 2000. Structure of the GAF domain, a ubiquitous signaling motif and a new class of cyclic GMP receptor. *EMBO J* **19**, 5288-99.
4. **McAllister-Lucas, L. M., W. K. Sonnenburg, A. Kadlecek, D. Seger, H. L. Trong, J. L. Colbran, M. K. Thomas, K. A. Walsh, S. H. Francis, J. D. Corbin, and et al.** 1993. The structure of a bovine lung cGMP-binding, cGMP-specific phosphodiesterase deduced from a cDNA clone. *J Biol Chem* **268**, 22863-73.
5. **McAllister-Lucas, L. M., T. L. Haik, J. L. Colbran, W. K. Sonnenburg, D. Seger, I. V. Turko, J. A. Beavo, S. H. Francis, and J. D. Corbin**. 1995. An essential aspartic acid at each of two allosteric cGMP-binding sites of a cGMP-specific phosphodiesterase. *J Biol Chem* **270**, 30671-9.
6. **Soderling, S. H., and J. A. Beavo**. 2000. Regulation of cAMP and cGMP signaling: new phosphodiesterases and new functions. *Curr Opin Cell Biol* **12**, 174-9.
7. **Kanacher, T., A. Schultz, J. U. Linder, and J. E. Schultz**. 2002. A GAF-domain-regulated adenylyl cyclase from Anabaena is a self-activating cAMP switch. *EMBO J* **21**, 3672-80.
8. **Martinez, S. E., A. Y. Wu, N. A. Glavas, X. B. Tang, S. Turley, W. G. Hol, and J. A. Beavo**. 2002. The two GAF domains in phosphodiesterase 2A have distinct roles in dimerization and in cGMP binding. *Proc Natl Acad Sci U S A* **99**, 13260-5.
9. **Bruder, S., J. U. Linder, S. E. Martinez, N. Zheng, J. A. Beavo, and J. E. Schultz**. 2005. The cyanobacterial tandem GAF domains from the cyaB2 adenylyl cyclase signal via both cAMP-binding sites. *Proc Natl Acad Sci U S A* **102**, 3088-92.
10. **Gross-Langenhoff, M., K. Hofbauer, J. Weber, A. Schultz, and J. E. Schultz**. 2006. cAMP is a ligand for the tandem GAF domain of human phosphodiesterase 10 and cGMP for the tandem GAF domain of phosphodiesterase 11. *J Biol Chem* **281**, 2841-6.
11. **Bruder, S., A. Schultz, and J. E. Schultz**. 2006. Characterization of the tandem GAF domain of human phosphodiesterase 5 using a cyanobacterial adenylyl cyclase as a reporter enzyme. *J Biol Chem* **281**, 19969-76.
12. **Hofbauer, K., A. Schultz, and J. E. Schultz**. 2008. Functional chimeras of the phosphodiesterase 5 and 10 tandem GAF domains. *J Biol Chem* **283**, 25164-70.
13. **Gross-Langenhoff, M., A. Stenzl, F. Altenberend, A. Schultz, and J. E. Schultz,** 2008. The properties of the phosphodiesterase 11A4 GAF domains are regulated by modi-fications in its N-terminal domain. *FEBS Journal* **275**, 1643-50.
14. **Scott, J. D., and T. Pawson**. 2000. Cell communication: the inside story. *Sci Am* **282**, 72-9.
15. **Sutherland, E. W., and T. W. Rall**. 1958. Fractionation and characterization of a cyclic adenine ribonucleotide formed by tissue particles. *J Biol Chem* **232**, 1077-91.

16. **Ashman, D. F., R. Lipton, M. M. Melicow, and T. D. Price**. 1963. Isolation of adenosine 3', 5'-monophosphate and guanosine 3', 5'-monophosphate from rat urine. *Biochem Biophys Res Commun* **11**, 330-4.
17. **Lipkin, D., W. H. Cook, and R. Markham**. 1959. Adenosine-3′: 5′-phosphoric Acid: A Proof of Structure. *J Am Chem Soc* **81**, 6198-203.
18. **Hurley, J. H.** 1998. The adenylyl and guanylyl cyclase superfamily. *Curr Opin Struct Biol* **8**, 770-77.
19. **Hurley, J. H.** 1999. Structure, Mechanism, and Regulation of Mammalian Adenylyl Cyclase. *J Biol Chem* **274**, 7599-602.
20. **Francis, S. H., I. V. Turko, and J. D. Corbin**. 2001. Cyclic nucleotide phosphodiesterases: relating structure and function. *Prog Nucleic Acid Res Mol Biol* **65**, 1-52.
21. **Beavo, J. A., R. S. Hansen, S. A. Harrison, R. L. Hurwitz, T. J. Martins, and M. C. Mumby**. 1982. Identification and properties of cyclic nucleotide phosphodiesterases. *Mol Cell Endocrinol* **28**, 387-410.
22. **Beavo, J. A., M. Conti, and R. J. Heaslip**. 1994. Multiple cyclic nucleotide phosphodiesterases. *Mol Pharmacol* **46**, 399-405.
23. **Conti, M., and J. Beavo**. 2007. Biochemistry and Physiology of Cyclic Nucleotide Phosphodiesterases: Essential Components in Cyclic Nucleotide Signaling. *Annu Rev Biochem* **76**, 481-511.
24. **Bender, A. T., and J. A. Beavo**. 2006. Cyclic nucleotide phosphodiesterases: molecular regulation to clinical use. *Pharmacol Rev* **58**, 488-520.
25. **Menniti, F. S., W. S. Faraci, and C. J. Schmidt**. 2006. Phosphodiesterases in the CNS: targets for drug development. *Nat Rev Drug Discov* **5**, 660-70.
26. **Zhang, K. Y. J., G. L. Card, Y. Suzuki, D. R. Artis, D. Fong, S. Gillette, D. Hsieh, J. Neiman, B. L. West, C. Zhang, M. V. Milburn, S. -H. Kim, J. Schlessinger, and G. Bollag,** 2004. A Glutamine Switch Mechanism for Nucleotide Selectivity by Phosphodiesterases. *Molecular Cell* **15**, 279-86.
27. **Wang, H., Y. Liu, J. Hou, M. Zheng, H. Robinson, and H. Ke**. 2007. Structural insight into substrate specificity of phosphodiesterase 10. *Proc Natl Acad Sci U S A* **104**, 5782-7.
28. **Xu, R. X., A. M. Hassell, D. Vanderwall, M. H. Lambert, W. D. Holmes, M. A. Luther, W. J. Rocque, M. V. Milburn, Y. Zhao, H. Ke, and R. T. Nolte**. 2000. Atomic structure of PDE4: insights into phosphodiesterase mechanism and specificity. *Science* **288**, 1822-5.
29. **Houslay, M. D., and D. R. Adams**. 2003. PDE4 cAMP phosphodiesterases: modular enzymes that orchestrate signalling cross-talk, desensitization and compartmentalization. *Biochem J* **370**, 1-18.
30. **Martinez, S. E., J. A. Beavo, and W. G. Hol**. 2002. GAF Domains: Two-Billion-Year-Old Molecular Switches that Bind Cyclic Nucleotides. *Mol Interv* **2**, 317-23.
31. **Handa, N., E. Mizohata, S. Kishishita, M. Toyama, S. Morita, T. Uchikubo-Kamo, R. Akasaka, K. Omori, J. Kotera, T. Terada, M. Shirouzu, and S. Yokoyama**. 2008. Crystal Structure of the GAF-B Domain from Human Phosphodiesterase 10A Complexed with Its Ligand, cAMP. *J Biol Chem* **283**, 19657-64.
32. **Heikaus, C. C., J. R. Stout, M. R. Sekharan, C. M. Eakin, P. Rajagopal, P. S. Brzovic, J. A. Beavo, and R. E. Klevit**. 2008. Solution structure of the cGMP binding GAF domain from phosphodiesterase 5: insights into nucleotide specificity, dimerization, and cGMP-dependent conformational change. *J Biol Chem* **283**, 22749-59.

33. **Pandit J, F. M., K. F. Fennell, K. S. Dillman, and F. S. Menniti** 2009. Mechanism for the allosteric regulation of phosphodiesterase 2A deduced from the X-ray structure of a near full-length construct. *Proc Natl Acad Sci U S A*. **106**, 18225-30.
34. **Anantharaman, V., E. V. Koonin, and L. Aravind**. 2001. Regulatory potential, phyletic distribution and evolution of ancient, intracellular small-molecule-binding domains. *J Mol Biol* **307**, 1271-92.
35. **Aravind, L., and C. P. Ponting**. 1997. The GAF domain: an evolutionary link between diverse phototransducing proteins. *Trends Biochem Sci* **22**, 458-9.
36. **Schultz, J., F. Milpetz, P. Bork, and C. P. Ponting**. 1998. SMART, a simple modular architecture research tool: identification of signaling domains. *Proc Natl Acad Sci U S A* **95**, 5857-64.
37. **Rybalkin, S. D., I. G. Rybalkina, M. Shimizu-Albergine, X. B. Tang, and J. A. Beavo**. 2003. PDE5 is converted to an activated state upon cGMP binding to the GAF A domain. *EMBO J* **22**, 469-78.
38. **Wu, A. Y., X. B. Tang, S. E. Martinez, K. Ikeda, and J. A. Beavo**. 2004. Molecular determinants for cyclic nucleotide binding to the regulatory domains of phosphodiesterase 2A. *J Biol Chem* **279**, 37928-38.
39. **Norton, A. W., M. R. D`Amours, H. J. Grazio, T. L. Hebert, and R. H. Cote**. 2000. Mechanism of Transducin Activation of Frog Rod Phototreceptor Phosphodiesterase. *J Biol Chem* **275**, 38611-19.
40. **Levdikov, V. M., E. Blagova, P. Joseph, A. L. Sonenshein, and A. J. Wilkinson**. 2006. The structure of CodY, a GTP- and isoleucine-responsive regulator of stationary phase and virulence in gram-positive bacteria. *J Biol Chem* **281**, 11366-73.
41. **Zoraghi, R., J. D. Corbin, and S. H. Francis.** 2004. Properties and functions of GAF domains in cyclic nucleotide phosphodiesterases and other proteins. *Mol Pharmacol* **65**, 267-78.
42. **Schultz, J. E.** 2008. Structural and Biochemical Aspects of Tandem GAF domains, in *cGMP: Generators, Effectors and Therapeutic Implications*, H. H. H. W. Schmidt, F. Hofmann, and J. -P. Stasch, Editors. Springer-Verlag Berlin Heidelberg, 93-109.
43. **Martinez, S. E., S. Bruder, A. Schultz, N. Zheng, J. E. Schultz, J. A. Beavo, and J. U. Linder**. 2005. Crystal structure of the tandem GAF domains from a cyanobacterial adenylyl cyclase: modes of ligand binding and dimerization. *Proc Natl Acad Sci U S A* **102**, 3082-7.
44. **Cheung, W. Y.** 1970. Cyclic 3',5'-nucleotide phosphodiesterase. Demonstration of an activator. *Biochem Biophys Res Commun* **38**, 533-8.
45. **Charbonneau, H., S. Kumar, J. P. Novack, D. K. Blumenthal, P. R. Griffin, J. Shabanowitz, D. F. Hunt, J. A. Beavo, and K. A. Walsh**. 1991. Evidence for domain organization within the 61-kDa calmodulin-dependent cyclic nucleotide phosphodiesterase from bovine brain. *Biochemistry* **30**, 7931-40.
46. **Loughney, K., T. J. Martins, E. A. Harris, K. Sadhu, J. B. Hicks, W. K. Sonnenburg, J. A. Beavo, and K. Ferguson**. 1996. Isolation and characterization of cDNAs corresponding to two human calcium, calmodulin-regulated, 3',5'-cyclic nucleotide phosphodiesterases. *J Biol Chem* **271**, 796-806.
47. **Yu, J., S. L. Wolda, A. L. Frazier, V. A. Florio, T. J. Martins, P. B. Snyder, E. A. Harris, K. N. McCaw, C. A. Farrell, B. Steiner, J. K. Bentley, J. A. Beavo, K. Ferguson, and R. Gelinas**. 1997. Identification and characterisation of a human calmodulin-stimulated phosphodiesterase PDE1B1. *Cell Signal* **9**, 519-29.

48. **Sonnenburg, W. K., D. Seger, K. S. Kwak, J. Huang, H. Charbonneau, and J. A. Beavo**. 1995. Identification of inhibitory and calmodulin-binding domains of the PDE1A1 and PDE1A2 calmodulin-stimulated cyclic nucleotide phosphodiesterases. *J Biol Chem* **270**, 30989-1000.
49. **Michibata, H., N. Yanaka, Y. Kanoh, K. Okumura, and K. Omori**. 2001. Human $Ca^{2+}$/calmodulin-dependent phosphodiesterase PDE1A: novel splice variants, their specific expression, genomic organization, and chromosomal localization. *Biochim Biophys Acta* **1517**, 278-87.
50. **Sharma, R. K., S. B. Das, A. Lakshmikuttyamma, P. Selvakumar, and A. Shrivastav**. 2006. Regulation of calmodulin-stimulated cyclic nucleotide phosphodiesterase (PDE1). *Int J Mol Med* **18**, 95-105.
51. **Bender, A. T.** 2006. Calmodulin-stimulated nucleotide phosphodiesterases, in *Cyclic Nucleotide Phosphodiesterases in Health and Disease,* J. A. Beavo, S. H. Fransis, and M. D. Houslay, Editors. CRC Press. 35-54.
52. **Yan, C., A. Z. Zhao, J. K. Bentley, K. Loughney, K. Ferguson, and J. A. Beavo**. 1995. Molecular cloning and characterization of a calmodulin-dependent phosphodiesterase enriched in olfactory sensory neurons. *Proc Natl Acad Sci U S A* **92**, 9677-81.
53. **Nikolaev, V. O., S. Gambaryan, S. Engelhardt, U. Walter, and M. J. Lohse**. 2005. Real-time monitoring of the PDE2 activity of live cells: hormone-stimulated cAMP hydrolysis is faster than hormone-stimulated cAMP synthesis. *J Biol Chem* **280**, 1716-9.
54. **Conti, M., W. Richter, C. Mehats, G. Livera, J. Y. Park, and C. Jin**. 2003. Cyclic AMP-specific PDE4 phosphodiesterases as critical components of cyclic AMP signaling. *J Biol Chem* **278**, 5493-6.
55. **Richter, W., S. L. Jin, and M. Conti**. 2005. Splice variants of the cyclic nucleotide phosphodiesterase PDE4D are differentially expressed and regulated in rat tissue. *Biochem J* **388**, 803-11.
56. **Sette, C., and M. Conti.** 1996. Phosphorylation and Activation of a cAMP-specific Phosphodiesterase by the cAMP-dependent Protein Kinase. *J Biol Chem* **271**, 16526-34.
57. **MacKenzie, S. J., G. S. Baillie, I. McPhee, C. MacKenzie, R. Seamons, T. McSorley, J. Millen, M. B. Beard, G. van Heeke, and M. D. Houslay**. 2002. Long PDE4 cAMP specific phosphodiesterases are activated by protein kinase A-mediated phosphorylation of a single serine residue in Upstream Conserved Region 1 (UCR1). *Br J Pharmacol* **136**, 421-33.
58. **MacKenzie, S. J., G. S. Baillie, I. McPhee, G. B. Bolger, and M. D. Houslay**. 2000. ERK2 mitogen-activated protein kinase binding, phosphorylation, and regulation of the PDE4D cAMP-specific phosphodiesterases. The involvement of COOH-terminal docking sites and NH2-terminal UCR regions. *J Biol Chem* **275**, 16609-17.
59. **Beard, M. B., A. E. Olsen, R. E. Jones, S. Erdogan, M. D. Houslay, and G. B. Bolger**. 2000. UCR1 and UCR2 domains unique to the cAMP-specific phosphodiesterase family form a discrete module via electrostatic interactions. *J Biol Chem* **275**, 10349-58.
60. **Richter, W., and M. Conti**. 2002. Dimerization of the type 4 cAMP-specific phosphodiesterases is mediated by the upstream conserved regions (UCRs). *J Biol Chem* **277**, 40212-21.
61. **Richter, W., and M. Conti**. 2004. The oligomerization state determines regulatory properties and inhibitor sensitivity of type 4 cAMP-specific phosphodiesterases. *J Biol Chem* **279**, 30338-48.

62. **Nemoz, G., C. Sette, and M. Conti.** 1997. Selective Activation of Rolipram-Sensitive, cAMP-Specific Phosphodiesterase Isoforms by Phosphatidic Acid. *Mol Pharmacol* **51**, 242-9.
63. **Grange, M., C. Sette, M. Cuomo, M. Conti, M. Lagarde, A. F. Prigent, and G. Nemoz**. 2000. The cAMP-specific phosphodiesterase PDE4D3 is regulated by phosphatidic acid binding. Consequences for cAMP signaling pathway and characterization of a phosphatidic acid binding site. *J Biol Chem* **275**, 33379-87.
64. **Houslay, M. D., G. S. Baillie, and D. H. Maurice**. 2007. cAMP-Specific phosphodiesterase-4 enzymes in the cardiovascular system: a molecular toolbox for generating compartmentalized cAMP signaling. *Circ Res* **100**, 950-66.
65. **Houslay, M. D., and D. R. Adams**. Putting the lid on phosphodiesterase 4. *Nat Biotechnol* **28**, 38-40.
66. **Houslay, M. D.** 2010. Underpinning compartmentalised cAMP signalling through targeted cAMP breakdown. *Trends Biochem Sci* **35**, 91-100.
67. **Baillie, G. S.** 2009. Compartmentalized signalling: spatial regulation of cAMP by the action of compartmentalized phosphodiesterases. *FEBS J* **276**, 1790-9.
68. **Houslay, M. D., and G. Milligan**. 1997. Tailoring cAMP-signalling responses through isoform multiplicity. *Trends Biochem Sci* **22**, 217-24.
69. **Huang, Z., Y. Ducharme, D. Macdonald, and A. Robichaud**. 2001. The next generation of PDE4 inhibitors. *Curr Opin Chem Biol* **5**, 432-8.
70. **Schmidt, D., G. Dent, and K. F. Rabe**. 1999. Selective phosphodiesterase inhibitors for the treatment of bronchial asthma and chronic obstructive pulmonary disease. *Clin Exp Allergy* **29 Suppl 2**, 99-109.
71. **Millar, J. K., B. S. Pickard, S. Mackie, R. James, S. Christie, S. R. Buchanan, M. P. Malloy, J. E. Chubb, E. Huston, G. S. Baillie, P. A. Thomson, E. V. Hill, N. J. Brandon, J. C. Rain, L. M. Camargo, P. J. Whiting, M. D. Houslay, D. H. Blackwood, W. J. Muir, and D. J. Porteous**. 2005. DISC1 and PDE4B are interacting genetic factors in schizophrenia that regulate cAMP signaling. *Science* **310**, 1187-91.
72. **Francis, S. H., T. M. Lincoln, and J. D. Corbin**. 1980. Characterization of a novel cGMP binding protein from rat lung. *J Biol Chem* **255**, 620-6.
73. **Coquil, J. F., D. J. Franks, J. N. Wells, M. Dupuis, and P. Hamet**. 1980. Characteristics of a new binding protein distinct from the kinase for guanosine 3':5'-monophosphate in rat platelets. *Biochim Biophys Acta* **631**, 148-65.
74. **Francis, S. H., E. P. Bessay, J. Kotera, K. A. Grimes, L. Liu, W. J. Thompson, and J. D. Corbin**. 2002. Phosphorylation of Isolated Human Phosphodiesterase-5 Regulatory Domain Induces an Apparent Conformational Change and Increases cGMP Binding Affinity. *J Biol Chem* **277**, 47581-47587.
75. **Corbin, J. D., I. V. Turko, A. Beasley, and S. H. Francis**. 2000. Phosphorylation of phosphodiesterase-5 by cyclic nucleotide-dependent protein kinase alters its catalytic and allosteric cGMP-binding activities. *Eur J Biochem* **267**, 2760-7.
76. **Bessay, E. P., M. A. Blount, R. Zoraghi, A. Beasley, K. A. Grimes, S. H. Francis, and J. D. Corbin**. 2008. Phosphorylation increases affinity of the phosphodiesterase-5 catalytic site for tadalafil. *J Pharmacol Exp Ther* **325**, 62-8.
77. **Corbin, J. D.** 2004. Mechanisms of action of PDE5 inhibition in erectile dysfunction. *Int J Impot Res* **16 Suppl 1**, S4-7.
78. **Corbin, J. D., S. H. Francis, and D. J. Webb**. 2002. Phosphodiesterase type 5 as a pharmacologic target in erectile dysfunction. *Urology* **60**, 4-11.
79. **Blount, M. A., A. Beasley, R. Zoraghi, K. R. Sekhar, E. P. Bessay, S. H. Francis, and J. D. Corbin**. 2004. Binding of tritiated sildenafil, tadalafil, or

vardenafil to the phosphodiesterase-5 catalytic site displays potency, specificity, heterogeneity, and cGMP stimulation. *Mol Pharmacol* **66**, 144-52.

80. **Corbin, J. D., and S. H. Francis**. 1999. Cyclic GMP phosphodiesterase-5: target of sildenafil. *J Biol Chem* **274**, 13729-32.
81. **Rybalkin, S. D., I. G. Rybalkina, R. Feil, F. Hofmann, and J. A. Beavo**. 2002. Regulation of cGMP-specific Phosphodiesterase (PDE5) Phoshorylation in Smooth Muscle Cells. *J Biol Chem* **277**, 3310-17.
82. **Hoeper, M. M.** 2005. Drug treatment of pulmonary arterial hypertension: current and future agents. *Drugs* **65**, 1337-54.
83. **Fujishige, K., J. Kotera, H. Michibata, K. Yuasa, S. Takebayashi, K. Okumura, and K. Omori**. 1999. Cloning and characterization of a novel human phosphodiesterase that hydrolyzes both cAMP and cGMP (PDE10A). *J Biol Chem* **274**, 18438-45.
84. **Soderling, S. H., S. J. Bayuga, and J. A. Beavo**. 1999. Isolation and characterization of a dual-substrate phosphodiesterase gene family: PDE10A. *Proc Natl Acad Sci U S A* **96**, 7071-6.
85. **Loughney, K., P. B. Snyder, L. Uher, G. J. Rosman, K. Ferguson, and V. A. Florio**. 1999. Isolation and characterization of PDE10A, a novel human 3′,5′-cyclic nucleotide phosphodiesterase. *Gene* **234**, 109-17.
86. **Fujishige, K., J. Kotera, K. Yuasa, and K. Omori**. 2000. The human phosphodiesterase PDE10A gene: Genomic organization and evolutionary relatedness with other PDEs containing GAF domains. *Eur J Biochem* **267**, 5943-51.
87. **Fujishige, K., J. Kotera, and K. Omori**. 1999. Striatum- and testis-specific phosphodiesterase PDE10A isolation and characterization of a rat PDE10A. *Eur J Biochem* **266**, 1118-27.
88. **Kotera, J., T. Sasaki, T. Kobayashi, K. Fujishige, Y. Yamashita, and K. Omori**. 2004. Subcellular localization of cyclic nucleotide phosphodiesterase type 10A variants, and alteration of the localization by cAMP-dependent protein kinase-dependent phosphorylation. *J Biol Chem* **279**, 4366-75.
89. **Kotera, J., K. Fujishige, K. Yuasa, and K. Omori**. 1999. Characterization and phosphorylation of PDE10A2, a novel alternative splice variant of human phosphodiesterase that hydrolyzes cAMP and cGMP. *Biochem Biophys Res Commun* **261**, 551-7.
90. **Linder, J. U., and J. E. Schultz**. 2003. The class III adenylyl cyclases: multi-purpose signalling modules. *Cell Signal* **15**, 1081-9.
91. **Linder, J. U.** 2006. Class III adenylyl cyclases: molecular mechanisms of catalysis and regulation. *Cell Mole Life Sciences* **63**, 1736-51.
92. **Sanger, F., S. Nicklen, and A. R. Coulson**. 1977. DNA sequencing with chain-terminating inhibitors. *Proc Natl Acad Sci U S A* **74**, 5463-7.
93. **Bradford, M. M.** 1976. A rapid and sensitive method for the quantitation of microgram quantities of protein utilizing the principle of protein-dye binding. *Anal Biochem* **72**, 248-54.
94. **Laemmli, U. K.** 1970. Cleavage of structural proteins during the assembly of the head of bacteriophage T4. *Nature* **227**, 680-5.
95. **Towbin, H., T. Staehelin, and J. Gordon**. 1979. Electrophoretic transfer of proteins from polyacrylamide gels to nitrocellulose sheets: procedure and some applications. *Proc Natl Acad Sci U S A* **76**, 4350-4.
96. **Salomon, Y., C. Londos, and M. Rodbell**. 1974. A highly sensitive adenylate cyclase assay. *Anal Biochem* **58**, 541-8.

97. **Diel, S., K. Klass, B. Wittig, and C. Kleuss**. 2006. Gbetagamma activation site in adenylyl cyclase type II. Adenylyl cyclase type III is inhibited by Gbetagamma. *J Biol Chem* **281**, 288-94.
98. **Gopalakrishna, R., and W. B. Anderson.** 1982. Ca $^{2+}$-induced hydrophobic site on calmodulin: application for purification of calmodulin by phenyl-sepharose affinity chromatography. *Biochem Biophys Res Commun* **104-2,** 830-6.
99. **Hofbauer, K.** (2007). Die GAF-Domänen der human Phosphodiesterase 10. *Dissertation der Universität Tübingen*.
100. **Bruder, S.** 2006. cAMP- und cGMP-bindende Tandem-GAF-Domänen – Biochemische Untersuchungen mit einer cyanobakteriellen Adenylatcyclase. *Dissertation der Universität Tübingen.*

# CURRICULUM VITAE


| | |
|---|---|
| **Name** | Ana Banjac |
| **Home address** | Wiesenstr. 52, 70794 Filderstadt |
| **E-Mail address** | ana.banjac@uni-tuebingen.de |
| **Date of birth** | December 22th, 1974, Cacak, Serbia |


***EDUCATION AND QUALIFICATIONS***

| | |
|---|---|
| **1981 - 1989** | Primary school, Cacak, Serbia |
| **1989 - 1993** | Secondary Grammar school, Gymnasium, Cacak, Serbia |
| **1994 - 2000** | Faculty of Pharmacy, University of Belgrade |
| **June 12th, 2001** | Final examination theme "Intermolecular bonds" |

***WORKING EXPERIENCE***

| | |
|---|---|
| **August 2001 - September 2002** | Trainee period in state pharmacies and a galenic laboratory Cacak and Belgrade, Serbia |
| **October 1st, 2002** | State examination |
| **from March, 2003 to July, 2005** | Permanently employed as a manager of a state pharmacy in Cacak, Serbia |
| **from March 2003 to July 2003** | As a professional consultant; lectures on physiology in primary and secondary schools. This project was supported by Ministries of Education and Sports and by Ministry of Health |

***PhD***

| | |
|---|---|
| **2006-2010** | Experimental work in Pharmaceutical Institut of Eberhard-Karls-University, Tübingen under the supervision of Prof.Dr.J.E.Schultz |

Filderstadt, May 1, 2011